

Visualization in Meteorology – A Survey of Techniques and Tools for Data Analysis Tasks

Marc Rautenhaus, Michael Böttinger, Stephan Siemen, Robert Hoffman,
Robert M. Kirby, Mahsa Mirzargar, Niklas Röber, and Rüdiger Westermann

Abstract—This article surveys the history and current state of the art of visualization in meteorology, focusing on visualization techniques and tools used for meteorological data analysis. We examine characteristics of meteorological data and analysis tasks, describe the development of computer graphics methods for visualization in meteorology from the 1960s to today, and visit the state of the art of visualization techniques and tools in operational weather forecasting and atmospheric research. We approach the topic from both the visualization and the meteorological side, showing visualization techniques commonly used in meteorological practice, and surveying recent studies in visualization research aimed at meteorological applications. Our overview covers visualization techniques from the fields of display design, 3D visualization, flow dynamics, feature-based visualization, comparative visualization and data fusion, uncertainty and ensemble visualization, interactive visual analysis, efficient rendering, and scalability and reproducibility. We discuss demands and challenges for visualization research targeting meteorological data analysis, highlighting aspects in demonstration of benefit, interactive visual analysis, seamless visualization, ensemble visualization, 3D visualization, and technical issues.

Index Terms—Visualization, meteorology, atmospheric science, weather forecasting, climatology, spatiotemporal data, survey.

1 INTRODUCTION

METEOROLOGY, the “study of the atmosphere and its phenomena” [1], is a recurrent application domain in research on visualization and display design, and one of great societal significance. Likewise, from the meteorological point of view, visualization is an important and ubiquitous tool in the daily work of weather forecasters and atmospheric researchers. As put by senior meteorologist M. McIntyre in 1988, human visual perception is the “most powerful of data interfaces between computers and humans” [2]. In modern meteorology, data from in-situ and remote sensing observations and from numerical simulation models are visualized [1], [3]; typical tasks include the *analysis* of data (frequently using multiple heterogeneous data sources) to understand the weather situation or a specific atmospheric process, *decision making*, and the *communication* of forecasts and research results. In recent years, an increase in observation density, numerical model resolutions, the number of simulated parameters, diversity of data sources, and use of ensemble methods to characterize model output uncertainty has resulted in increased data size and complexity and, hence, in higher challenges for visualization.

A number of overview articles have explored aspects

of visualization in meteorology. Early surveys by Papathomas, Schiavone, and Julesz [4], [5] reported on the usage of computer graphics techniques for the visualization of meteorological data in the 1980s. Subsequent summaries by Böttinger et al. [6], Middleton et al. [7], and Nocke et al. [8] described, from a meteorological research point of view, tools and techniques used in weather and climate research; Nocke [9] recently provided a situation analysis of scientific data visualization in climate research. Monmonier [10] provided a history of meteorological map making, and Trafton and Hoffman [11] discussed activities in cognitive engineering to improve meteorological display technology. Recently, Stephens et al. [12] reviewed how probabilistic information is communicated in climate and weather science, and Nocke et al. [13] explored the usage of visual analytics to analyze climate networks. None of these articles, however, provided a comprehensive overview of current visualization techniques and tools in meteorology and of the state of the art of visualization research aimed at advancing meteorological visualization.

Such an overview is the purpose of the present article. Our objective is to provide the visualization researcher with a summary of visualization techniques and tools that are in current use at operational meteorological centers and in meteorological research environments, to survey the research literature related to visualization in meteorology, and to identify important open issues in meteorological visualization research. As illustrated in Fig. 1a, visualization techniques for data analysis, decision making, and communication overlap; to limit the scope of our survey, we focus on visualization for data analysis tasks. While effective visualization techniques for communication and decision making are equally important, they provide enough material for overviews on their own (e.g., cf. Stephens et al. [12] and Schneider [14]).

- M. Rautenhaus and R. Westermann are with the Computer Graphics & Visualization Group, Technische Universität München, Garching, Germany. E-mail: {marc.rautenhaus, westermann}@tum.de
- M. Böttinger and N. Röber are with the Deutsches Klimarechenzentrum GmbH, Hamburg, Germany. E-mail: {boettinger, roeber}@dkrz.de
- S. Siemen is with the European Centre for Medium-Range Weather Forecasts, Reading, UK. E-mail: stephan.siem@ecmwf.int
- R. Hoffman is with the Institute for Human and Machine Cognition, Pensacola, USA. E-mail: rhoffman@ihmc.us
- R. M. Kirby is with the Scientific Computing and Imaging Institute, University of Utah, Salt Lake City, USA. E-mail: kirby@cs.utah.edu
- M. Mirzargar is with the Computer Science Department, University of Miami, Miami, USA. E-mail: mirzargar@cs.miami.edu

Manuscript received February XX, 2017; revised November YY, 2017.

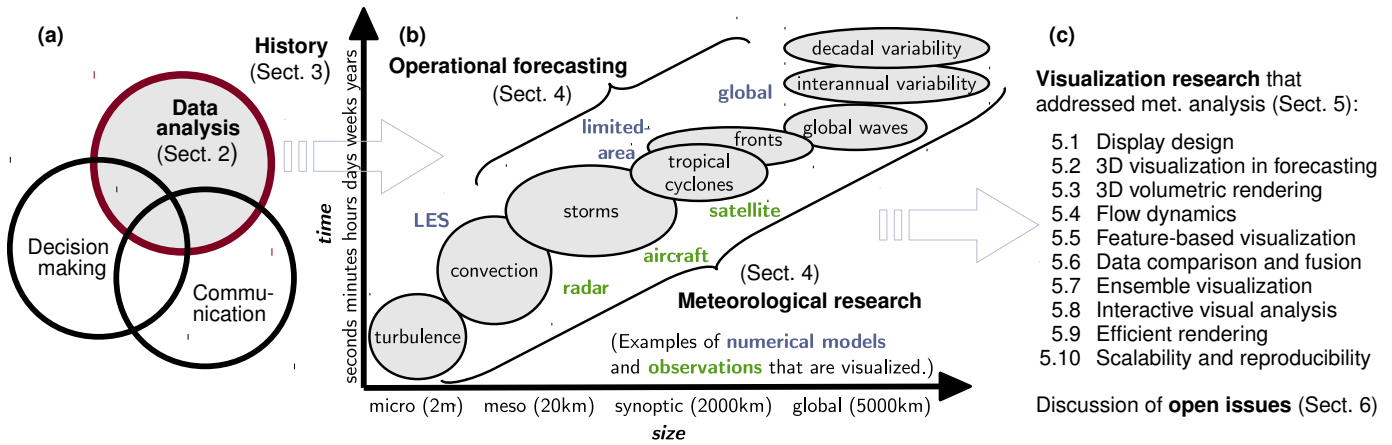


Fig. 1. Overview of the survey with links to the corresponding sections. (a) Visualization in meteorology is relevant for the overlapping areas of data analysis, decision making and communication. In this survey, we focus on data analysis. (b) Different scales of atmospheric processes are analyzed by weather forecasters and atmospheric researchers; data to be visualized originates from numerical models and observations. Forecasting is mainly concerned with the meso and synoptic scales; atmospheric research considers all scales. (c) Surveyed visualization research.

We structure the article as follows. To make the reader aware of domain-specific requirements for visualization, characteristics of meteorological analysis tasks and data are described in Sect. 2, followed by a brief history of meteorological visualization in Sect. 3. Section 4 describes the state of the art in visualization in the application domain, considering operational forecasting and meteorological research environments. The reader is provided with an overview of visualization in day-to-day meteorological practice and made aware of challenges. The state of the art in visualization research that is related to meteorology is surveyed in Sect. 5, which highlights techniques with the potential to improve on current practice. A summary of Sects. 2 to 5 is followed by a discussion of what we view as being the most important open issues in meteorological visualization in Sect. 6; the article is concluded in Sect. 7.

2 METEOROLOGICAL DATA AND ANALYSIS TASKS

Meteorological phenomena and processes encompass a wide range of spatiotemporal scales, from small-scale turbulence to global climate (illustrated in Fig. 1b). Visualization requirements depend on the purpose of the analysis, the scale of the process to be analyzed, and the characteristics of the data used. For instance, meteorologists aiming at understanding *weather* (the condition of the atmosphere at any particular place and time [1]) may focus on visualizing the development of a particular storm; researchers investigating *climate* (the “statistical weather” of a particular region over a specified time interval, usually over at least 20 to 30 years [15, Ann. 3]) could focus on visualizing statistical quantities (e.g., a change in mean summer precipitation).

2.1 Weather forecasting vs. atmospheric research

Due to different requirements for visualization techniques and tools, Papathomas et al. [4] and Koppert et al. [16] distinguished between the use of visualization in *operational weather forecast settings* versus *atmospheric research settings*. Operational forecasting focuses on atmospheric processes at mesoscale and synoptic scale (cf. Fig. 1b), covering tasks from *nowcasting* (prediction of, e.g., thunderstorms in the

next two hours) over *medium-range forecasting* (five to seven days into the future) to *seasonal forecasting* (statistical characteristics of the next months) [17, App. I-4]. The operational computational chain at weather centers covers the assimilation of routine observations (e.g., surface stations, satellites) into numerical weather prediction (NWP) models, the numerical prediction itself, post-processing, and visualization of observations and NWP data [3], [18]. Despite increasingly automated procedures, the human forecaster and, thus, visualizations interpreted by the forecaster, continue to play a crucial role [3]; forecasting results depend on the forecaster’s ability to envision a *dynamic mental model* of the weather from available data visualizations [11], [19]. This model reflects his/her understanding of qualitative/conceptual information (e.g., images of the internal structure and dynamics of storm clouds), as well as of numerical information (e.g., data about winds, air pressure changes, etc.) [19].

Innes and Dorling [3] provided an overview of typical forecaster tasks. A forecaster follows specific objectives (weather prediction for a particular place, time, and purpose), and is subject to time constraints. For example, a common task is to estimate the uncertainty of NWP output; often using ensemble predictions (Sect. 2.3) to judge a model’s uncertainty and to gain information about potential forecast scenarios and the risk of severe weather events. Another example is the application of knowledge about model characteristics (e.g., systematic errors and biases) to improve the forecast. Forecasters inspect and integrate a great number of complex visualizations and data sources; estimates are in the range of eight or more different data type displays for forecasts in non-severe situations [19]. Because the pertinent information usually is not displayed in any one single visualization, forecasters must mentally integrate that information into a coherent whole to make a prediction about the future weather. In this respect, one of the challenges today is the sheer volume of NWP output that needs to be explored and interpreted [3].

In meteorological research environments, the objectives of a scientist can include many other things in addition to “understand and predict the weather”; e.g., field observations are analyzed, and numerical models are developed

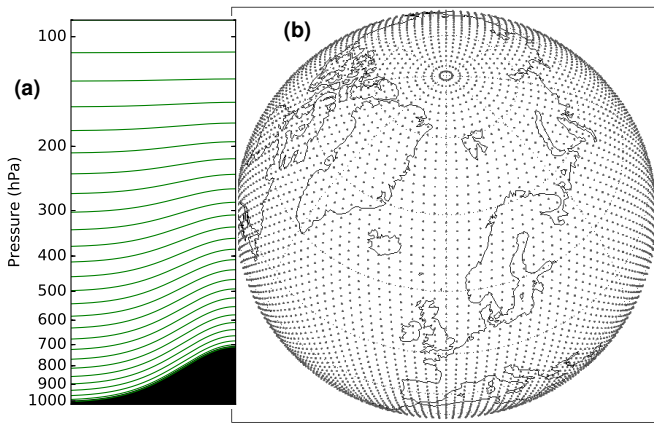


Fig. 2. Examples of grids used in numerical weather prediction models. (a) The vertical hybrid sigma-pressure coordinate prevents intersection of lower model levels (green lines) with the surface orography (black) by “following” the terrain. (b) The reduced Gaussian grid [28] keeps the distance between grid points approximately constant by reducing the number of points per parallel towards the pole. (Courtesy of ECMWF.)

and evaluated. In contrast to operational environments, visualization requirements are not necessarily known and fixed a priori. Processes from the microscale to climate variation (cf. Fig. 1b) are targeted; the increased diversity of data and analysis tasks requires an increased diversity of visualization techniques. Time is a much less limiting factor; a researcher has more time to create, interact with, and interpret a visualization.

2.2 Heterogeneity of data sources

Modern meteorology employs data from atmospheric observations and numerical computer model output (data from laboratory experiments and idealized mathematical models are used as well). Data come in different modalities; also, coordinate systems differ. For example, pressure is used as the standard vertical coordinate, but geometric height and potential temperature are also frequently encountered [1].

Atmospheric computer models include fluid flow, air chemistry, Lagrangian particle, and radiative transfer models, with different models targeting different scales of motion (cf. Fig. 1b; the interested reader is referred to, e.g., [3], [20]). The topology of the data grids is important to visualization algorithms (e.g., [21], [22]). Horizontal grid topologies include regular and rotated grids for models covering a limited area (e.g., [23], [24], [25]), and, as illustrated in Fig. 2, unstructured (e.g., icosahedral and reduced Gaussian) grids for global models (e.g., [26], [27]). Grid spacings range from the order of meters to hundreds of kilometers. To avoid intersection of model levels with the earth’s terrain, many models use “terrain-following” vertical coordinates (Fig. 2).

Data from atmospheric models are frequently encountered in the visualization literature. Examples include the European Centre for Medium-Range Weather Forecasts (ECMWF) Integrated Forecast System (IFS, [26]) as a global model and the Weather Research & Forecasting Model (WRF, [23]) as a limited-area model. New-generation global models manifest efforts towards *seamless prediction* [29], [30], their icosahedral grids can be refined in selected regions to replace limited-area models (e.g., [31], [27]). Climate

models are similar to global NWP models but run at coarser resolutions to facilitate longer integration times (e.g., [32]), large-eddy simulation (LES) models explicitly resolve small-scale atmospheric phenomena (e.g., convection; e.g. [25]).

Observational data come routinely from surface stations, radiosonde soundings, weather radar, meteorological satellites, aircraft and ship sensors, and further in-situ and remote sensing instruments [3, Ch. 3]. They are distributed through World Meteorological Organization (WMO) systems [33]. Further observations originate from research experiments [34], e.g., field campaigns using sensors on aircraft, ships, and at the surface. Data modality and sampling resolution of observations varies significantly, making it challenging to co-locate measurements from different sensors. For example, a network of surface stations yields scattered 2D data, a volumetric radar scan data on an irregular, rotated, stretched grid.

2.3 Uncertainty and ensemble modeling

Uncertainty plays an important role in both forecasting and research, and poses significant challenges to visualization (where it has been broadly identified as a key challenge as well; e.g., [35], [36]). Uncertainty information in forecasting is derived, e.g., from the comparison of different NWP models, from model output statistics (MOS) techniques (statistical correction of NWP output often based on past observations; e.g., [37]), and from ensemble methods [38], [39]. In their recent review of the state of numerical weather prediction, Bauer et al. [30] identify ensemble methods as one of three areas that present the most challenging science questions in weather prediction in the next decade.

NWP ensembles typically represent uncertainty due to initial condition errors and model imperfections. The equations of motion have a *chaotic* nature [40], and small changes in, e.g., initial conditions can lead to fundamentally different solutions. Limits of predictability are estimated to be on the order of about 10 days, depending on atmospheric state and depending on what specific atmospheric parameters are the focus of the prediction [41], [42]. A finite sample of initial atmospheric states (on the order of 20 to 50; [37], [39], [40]) is integrated in time; this ensemble of forecasts is interpreted to approximate the probability distribution (which is of general shape and can be multi-modal) of future atmospheric states. Examples of NWP ensemble systems include the ECMWF Ensemble Prediction System (ENS, 51 members; [40, Ch. 17]) and the U.S. National Weather Service (NWS) Global Ensemble Forecast System (GEFS, 21 members; [43]). Common practice is to run a high-resolution forecast (often called *deterministic*) using the “best” initial conditions [38], and to run the ensemble at lower resolution. With ensembles, grid topologies can pose additional challenges to visualization. For example, terrain-following coordinates may lead to different vertical locations for the same grid point in different members [22].

In different contexts (e.g., climate research), ensemble methods are used as well, e.g., for estimation of the internal variability in long term climate projections [44], [45] and for decadal climate predictions [46]. Here, ensembles based on perturbed physics and on multiple models are commonly encountered (e.g., [47], [48]).

3 HISTORY OF VISUALIZATION IN METEOROLOGY

Traditionally, meteorologists and forecasters have employed a variety of hand-drawn 2D meteorological charts and diagrams. In his (pre-computer era) book on meteorological analysis, Saucier [49] classified depictions in usage in the 1950s into meteorological maps, cross-section charts, vertical sounding charts, and time-section charts. These 2D depictions of meteorological observations (their historical evolution was described by Monmonier [10]) typically included contour lines, wind vectors, barbs, or streamlines.

3.1 Computer-based visualization 1960-1990

As reported by Papathomas et al. [4], the earliest computer-based visualization tool specific to meteorology was the National Center for Atmospheric Research (NCAR) Graphics package developed in the late 1960s. As a notable example, Washington et al. [50] presented 2D contour lines of simulation data from the NCAR general circulation model [51] displayed on a cathode ray tube screen. The first computer animated movies of atmospheric simulations were created in the 1970s. Grotjahn and Chervin [52] described the creation of (still monochrome) movies at NCAR. They already used 3D perspective views; an example is shown in Fig. 3a. At the same time, interest in “true” 3D displays grew and methods were developed to generate stereoscopic projections, first of observational (mainly satellite) data [53], [54], [55], [56], but also of simulation data [57].

At the University of Wisconsin-Madison, the *Man computer Interactive Data Access System* (McIDAS), a pioneering workstation system to process and view meteorological observation data, had been developed since 1973 [58], [59], [60]. In the mid-1980s, a stereographic terminal was developed, and Hibbard [56], [61] reported on extensive experiments with monochrome 3D stereo visualization. In the 1980s, high attention was given to psychophysical aspects, specifically visual perception (cf. [4], [5], [57]). In this line, Hibbard [56] discussed challenges of 3D visualization and perception, including the correct usage of visual cues to create an illusion of depth, choosing a good aspect ratio to avoid misleading angles and slopes in the display, system performance and user handling. He presented 3D views of satellite cloud images, wind trajectories, contour surfaces, and radar data, noting that the displays required improvement in particular with respect to spatial perception (the “location problem” as he called it), use of color, combined display of multiple variables, and efficiency for better interactivity. In a similar effort, Haar et al. [62] presented 3D displays for satellite and radar data, discussing application to pilot briefing, forecasting and research, and teaching.

McIDAS was extended to handle simulation data and color [64]. Figs. 3b and c show examples from Hibbard et al. [63], who described its application to a model study. In addition to the techniques for observations presented by Hibbard [56], they used isosurfaces of potential vorticity to depict the tropopause on top of a topographic map and contour lines of surface pressure. Particle trajectories were rendered as shaded tubes. Hibbard et al. [63], [65] stressed the need for an interactive system to create such visualizations, as adjustments still required several hours to recompute an image. Also in the late 1980s, Wilhelmson

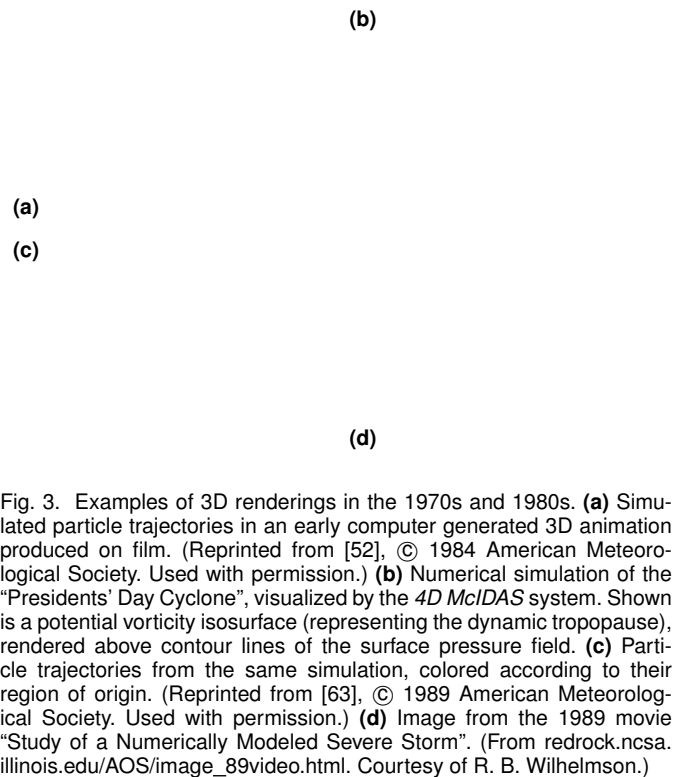


Fig. 3. Examples of 3D renderings in the 1970s and 1980s. (a) Simulated particle trajectories in an early computer generated 3D animation produced on film. (Reprinted from [52], © 1984 American Meteorological Society. Used with permission.) (b) Numerical simulation of the “Presidents’ Day Cyclone”, visualized by the 4D McIDAS system. Shown is a potential vorticity isosurface (representing the dynamic tropopause), rendered above contour lines of the surface pressure field. (c) Particle trajectories from the same simulation, colored according to their region of origin. (Reprinted from [63], © 1989 American Meteorological Society. Used with permission.) (d) Image from the 1989 movie “Study of a Numerically Modeled Severe Storm”. (From redrock.ncsa.illinois.edu/AOS/image_89video.html. Courtesy of R. B. Wilhelmson.)

Fig. 4. Screenshot of the Vis5D visualization tool, showing a display combining different visualization types available in the software: 2D contour lines, 2D color mapping, terrain, isosurface, and volume rendering. (Reprinted from [67, p. 674], © 2005, with permission from Elsevier.)

et al. [66] raised attention (cf. [7]) with story-boarded 3D animation movies. Fig. 3d shows an image from the 1989 video “Study of a Numerically Modeled Severe Storm”. Creating the movie was a major undertaking, requiring multiple scientific animators, script writers, artistic consultants, and postproduction personnel over an 11-month period [66].

Further details on visualization activities up to the late 1980s can be found in earlier surveys [4], [5], [7].

3.2 Interactive workstations

Since around 1990, workstations with increasingly powerful graphics accelerators enabled the development of interactive visualization tools. To create an interactive McIDAS system, Hibbard et al. developed the *Vis5D* software [67], [68], [69], [70]. It became a major 3D visualization tool

in meteorology in subsequent years [7], [67]. For instance, Vis5D was used at the German Climate Computing Center (DKRZ) [6], coupled with ECMWF's Metview meteorological workstation [71], and used as basis for a 3D forecasting workstation (cf. Sect. 5.2). Fig. 4 shows a screenshot of the last Vis5D release, described by Hibbard [67]. Data could be displayed interactively as 2D contour lines or pseudo-colors on horizontal and vertical sections, as 3D isosurfaces, and as volume rendering. Wind data could be depicted as vector glyphs, streamlines and path lines. A topographical map could be displayed as geo-reference. Vis5D provided support for comparing multiple datasets, multiple displays could be “grouped” and synchronized. Development of Vis5D ceased in the early 2000s [67].

A number of further 3D visualization tools appeared in the 1990s, mostly general-purpose, commercial, and not primarily targeted at meteorology. Systems used in the atmospheric sciences were listed by Schröder [72], Böttinger et al. [6], and Middleton et al. [7]. Examples include the commercial systems *Application Visualization System* (AVS) [73], [74], *Iris Explorer* [75], the *IBM Data Explorer* [76], [77] (DX; later made open-source as *OpenDX*; discontinued in 2007), and *amira* [78] (now *Avizo*). However, these tools were primarily used by visualization specialists, as Böttinger et al. [6] and Middleton et al. [7] pointed out. Atmospheric scientists in their daily work relied mainly on command-driven 2D plotting and analysis tools [6], [7].

4 VISUALIZATION IN METEOROLOGY TODAY

Today, the well established meteorological charts and diagrams listed at the beginning of Sect. 3 (see [10], [49]) are still in the center of both operational forecast visualization and visual data analysis in meteorological research.

Operational meteorology is still dominated by 2D visualization, despite the efforts with respect to interactive 3D visualization in the 1980s and 1990s. Major reasons include that forecasters are mainly concerned with horizontal movements of weather features (for which depiction on a 2D map is appropriate), the clarity of 2D maps with respect to spatial perception and conveyance of quantitative information, and historical reasons (forecasters have traditionally been trained with 2D visualization). 2D images also integrate well with Geographic Information Systems used by emergency services and are established to communicate weather information to the public. In recent years, feature-based and ensemble visualization methods have gained increased importance.

In meteorological research, visualization techniques and tools are much more diverse than those encountered in operational settings, reflecting the (in comparison to forecasting) larger diversity of scientific questions being investigated. Similar to operational forecasting, 2D visualizations dominate meteorological research environments, although 3D techniques are more common than in forecasting.

In the following, we survey the state of the art in visualization in operational environments (e.g., at national meteorological centers) and meteorological research settings. Major visualization tasks are listed in Table 1, which provides a summary and a categorization of visualization techniques employed in practice, grouped by operational meteorology and research.

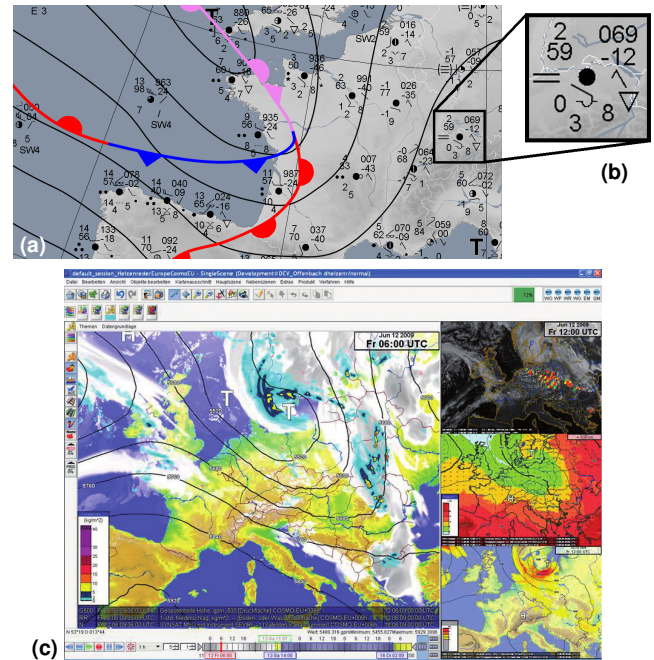


Fig. 5. Standard visualizations in weather forecasting. (a) Operational surface map, showing contour lines of surface pressure, analyzed fronts, and (b) station data depicted using WMO glyphs (© 2016 Deutscher Wetterdienst. Used with permission.) (c) The *NinJo* forecasting workstation features multiple views that offer a variety of 2D visualization methods to depict observations and numerical prediction data. (Reprinted from [80], © 2010 Deutscher Wetterdienst. Used with permission.)

4.1 Analysis of observation and simulation data

The depiction of observation and numerical model data on maps plays a central role in meteorology. As shown in Fig. 5a, surface data are routinely plotted using contour lines to depict pressure, wind barbs to show wind flow, and glyphs to depict station observations and analyzed features including, e.g., fronts. The styling of the glyphs is mandated by the WMO [17]; they represent aspects of the observations (e.g., precipitation type and cloud cover). Upper level data are plotted on standardized pressure level charts [17], including the 500 hPa level often used as representative for large scale atmospheric flow at mid-troposphere (cf. Figs. 7 and 9). For specific purposes, vertical coordinates other than pressure are used (cf. Sect. 2.2), including potential vorticity (e.g., to display the height of the tropopause) and potential temperature. Meteorological maps are created for many different scales, from local to global maps. From the early days of hand-plotted maps, different cartographic projections have played an important role due to their attempts to conserve scale, angle, and area [79]. For example, a map projection widely used by European forecasters is the polar stereographic projection; it accurately portrays weather systems moving over the North Atlantic.

Typically, multiple observed and/or forecast parameters are combined in a single image. Also, juxtaposition of different maps is heavily used, as shown in Fig. 5b in a screenshot of the *NinJo workstation* (the visualization software operationally used, e.g., at the German Weather Service (DWD)). Temporal evolution of spatial fields is usually inferred from time animation of the maps; time evolution of a forecast at a particular location is displayed by means of a *meteogram*.

TABLE 1

Categorization and summary of visualization techniques commonly used in operational weather forecasting and meteorological research, and topics that have been addressed in visualization research. Links to sections and figures in this article are abbreviated with *S* and *F*, respectively.

	Operational weather forecasting (examples of tasks: analyze weather situation and its time evolution, analyze and compare NWP models and observations, judge NWP uncertainty and estimate risk)	Meteorological research (examples of tasks: analyze observations and model data w.r.t. many possible objectives, e.g., analysis of a specific feature, explorative analysis, statistical analysis)	Research on met. visualization (published techniques to improve on common practice; they are mostly not directly available to meteorological researchers in a common visualization tool)
Visual mapping of observations & simulations	2D depiction predominates (S4, S4.1): surface & upper-level maps (F5), cross-section charts, vertical profiles (F7c), domain-specific glyphs and diagrams (F5-11), synthetic satellite images (F6b)	2D visualization as in forecasting (S4, S4.1), some 3D visual mapping (iso-surfaces, volume rendering, streamlines and trajectories/path lines, S4.4, F4, F13, F16), domain-specific diagrams	Advice on color and map making (S5.1), visual salience (S5.1), 2D flow display improvements (S5.1, F14), 3D feasibility studies for forecasting (S5.2, F15, F16), 3D cloud rendering (S5.3)
Analysis of flow & temporal evolution	Animation (S4.1), meteograms (F10) and time-section charts (S3), overlay of time steps, wind barbs (F14a), streamlines, trajectories/path lines, Lagrangian particles	As in forecasting, criterion-based trajectory visualization, domain-specific diagrams including Hovmöller diagrams (S4.1)	Approaches for streamlines and path lines (S5.4), dynamic flow displays (S5.4), Lagrangian coherent structures (S5.4), feature-based flow visualization (S5.5)
Detection & tracking of atmospheric features	Time evolution (S4.1) and uncertainty (spaghettis, probabilities, S4.2) of, e.g., convective storms (F6), extratropical cyclone features (e.g., fronts, F11), tropical cyclones	As in forecasting but with more diverse feature detection targets and approaches (e.g., jet streams, clouds), often for statistical analysis (S4.1, S5.5)	Feature tracking in virtual reality, critical points, optical flow, image-based techniques, feature-based flow visualization (S5.5)
Comparison & fusion of heterogeneous data	Side-by-side depiction, overlay (F5), regridding to common grid, difference plots, depiction of model data as observations, e.g., synthetic satellite images (S4.1, F6b)	As in forecasting but with more diverse data sources (S2.2)	IVA to compare model output, overlay, similarity measures, filling of spatio-temporal gaps in data from heterogeneous sources, segmentation, streamlines in multi-resolution data (S5.6)
Analysis of uncertainty in simulations	2D depiction (S4.2): stamp maps, spaghetti plots of contour lines (F7a) and features (F11), ensemble mean and standard deviation (F7b), ensemble probabilities, extreme forecast index (F8), clustering (F9), ensemble meteograms (F10)	As in forecasting, distinct visual channels (e.g., stippling), interactive approaches (ensemble space navigation, interactive ensemble statistics, brushing and linking), 3D approaches (e.g., depiction of probabilities, height mapping) (S4.2)	Perceptual design studies (S5.1, S5.7), visual abstractions as alternatives to spaghetti plots (S5.7, F18), interactive exploration, linked views, abstract views, 3D spatial displays (F16), time series, multi-modal distribution visualization, flow uncertainty (S5.7)
Usage of interactivity in workflows	Operational meteorological workstations support interactive 2D visualization (e.g., pan, zoom, map styling) (F5c, S4.3)	Command-driven 2D tools most common due to flexibility and reproducibility (S4.3), some interactive 3D analysis (S4.4), little IVA (F12, S5.8)	Linked views, brushing & linking, hypothesis generation, interactive statistical analysis (S5.8), IVA for comparative visualization (S5.6)
Technical aspects	Web-based remote visualization (OGC web services, S4.3), scalability challenges (S5.10, S6)	Increasing data volumes (scalability, data compression, remote rendering, S4.3, S4.4, S5.10), reproducibility (S4.3, S5.10), efficient GPU-based 3D rendering directly using model grids (S5.9), virtual reality (S5.3)	

Examples are shown, e.g., in Schultz et al. [81]. Temporal movement of air masses is frequently visualized by 2D depiction of 3D trajectories (i.e., path lines; e.g., [82]), often filtered and colored according to specific criteria. *Vertical cross-sections*, typically along a line between two locations, are used to analyze the vertical structure of the atmosphere. Domain specific diagrams frequently used in operations include *Skew-T* diagrams and *tephigrams* to analyze vertical profiles (e.g., observations from radiosonde ascents, an example can be found in [81]), additional examples used in research include Hovmöller diagrams (space-time diagrams; e.g., [83]) and Taylor diagrams (model evaluation, [84]). Also, results of statistical analyses including principal component analysis, e.g., of recurring patterns in the climate system, are frequently plotted on maps (e.g., [37]).

In recent years, feature-based (also referred to as object-based) visualization techniques have gained importance in operational forecasting. Commonly analyzed features are convective storms and mesocyclones (e.g., [86], [87]), synoptic-scale extratropical cyclonic features (fronts and low pressure centers) [88], and tropical cyclones [89]. Features are detected from satellite/radar observations and from

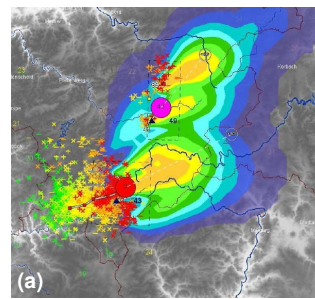


Fig. 6. Visualizations in operational forecasting. (a) Storm cells detected and tracked in combined observational and model data (red and purple circles indicate convective cells, dotted lines expected tracks), visualized together with lightning observation data (crosses colored by observation time) and MOS-derived probabilities of severe precipitation (filled contours). (© 2011 Deutscher Wetterdienst. Courtesy of D. Heizenreder.) (b) Synthetic satellite image. Visible radiances are approximated using a neural network that takes NWP data as input. (Reprinted from [85], © 2012 American Meteorological Society. Used with permission.)

NWP output. Fig. 6a shows an example of the DWD *Now-CastMIX* and *KONRAD* systems (e.g., see the overview by Joe et al. [90], and references therein), which output the

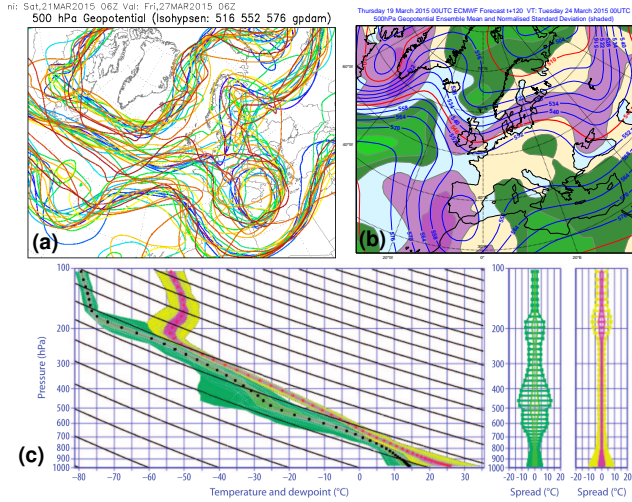


Fig. 7. Ensemble forecast products. (a) “Spaghetti plot”, comparing contour lines of three isovalues of the 500 hPa geopotential height field of an NCEP GEFS forecast at 144 lead time. (Courtesy of G. Müller, www.wetterzentrale.de.) (b) ECMWF forecast product showing ensemble mean of 500 hPa geopotential height (contour lines) and normalized standard deviation of the same field (filled contours). (Courtesy of ECMWF.) (c) Ensemble vertical profile displaying temperature (yellow/magenta) and dewpoint (green) at a single location. Colors indicate ranges of probability (0-25%, 25-75%, 75-100% bands). (Reprinted from [104]. Courtesy of I. Ihász, Hungarian Meteorological Service.)

locations of thunderstorm cells, as well as their track and probability fields for impact in the near future. In research, uses of feature-based visualization also include statistical data analysis, e.g., climatologies of feature occurrence [91], [92]. For comparative visualization, model output is visualized in ways corresponding to observations, an example is rendering simulated clouds as seen from a satellite (e.g., [85], [93]). Such images are frequently used by forecasters; Fig. 6b shows an example of an approach using neural networks for rendering to approximate the displayed cloud-top radiances.

4.2 Analysis of simulation uncertainty

Visualization of model uncertainties is of particular importance in forecasting, but also in research for, e.g., climate predictions. Early approaches date back to the 1960s [94], [95]; in operational forecasting today, output from MOS techniques and ensemble output (cf. Sect. 2.3) are visualized. For example, Fig. 6a displays uncertainty information from an operational nowcasting MOS technique. The books by Wilks [37] and Inness and Dorling [3] contain overviews of general meteorological uncertainty visualization techniques; several articles described ensemble visualization products in use at national weather centers [96], [97], [98], [99], [100], [101], [102]. A set of basic guidelines on how to communicate forecast uncertainty is available from the WMO [103]. Note that all techniques in the above references (and presented in this section) solely rely on 2D visualization.

A direct way to visualize ensemble output are small multiples referred to as *stamp maps* (examples can be found in [3, Fig. 5.6] and [18, Fig. 2.9]). In stamp maps, individual details are not discernible, but differences in large-scale features (e.g., location and strength of a cyclone) can be

Anomalous weather predicted by EPS: Thursday 26 March 2015 at 12 UTC
1000 hPa Z ensemble mean (Tuesday 31 March 2015 at 12 UTC)
and EFI values for Total precipitation, maximum 10m wind gust and mean 2m temperature (all 24h)
valid for 24 hours from Tuesday 31 March 2015 at 00 UTC to Wednesday 01 April 2015 at 00 UTC

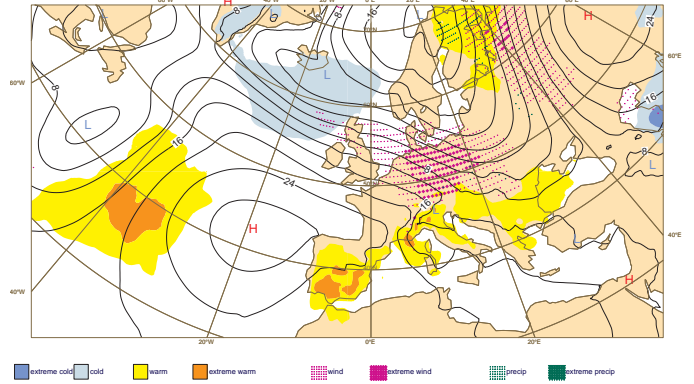


Fig. 8. The ECMWF extreme forecast index relates ensemble predictions to model climatology to detect anomalous weather conditions in the forecast. Shown is the EFI computed at five days lead time for 31 March 2015. On this day, storm “Niklas” hit central Europe with gale-force winds. Note how five days prior to the event the EFI predicted extreme winds over large parts of Germany. (Courtesy of ECMWF.)

recognized by the forecaster [96]. Alternatively, *spaghetti plots* as shown in Fig. 7a display selected contour values of all ensemble members in a single image. Wilks [37] noted that spaghetti plots have proven to be useful in visualizing the time evolution of the forecast flow, with the contour lines diverging as lead time increases. A disadvantage of spaghetti plots, however, is that they become illegible when members diverge too much; also, care needs to be taken in interpretation as the distance of the contour lines depends on the gradient of the underlying field [96].

Displays of summary statistics computed per model grid-point are also common. Typical visualizations include maps of probabilities of the occurrence of an event, and of ensemble mean and standard deviation (the mean is on average more skillful than any single member; the standard deviation or *spread* indicates forecast uncertainty [3]). Fig. 7b shows an example, indicating areas of a geopotential height forecast that are most affected by uncertainty (large spread). Probability maps (an example can be found in [105, Fig. 13.4]) are generated mainly for surface parameters relevant for weather warnings (e.g., wind speed, temperature, and precipitation). They are frequently computed over a time interval. For example, probabilities for extreme wind gusts are computed over a 24 hour period at ECMWF, as it is considered more important to know *that* an extreme event will occur rather than *when exactly* it will occur [102]. Probabilities are also commonly computed for areas encompassing multiple grid boxes to determine whether an event can occur *somewhere in a given region*. Similar depictions are also applied to other types of meteorological diagrams. For example, Fig. 7c shows an ensemble vertical profile used by the Hungarian Meteorological Service [104].

A display that summarizes regions in which severe weather events may occur are maps of the *extreme forecast index* (EFI) [106], a measure that relates forecast probabilities to the model climate to detect forecast conditions that largely depart from “normal conditions”. The EFI is used, e.g., to generate warnings of extreme winds [107].

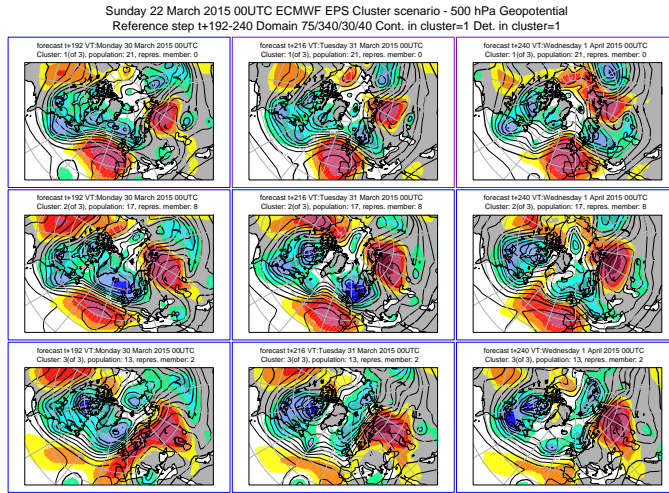


Fig. 9. Example of a cluster product, based on 500 hPa geopotential height over Europe forecast by ECMWF. Three clusters (rows) of the ensemble forecast are valid at (left) 192, (middle) 216, and (right) 240 hours lead time. The clusters are represented by the member closest to the cluster center. Note the different extent of the trough over northern Europe. The color of the frames corresponds to the large-scale weather regime to which the cluster is most similar. (Courtesy of ECMWF.)

Fig. 8 shows an example of an ECMWF forecast, indicating extreme winds over large parts of Germany.

To identify similarities within ensemble members, they are commonly objectively clustered [108], [109]. Fig. 9 shows an operational example from ECMWF. The 51 ensemble members, as well as the high-resolution deterministic forecast, are grouped into a small number (a maximum of six) of clusters according to their similarity in 500 hPa geopotential height over Europe in a given time window [108]. The clusters are represented by the members closest to their center, and assigned to one of four large-scale weather regimes (color of the cluster frame in Fig. 9 [108]; forecast skill of the ensemble depends on the weather regime [110]).

For point forecasts (i.e., for a specific location), *ensemble meteograms* show time series of box plots (e.g., [37]) of forecast variables. Fig. 10 shows an operational example from ECMWF. Forecast information are accumulated into daily mean and displayed together with model climate information, showing how the current forecast weather deviates from the “norm”. The overlaid boxplots show if the ensemble forecast contains more information than climatology (in the example, cloud cover and temperature forecasts in the last few days hardly differ from climatology). The diagram additionally contains wind roses to display the distribution of wind direction. Wind roses are traditionally used to show distributions of wind direction over a time period (e.g., [111], [112]); here, they are used to show both temporal and ensemble information (distribution of all members over one day), with wind directions clustered into octants. In addition, *plume plots*, a combination of spaghetti plots and probability maps, are used to display the temporal evolution of further meteorological quantities at the location of interest (an example can be found in [18, Fig. 2.17]).

A feature-based method to visualize the evolution of cyclonic features in ensemble forecasts [88], [113], [114], [115] is operated by the UK Met Office and ECMWF. The example

ENS Meteogram

München, Germany 48.02°N 11.2°E (EPS land point) 512 m

Extended Range Forecast based on ENS distribution Thursday 19 March 2015 00 UTC

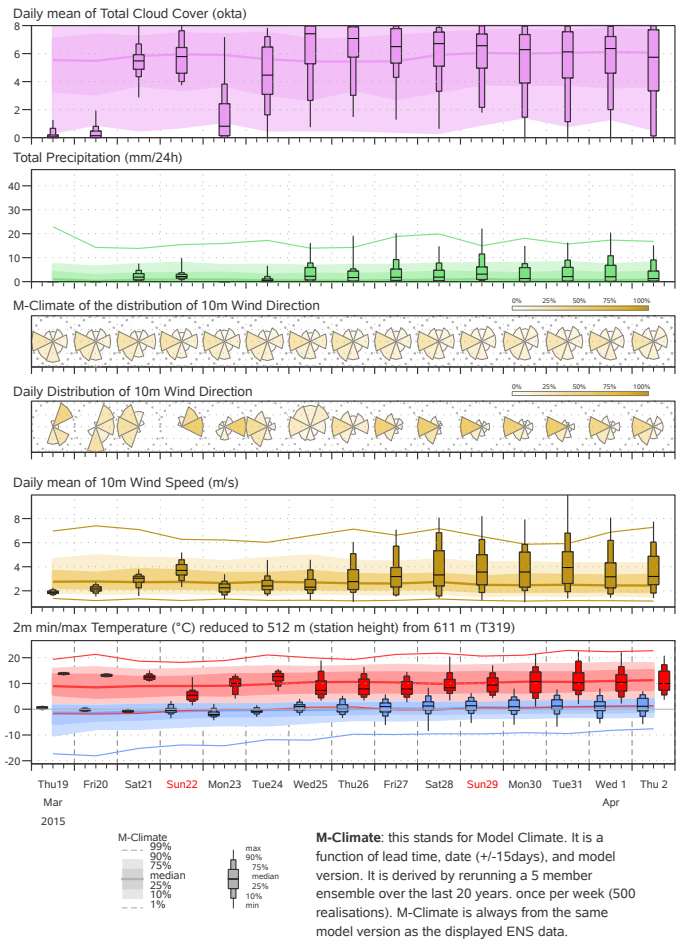


Fig. 10. Example of an ECMWF 15-day ensemble meteogram, depicting time series of surface parameters of a forecast initialized on 19 March 2015 for Munich, Germany. The ensemble distribution is displayed by means of boxplots. This diagram relates forecast daily averages to the model climate (colored background bars). Note how in the daily mean of 10 m wind speed the possibility of high wind speeds on 31 March 2015 (12-day forecast) is predicted (box plot whisker extending over 10 ms^{-1} ; the same event as in Fig. 8). (Courtesy of ECMWF.)

in Fig. 11 shows surface cold and warm fronts detected in the individual ensemble members as line features in a spaghetti plot. Alternative visualizations are available at ECMWF to view the individual ensemble member’s features (e.g., animation). Further cyclonic features (e.g., center of low pressure systems, developing waves) are also available.

The visualization products surveyed so far depict short and medium-range forecasts. With respect to seasonal forecasts, visualizations mainly show probabilities and anomalies of the predicted quantities from the climatological means (see [3, Ch. 7.4] for examples of displays). Also, specialized ensemble products are in use to provide uncertainty information requested by “sophisticated users” [99] such as emergency managers. Visualizations include, for example, forecasts of turbulence regions for aviation [116] and extratropical storm and hurricane forecasts [117], [118]. Stephenson and Doblas-Reyes [119] discussed further statistical approaches to summarizing, displaying and interpreting output from ensemble predictions.

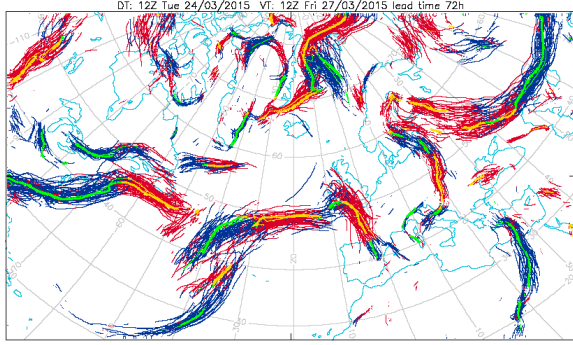


Fig. 11. Example of a spaghetti plot depicting surface fronts detected with the Hewson and Titley [88] algorithm (red lines depict warm fronts, blue lines cold fronts). Shown is an ensemble forecast valid at 72 hours lead time. (Courtesy of ECMWF.)

In meteorological research, many of the above ensemble visualization techniques are also used (e.g., spaghetti plots [120], [121]). However, as ensembles are also created with different techniques and following different scientific questions (cf. Sect. 2.3), demands for ensemble visualization are more diverse than in forecasting. For example, in climate research stippling overlaid on maps is a popular technique to depict uncertainty (e.g., [122]). Ensemble visualization capabilities of off-the-shelf visualization tools used in meteorological research were described by Potter et al. [123] and Böttinger et al. [122]. For example, the latter article showed how the uncertainty in 2D fields obtained from ensembles of decadal climate simulations can be visualized by means of static maps, interactive 3D views, and interactive brushing and linking techniques.

4.3 Implementations: workflows and challenges

In operational meteorology, the presented visualization techniques are commonly implemented in meteorological workstation systems that provide predefined visualization products that often can be interactively refined. As an example, the *NinJo* workstation [80] shown in Fig. 5c (used in Germany, Switzerland, Denmark and Canada) is based on 2D visualization methods and supports multiple views to simultaneously display different observed and forecast parameters. *NinJo* provides sophisticated time navigation, and meteorological charts including vertical soundings and time series can be displayed and analyzed interactively. Further examples include *AWIPS-II* [124] (U.S. NWS), *Diana* [125], [126] (Norwegian Meteorological Institute), *Synergie* [127] (Météo-France), and *VisualWeather* [128]. Daabeck [129] surveyed operational workstations in use in Europe as of 2005, for recent information we refer to the European Working Group on Operational Meteorological Workstations [130].

Visualization software for special-purpose forecast settings mostly provides standard meteorological maps and diagrams as well; examples include tools for teaching at universities (e.g., [81], [131]) and for forecasting during atmospheric research campaigns (e.g., [132], [133]). Standard charts are frequently augmented with additional information; e.g., the German Aerospace Center (DLR) *Mission Support System* (MSS) [133] visualizes forecast data along with flight track information to allow scientists to judge expected instrument behavior.

A technical challenge for operational comparative analysis of different NWP models is the exchange of forecast visualizations among weather centers. Standardized web-based visualization services have become common for remote visualization (cf. the Open Geospatial Consortium MetOcean domain working group [134]), examples of web-based interfaces include the ECMWF *ecCharts* system [135] and the Royal Netherlands Meteorological Institute's (KNMI) *ADAGUC* [136] web interface.

In meteorological research, data analysis and visualization tools typically employ a mostly command-driven and script-based workflow, providing functions for data import and remapping, statistical analysis, and visualization. The functionality offered by the various tools overlaps widely (cf. [7]), examples include the *NCAR Command Language* NCL [137], *GrADS* [138], *Ferret* [139], and *GMT* [140], as well as the general-purpose languages *Python* [141], *IDL* [142], and *Matlab* [143]. ECMWF's open-source *Metview* system [144], [145] takes a hybrid role; in addition to being scriptable it features a graphical user interface to allow scientists, e.g., to interactively create graphical products and then convert the visualization generation to operational scripts.

Nocke [9] attributed the popularity of script-based systems to the importance of comparability and reproducibility in the application domain. He noted that discussions with climate scientists revealed a kind of “*mistrust in interactivity*”, due to the “*arbitrariness*” that interactive adjustments introduce into the generation of visualizations. Additionally, Schulz et al. [146] stated that climate researchers tended to pursue analysis tasks with visualization techniques that they can directly re-use in publications. Nocke [9] noted, however, that in recent years in particular young scientists have become more accustomed to utilizing interactive features in visualization software, resulting in a “*rising acceptance of interactive visualization, however, still mainly for the purpose of presentation*.” Interactive visualization software for meteorological research mostly comes with a focus on 3D visualization, it is surveyed in Sect. 4.4.

Further practical challenges meteorological researchers are confronted with include increasing data volumes (most interactive visualization tools lack scalability for large grids; cf. Sect. 5.10), support of a given tool for data types output by a specific numerical model or observation system (e.g., for the development of numerical models it is essential to visualize model output on original grids, however, only few visualization tools support direct import and display of irregular model grids; cf. Fig. 12), and missing knowledge about suitable visualization techniques. For example, Nocke [9] noted that researchers in the climate sciences are often familiar with one or two visualization tools only, an issue Nocke et al. [147] approached with *SimEnvVis*, a framework that supports the researcher in finding the most suitable visualization technique for the task at hand.

4.4 Interactive (and) 3D depiction: mainly in research

While 2D visualization techniques dominate forecasting environments, 3D displays are used in rare occasions. For example, KNMI has developed *Weather3DeXplorer* (W3DX) [148], a 3D visualization framework based on the *Visualization Toolkit* (VTK, [149]). W3DX is used at KNMI to explore

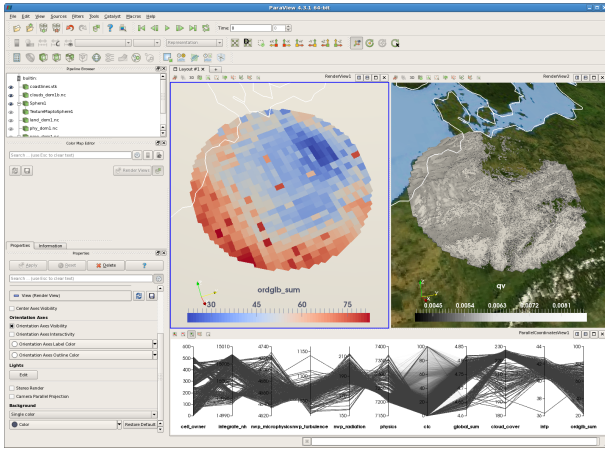


Fig. 12. For the development of numerical models, visualization of the data on its original model grid is very important. Side-by-side visualizations of atmospheric variables along with simulation performance data can be used for debugging and optimization. This example, created with ParaView, shows (left view) load balance inefficiencies for the 512 processors used, along with (right view) simulated specific humidity.

operational NWP models using immersive stereo projection of, e.g., isosurfaces and path lines. 2D and 3D model data can be visualized with radar and satellite observations and ground-based measurements [150] for comparison. W3DX is used in the operational weather room for forecaster briefings and in research settings to study model behavior during severe weather events [151]. The W3DX website [148] lists a number of examples and presentation videos. In addition, a number of projects have conducted feasibility studies to evaluate the value of 3D techniques in forecasting. We survey these visualization studies in Sect. 5.2.

In meteorological research, 3D visualization is more frequently used than in operational forecast environments, though from our experience still much less than 2D. As stated in Sect. 3, Vis5D was the first popular and widespread tool in the 1990s, widely used into the 2000s. More recently, prominent tools include the *Integrated Data Viewer* (IDV), *Vapor*, and the general-purpose tool *ParaView*.

Besides their work on Vis5D, Hibbard et al. in the early 1990s started work on the *Visualization for Algorithm Development* (VisAD) library [69], [152], with the goal of simplifying the visualization of multiple heterogeneous data types. The VisAD Java implementation [153], [154] has become the basis for a number of meteorological visualization tools [155], in particular, the Unidata IDV [156], [157] and the latest version of McIDAS [158]. IDV, for example, supports a variety of 2D and 3D visualization methods similar to Vis5D, as well as basic ensemble techniques (e.g., spaghetti plots) and meteorological charts including vertical soundings and observation plots. IDV provides 3D stereo support and a “fly-through” option. For example, Yalda et al. [159] used IDV’s 3D capabilities for interactive immersion learning.

Vapor [161], [162] is an open-source 3D visualization software developed by NCAR. A recent example of its use is shown in Fig. 13, reproduced from Orf et al. [160], [163], who investigated a tornado embedded into a supercell thunderstorm. *Vapor*’s visualization techniques include, e.g., 3D isosurface and volume rendering (cf. Fig. 13), 2D color mapped planes, steady and unsteady flow lines, and 2D

Fig. 13. Example of a visualization created with Vapor, showing a tornado embedded within a supercell thunderstorm. (Reprinted from [160, p. 33], © 2016, with permission from Elsevier.)

contour lines. A particular feature is a wavelet-compressed data format [161], [162], [164], allowing progressive access to multiple resolution levels of the data and enabling the user to switch to a coarser, compressed version at runtime. For high-resolution datasets whose size surpasses the available memory, subregions can be selected and the full resolution be loaded for the subregion only. Currently, all data in Vapor are assumed to arise from a single numerical experiment (i.e., comparative visualization of multiple datasets as required, e.g., for ensemble visualization, is not possible), and there is a restriction to structured, regular grids (although the grid spacing need not be uniform). A current development effort opens Vapor to unstructured grids [165].

On a broader scope, the general-purpose visualization tool *ParaView* [166], [167] can be used to display meteorological data, providing additional techniques, for example, for interactive visual analysis including brushing and linking. For instance, Dyer and Amburn [168] investigated how ParaView can be used in a graduate meteorology course. While not specifically designed for meteorological data, ParaView supports some meteorological data formats. For example, DKRZ has developed a reader for unstructured ICON output and simulation performance data that can be used to study not only the atmospheric variables but also the efficiency of the simulation [169]. An example is provided in Fig. 12. A tutorial on the use of ParaView for visualizing climate datasets has been published by DKRZ [170].

Further open-source general-purpose visualization tools are also applied (e.g., *OpenDX*; cf. Sect. 3), however, commercial 3D visualization codes are rarely used in atmospheric research. Notably, *Avizo* [171] (formerly *amira*) in its “climatology profile” is regularly used at DKRZ for the visualization of climate simulations (cf. the DKRZ tutorial [172]). For instance, Röber et al. [173] used Avizo to visualize the output of a small-scale simulation covering the city of Hamburg. Avizo was also used in a recent case study by Theußl et al. [174], who presented several visualizations of a simulated cyclonic storm over the Arabian Sea. Virtual-globe-based visualization has also been applied, for instance, to visualize severe weather products [175] and satellite and sounding data [176], [177], to volume-render typhoon simulations [178], and to analyze the dispersion of volcanic ash and possible encounters with aircraft [179]. Sun et al. [180] discussed usage of virtual globes for climate research, and Wang et al. [181] integrated a microscale atmospheric model to visualize flow over complex terrain.

5 VISUALIZATION RESEARCH

Many aspects of meteorological visualization have been investigated in the visualization community to advance the state of the art in the application domain surveyed in Sect. 4; our objective for this section is to provide an overview of techniques that are not yet commonly used in meteorological practice. Our selection of articles is based on research that either directly targeted a visualization challenge in meteorology, or that included a predominant case study that illustrates the application of a proposed method to meteorological data. For instance, a number of studies used a dataset of *Hurricane Isabel*, a WRF simulation that was first used in the IEEE visualization contest 2004 [182]. In the following, we survey the literature in an annotated-bibliography style. For each of the categories used to summarize the state of the art in Sect. 4, Table 1 lists visualization topics that have been investigated in the literature. Links are provided to the subsections in this section (an overview of which is given in Fig. 1c), references to individual studies are given in the text. Note that for each of these topics there is already a significant volume of published literature that has not focused on atmospheric data. We point out overview articles where applicable.

5.1 Display design

The design of a meteorological visualization is crucial to the human ability to comprehend the displayed data and to build a mental model thereof [19], as manifested in a number of studies that give advice on how to make meteorological maps and that investigate cognitive issues of how specific visualization elements are perceived. For example, advice on how to use color in meteorological maps was given by Hoffman et al. [183], Teuling et al. [184] and, recently, Stauffer et al. [185]. Stauffer et al. discussed the use of the perceptual linear hue-chroma-luminance (HCL) color space in meteorology, emphasizing benefits including better readability and more effective conveyance of complex concepts, but also noting the importance of considering the specific task at hand for choosing effective colors. Further specific guidance in meteorological map making, in particular with respect to mapping uncertain variables, was provided by Kaye et al. [186] and Retchless and Brewer [187]. For instance, the latter study evaluated how combinations of color and pattern can be used to map climate change parameters with uncertainty. Dasgupta et al. [188] evaluated maps and further visualizations created by climate scientists, identifying a number of issues and offering improvements. They provided a list of design guidelines, discussing, amongst others, color and visual saliency. Studies from the cognitive sciences and human-machine interaction have also addressed meteorological issues (for a general overview on implications of cognitive science research for the design of visual-spatial displays we refer to [189]). For example, Hegarty et al. [190] investigated the effects of salience of the depiction of specific forecast variables on a weather map on typical inference tasks. They noted that weather maps should be designed to make task-relevant information salient in a display. Trafton and Hoffman [11] suggested improvements to meteorological visualizations and tools, based on notions of human-centric computing. Bowden et

Fig. 14. The improved wind barbs approach by Pilar and Ware [199]. A wind field depicted by (a) traditional wind barbs and (b) a combination of stream lines and wind barbs. Small structures in the wind field that are missed by the visualization in (a) are captured in (b). (Reprinted from [199], © 2013 IEEE. Used with permission.)

al. [191] argued for increased usage of eye tracking as a method to study forecaster’s cognitive processes when viewing meteorological displays. They studied a forecaster’s eye movements during the interpretation of precipitation radar maps, showing that attention was put on different parts of the display depending on the weather scenario.

A number of studies investigated display design with respect to visualizing atmospheric flow, e.g., considering vector glyphs, streamlines, and flow texture representations (e.g., [192], [193], [194]). Publications date back to suggestions to improve wind rose displays in the 1970s [195], [196]; a recent example is Martin et al. [194], who conducted a study investigating the user’s ability to determine magnitude and direction of a wind field from wind barbs. They found, e.g., that their observers had a tendency to underestimate wind speed in particular when asked to determine the average velocity over an area. Ware and Plumlee [197] investigated how 2D weather maps displaying three or more variables can be improved. Alternative approaches to depict the wind vector field and multiple scalar variables were explored, using static and animated displays with different color, texture, and glyph schemes to target distinct perceptual channels. Ware and Plumlee [197] evaluated their approaches with a user study, noting, for instance, the effectiveness of a wind depiction by animated particle traces (in this respect, cf. Beccario’s web implementation [198]). Fig. 14 shows results from Pilar and Ware [199], who investigated how the 2D display of streamlines and wind barbs can be improved. In their work, wind barbs (and alternatively arrow glyphs) are placed along streamlines to combine advantages of both approaches to visualize the flow field. The streamlines achieve a better spatial sampling of the flow, capturing small scale structures sometimes missed by regularly placed wind barbs. They also have the advantage of everywhere being tangential to the flow (which wind barbs are only at their tip). Yet, the approach by Pilar and Ware [199] maintains the advantages of a glyph-based depiction of flow velocity and direction; also, the “traditional” wind barb depiction that meteorologists are used to is maintained (Fig. 14b).

5.2 3D visualization in forecasting

Sect. 4.4 presented options that meteorological visualization tools offer with respect to 3D rendering. As noted, 3D visualization is used more often in atmospheric research than in forecasting, however, in both forecasting and research

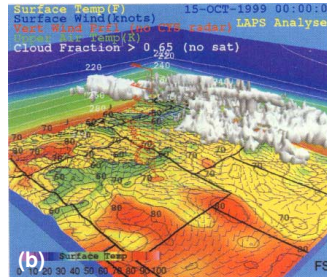


Fig. 15. (a) The 3D forecasting tool presented by Treinish et al. [200], [201], [202], based on the then-commercial IBM Data Explorer. (Reprinted from [202], © 1998 IEEE. Used with permission.) (b) Screenshot of the D3D forecasting tool built in the late 1990s at the U.S. Forecast Systems Laboratory, as presented by McCaslin et al. [203]. The tool was based on Vis5D (cf. Fig. 4), however, featured a different user interface that matched the interface of the 2D AWIPS D2D software in use at the NWS Weather Forecast Offices. (Reprinted from [203]. Courtesy of P. T. McCaslin, P. A. McDonald, and E. J. Szoke.)

much less than 2D visualization. With respect to forecasting, a number of projects have conducted feasibility studies on using 3D visual mappings, investigating whether 3D visualization can be of advantage in the weather room.

Treinish and Rothfus [200], [201], [202] reported on experiments during the 1996 Olympic Games in Atlanta. A forecast visualization tool based on the IBM Data Explorer [76] was designed, a screenshot of which is shown in Fig. 15a. The tool offered visualization functions similar to Vis5D (including 3D isosurfaces and volume rendering, 2D filled and line contours, wind vectors, a probe for vertical profiles). Functionality for different visualization tasks was separated into “classes” of sub-tools, each featuring specialized methods for data exploration, analysis, and communication [202]. Treinish [202] described a typical workflow of the system, focused on first interacting with the visualization to select a suitable combination of forecast variables, then creating a time animation of the selected scene. Treinish and Rothfus [201] concluded that an advantage of their 3D methods was the elimination of interpreting numerous 2D images, helping mental model building (cf. Sect. 2.1) by making conceptual models “*immediately obvious*” in 3D.

At the same time, Schröder, Lux, Koppert et al. [16], [72], [204] presented RASSIN (also named *VISUAL*), a 3D forecasting system for usage within DWD. Focus was put on visualizing directly from the rotated grid and terrain-following vertical coordinates of a DWD model. Similar to the approach by Treinish and Rothfus [201], RASSIN provided functionality to display 2D sections and 3D isosurfaces. Discussing an operational test of the software, Koppert et al. [16] pointed out the importance of system performance for user acceptance, and highlighted the need for common concepts of operations (user interface, workflow) when forecasters are asked to transition from a 2D to a 3D environment. On the same software basis, the system *TriVis* for media usage was developed [205], [206], [207].

Around 2000, McCaslin, Szoke et al. [203], [208] presented *D3D*, a 3D software built at the U.S. Forecast Systems Laboratory (FSL) on top of Vis5D. To ensure common concepts of operation, the Vis5D user interface was rewritten to match that of the 2D *AWIPS D2D* software already in use at the NWS Weather Forecast Offices (WFOs). Szoke et al.

[208] provided an overview of the tool’s functionality. *D3D* provided a more extensive array of visualization methods than the approaches by Treinish et al. and by Schröder et al., including 3D isosurfaces and volume rendering, 2D horizontal and vertical sections, vertical soundings and data probes, and trajectories. Fig. 15b shows an example. Notably, “real-time forecast exercises” were conducted to evaluate the value of 3D visualization. Case studies were presented, including usage of *D3D* for the examination of tropical cyclones [209], the usage of 3D trajectories [210], and the analysis of the synoptic situation during a tornado outbreak [211]. Szoke et al. [212] reported reluctance of forecasters to switch from 2D to 3D, but also stated that forecasters trained with *D3D* found forecast analysis in 3D more effective, e.g., by reducing the chance to miss a critical feature by not examining the ‘correct’ 2D level. Szoke et al. [212] pointed out problems with spatial perception, an issue they approached with a switch to toggle an overhead view, as well as with a vertically movable background map that could be elevated to the height of an isosurface. They also positively reported on the interactivity introduced by their system. Interactively moveable vertical soundings and cross sections, for example, were very well perceived by the forecasters [212]. Szoke et al. [212] concluded that there needs to be training in how to best use 3D depiction in forecasting, and suggested to teach university courses with 3D visualization, in order to make the next generation of meteorologists familiar with the concepts.

Recently, Rautenhaus et al. [22], [213] presented the open-source forecast visualization tool *Met.3D*, developed in the context of weather forecasting during aircraft-based field campaigns. Fig. 16 shows example visualizations. *Met.3D* combines interactive visualization similar to *D3D* with ensemble visualization; the tool supports GPU-accelerated 2D horizontal and vertical sections as well as 3D rendering. In particular, the system closely reproduces the look of 2D sections of the DLR MSS [133] (cf. Sect. 4.3), thereby aiming at the creation of a “bridge from 2D to 3D” to achieve acceptance with forecasters trained with the 2D MSS (Fig. 16; cf. [18], [22]). *Met.3D* introduces a number of state-of-the-art computer graphics techniques to the meteorological application, e.g., 3D spatial perception is increased by the usage of shadows and vertical poles (Fig. 16a). The system’s ensemble support enables the user to animate through the ensemble members and to display ensemble statistics that are computed on-the-fly from the input data (e.g., mean and standard deviation; Fig. 16b). Rautenhaus et al. [214] applied *Met.3D* to forecasting Warm Conveyor Belt features (airstreams in extratropical cyclones) and presented a detailed case study of how interactive 3D ensemble visualization can be applied to practical forecasting. Recent information can be found on the project website [215].

5.3 3D volumetric rendering

Visualization research has considered various further aspects of 3D rendering applied to atmospheric data. For example, a case study demonstrating the use of multi-dimensional transfer functions for rendering multivariate 3D weather simulations on Cartesian grids was conducted by Kniss et al. [216], and a number of different rendering options for meteorological data including rainfall and clouds

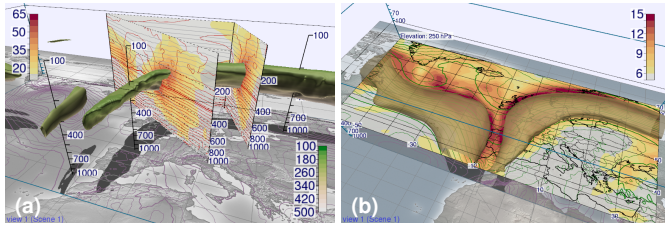


Fig. 16. ECMWF ensemble prediction data visualized with Met.3D [22], illustrating combined 2D and 3D visualization and the tool's ensemble support. (a) An interactively movable vertical section using color mapping (wind speed) and contour lines (potential temperature) is rendered with a wind speed isosurface showing the jet stream. Spatial perception is improved by shadows and vertical poles. (b) An isosurface of ensemble mean wind speed is augmented by a horizontal section showing wind speed standard deviation. (Reprinted from [22], © Author(s) 2015. CC Attribution 3.0 License.)

have been presented by Song et al. [217]. They discussed resampling issues for the handling of different model grids as well as data-dependent rendering options. Arthus et al. [218] presented an approach using 3D visualization to analyze campaign observations, and Berberich et al. [219] implemented GPU-based direct volume rendering techniques via VTK and OpenGL to visualize hurricane simulations. They conducted a user study to compare the effectiveness of direct volume rendering techniques and isosurface rendering, noting that their users preferred direct volume rendering. 3D visualization was also investigated with respect to virtual reality environments [67], [220], including a virtual workbench for the analysis of cumulus clouds simulated by LES models [221] and usage of immersive virtual reality visualization for teaching in meteorology classes [222], [223]. Recently, Helbig et al. [224], [225] designed *MEVA*, a system using tools including ParaView and the *Unity* game engine to enable the exploration of heterogeneous data using multiple 3D virtual reality devices. In a case study, *MEVA* was applied to create 3D visualizations of WRF simulations of a supercell thunderstorm and to compare model output at different resolutions and observations.

Realistic rendering of simulated and observed clouds has not commonly been used for meteorological analysis, except for radiative-transfer-based methods to generate synthetic satellite imagery from NWP output (cf. Sect. 4.1). Meteorological applications have mainly relied on isosurfaces (cf. Figs. 3 and 15) and volume rendering (cf. Figs. 4 and 13). In visualization, early texture-based approaches were proposed in the 1980s by Gardner [226] and Max et al. [227], [228]. Physics-based rendering of cloud data was investigated by Riley et al. [21], [229], [230], who devised optical and illumination models based on extinction and scattering of simulated cloud particle properties. They discussed the rendering of optical effects including backscatter glory and rainbows [230] and applied the methods to WRF simulations [21]. Ueng and Wang [231] used splatting of 2D billboards in combination with precomputed lightmaps to render clouds from Doppler radar data. Note that, however, the physical parameters most relevant for a realistic visualization of a cloud (e.g., droplet size distributions to compute correct scattering) are not resolved by most atmospheric models (except for specific small-scale simulations)

and need to be parametrized, imposing limits on achievable realism. Cloud rendering has, however, been used for public media visualization. Trembilski [232] addressed the realistic synthesis and rendering of clouds, and Hergenroether et al. [233] presented an interpolation scheme to achieve smooth animation from a discrete set of time-varying clouds. Also, real-time cloud rendering has been studied for applications including computer games and flight simulators. Examples include the studies by Dobashi et al. [234], [235] and Harris et al. [236], [237], who introduced cloud billboards and particle-based simulation of first-order scattering events in clouds. Hufnagel and Held [238] summarized the state of the art in this field.

5.4 Flow dynamics

Flow visualization techniques including wind barb and arrow glyphs, and streamlines are accessible to meteorologists as surveyed in Sect. 4; path lines (in meteorology referred to as trajectories) are usually computed using Lagrangian particle models (cf. Sect. 2.2; e.g., [82]). Many advanced techniques have been proposed in the visualization literature (cf., e.g., [239], [240]), however, only few directly targeted atmospheric data (e.g., [241], [242], [243], [244], surveyed below). More frequently, flow visualization studies use an atmospheric dataset as one of multiple examples. A complete list of these papers is outside the scope of this survey, but we provide links to topics that in our opinion are of interest to the meteorological community.

For instance, visual analysis of stream and path line datasets is of interest when compared to Lagrangian analysis in meteorology (e.g., see Sprenger and Wernli [82], where importance criteria are used to select air parcel path lines to detect regions and processes of relevance to the analysis). For example, Kendall et al. [245] used an approach related to Sprenger and Wernli [82] to visualize flow features based on query trees that describe the geometry of integral lines by means of combined criteria. They integrated their method into a scalable visual analysis software and applied it to atmospheric and oceanographic datasets. The Hurricane Isabel dataset was used by Edmunds et al. [246] for automatic stream surface seeding and by Guo et al. [247], who proposed an approach to improve brushing-and-linking techniques for path line rendering. Distances between data samples at the positions of advected particles are projected into 2D space for feature identification and selection; the method is applied to two atmospheric simulation examples. The aspect of analyzing scale interactions for tropical cyclone formation was discussed by Shen et al. [248], [249]. In their study, opacity is used to control streamline transparency at different heights to visualize scale interactions, e.g., between the outflow of Hurricane Katrina and the jet stream. As an alternative to Lagrangian flow visualization, Maskey and Newman [244] investigated the use of directional textures for visualizing atmospheric data. A conducted user study suggested the usefulness particularly for multivariate weather data.

The usage of animation to achieve dynamic flow visualization has been investigated in 2D by Jobard, Lefer et al. [250], [251], [252]. Lefer et al. [251] used a so-called *Motion Map* to animate a dense set of colored streamlines, Jobard

and Lefer [250] discussed challenges to update evenly-spaced streamlines when animating over time-varying wind fields. Jobard et al. [252] animated arrow plots. In 3D, the potential of GPU particle tracing to interactively visualize time dependent climate simulation data was examined by Cuntz et al. [241]. The article focuses on technical aspects, discussing, e.g., the method's performance with respect to GPU computational power and bandwidth. Investigating a different animation aspect, Yu et al. [253] studied automatic storytelling. Their method automatically computes a suitable camera path to generate animations of time-varying datasets and is applied to the Hurricane Isabel dataset.

Finite-time Lyapunov exponent (FTLE) fields and Lagrangian coherent structures (LCS) can be used as a tool to study the transport behavior of unsteady flow (meteorological examples include [254], [255]). Discussing a complete meteorological analysis of Hurricane Isabel, Sapsis and Haller [256] used 3D visualizations of *inertial* LCS (ILCS). They depict attracting and repelling ILCS and demonstrate by comparison with conventional meteorological fields how the structures can be used to identify, e.g., the eyewall of the hurricane. Recently, Guo et al. [257] extended the FTLE and LCS concepts to uncertain data (cf. Sect. 5.7), applying their method to weather forecast data. Using a different quantity, but also derived from temporal changes in 3D simulation data, Jänicke et al. [258] presented a method based on local statistical complexity to identify regions with anomalous temporal behavior. Applying the method to climate simulation data, they compared their measure to temperature anomalies computed from long-term time series, finding that they were able to detect comparable regions.

5.5 Feature-based visualization

Methods for feature detection and tracking are used in operational forecasting as summarized in Table 1; in atmospheric research, a primary application is statistical data analysis (cf. Sect. 4.1). In visualization, feature tracking has been widely used for general flow visualization [259]. Meteorological applications include the studies by Griffith et al. [260] and Heus et al. [261], who investigated the tracking of cumulus clouds simulated by an LES model. They embedded feature tracking based on connected components into a virtual reality environment, allowing the user to select the cloud to be tracked using a virtual workbench [221]. Also investigating clouds, vortex detection methods were applied by Orf et al. [262] to detect and track features in simulated 3D supercell thunderstorms. Recently, Doraiswamy et al. [242] presented a visualization framework to track cloud movements via computer vision techniques applied to satellite images. The authors used computational topology and optical flow techniques to analyze the multi-scale characteristics of tropical convective phenomena, visualizing the envelopes of cloud clusters and movement directions of individual clouds. In a similar line, Peng et al. [263] reported on a GPU-accelerated approach for tracking features represented by labeled regions in imagery datasets that largely exceed GPU memory. They illustrate their method with a large precipitation radar dataset, tracking regions where precipitation exceeds a defined threshold. Further examples include Lee et al. [243], who track events of the

Madden-Julian Oscillation in a climate simulation, depicting the results in a GoogleEarth based display, and Caban et al. [264], who introduced a feature-tracking method based on textures to visualize dynamic changes in volumetric data and track features in simulations of Hurricanes Bonnie and Katrina. Critical-point-based flow field visualization was investigated by Wong et al. [265], who introduced a technique based on vorticity to eliminate “less interesting” critical points from atmospheric simulations. In a typhoon simulation, they detected features characterized by strong shear and circulation and represented potential locations of weather instability. Recently, Kern et al. [266] presented a 3D method to detect and visualize jet-stream core lines in atmospheric flow.

5.6 Data comparison and fusion

Comparison of atmospheric data is a frequent challenge both in operational forecasting and research (cf. Sect. 2). Tasks include comparing the same quantity but from different sources (e.g., the evaluation of numerical models with observations or the comparison of different numerical models), as well as the comparison of structures in different fields (e.g., temperature to humidity). A closely related task is the fusion of data from heterogeneous sources (often multimodal and partially incomplete) to obtain a coherent picture of the atmosphere. There are approaches to data fusion in forecasting (e.g., [267]), also, the 2014 IEEE Visualization contest (analysis of volcanic ash dispersion by visualizing data from multiple sources [182]) provides a representative example.

Comparison has also been addressed in the visualization community (for general references see [268], [269, Ch. 28]), with studies targeting comparison on data, image, and feature levels [270]. Only few studies, however, have explicitly considered meteorological data. For example, Nocke et al. [147] discussed the challenges of comparative visualization of climate related model output and introduced the *SimEnvVis* framework to reduce obstacles for atmospheric researchers to use unfamiliar visualization techniques. With respect to model comparison, Poco et al. [271], [272] proposed interactive visual analysis (IVA; cf. Sect. 5.8) methods to compare the output of climate models based on coordinated multiple views and a proposed “visual reconciliation” workflow. The user interacts with linked views of abstract similarity measures and data displays to iteratively explore model similarities. The system has commonalities with approaches from the meteorological community. Here, an example is *ESMValTool* [45], a script-based system designed to evaluate climate models with observations based on a large number of diagnostics and performance metrics. Visualizations generated by the tool, however, are currently created with standard software discussed in Sect. 4.3 (e.g., NCL), and are static. With respect to model evaluation, Wang et al. [273] proposed a feature-based comparison method to verify precipitation forecasts. They used Gaussian mixture models to extract rain bands from observations and forecast data and use coordinated views for comparison.

The comparison of multiple fields is in the most simple way approached by the overlay of, e.g., color, contour lines, and glyphs. Also, statistical approaches can be used to

wind field simulations, including improved strategies for streamline seeding based on vector field filtering.

5.7 Ensemble visualization

The demands of meteorologists with respect to analyzing ensemble datasets have in recent years provided much motivation for visualization studies. From the visualization point of view, ensemble visualization is part of uncertainty visualization, a topic that has received significant attention [35], [36], [282], [283], [284], [285]. Irrespective of the application domain that uses ensemble visualization, Obermaier and Joy [286] classified ensemble visualization tasks into two categories, *location-based methods* and *feature-based methods*. The two concepts directly map to ensemble visualization techniques used in meteorology. Location-based methods aim at visualizing properties of an ensemble at fixed locations, with examples including maps of mean and standard deviation (Fig. 7) and EFI maps (Fig. 8). Feature-based techniques, on the other hand, focus on comparative visualization of features extracted from the individual ensemble members. Examples include spaghetti plots of contour lines (Fig. 7) and frontal features (Fig. 11).

A number of recent visualization studies have been published with direct reference to meteorology. The depiction of uncertainty is also of high importance for communication and decision making; several studies have been published in this respect as well. For instance, Nadav-Greenberg et al. [287] investigated the effect of visualizations on understanding and use of uncertainty in wind speed forecasts in decision making; Savelli and Joslyn [288] studied the effect of visualizing predictive intervals of temperature forecasts for communication purposes. The articles by Kaye et al. [186] and Retchless and Brewer [187], providing advice on representing and communicating uncertainty on meteorological maps, have been surveyed in Sect. 5.1. For further links with respect to communication, we refer to Stephens et al. [12], who link uncertainty communication methods from weather forecasting to climate change communication.

With respect to data analysis, a topic subject to a number of studies has been the design of alternative depictions of spaghetti plots. For example, Whitaker et al. [289] and Mirzargar et al. [290] generalized boxplots to *contour boxplots* and *curve boxplots* as alternatives to spaghetti plots. As shown in Fig. 18a, their figures highlight the median contour line and show percentiles and outliers of the original ensemble of contours or tracks. Similarly, Sanyal et al. [291] enhanced spaghetti plots by glyphs and confidence ribbons to highlight the Euclidean spread of 2D contour ensembles. Ferstl et al. [292] clustered 2D and 3D streamlines, path lines, and feature tracks. They visualized the results as 2D and 3D lobes that show a median line and the variability of the lines in the cluster (*variability plots*). Fig. 18b shows an extension of the method to arbitrary contour lines, presented by Ferstl et al. [293], [294]. Contour lines were clustered for individual time steps as well as for time-dependent data, visualizing stacked plots that display the temporal development of the clusters (i.e. forecast scenarios) in a single view [294].

Both Mirzargar et al. [290] and Ferstl et al. [292] applied their method to the depiction of 2D hurricane track ensembles, an application that has received attention by a number

Fig. 17. Topology-based segmentation for data fusion, as proposed by Kuhn et al. [278]. The method fuses data from different atmospheric observations and simulations; this example shows data from the 2014 IEEE Visualization contest [182]. (Reprinted from [278, p. 44], © 2017 Springer International Publishing AG. With permission of Springer.)

compute similarities (e.g., in a simple form the correlation coefficient) [37]. With respect to overlay, Tang et al. [274] have investigated the use of textures to overlay multiple parameters of climate data. Similarity measures for comparing meteorological data have been used in a number of studies [275], [276], [277]. Jänicke et al. [276] proposed a local statistical complexity measure. They showed that it is able to highlight regions of high spatio-temporal variability in an overlay plot of simulated wind and evaporation, in which structures are otherwise hard to discern. Similarly, Nagaraj et al. [277] presented a gradient-based local comparison measure that is able to highlight, for instance, frontal structures. A correlation measure combined with a proposed “multifield-graph” was used by Sauber et al. [275]. Analyzing the Hurricane Isabel dataset, they demonstrated how the approach allows to quickly identify fields and regions with strong correlation.

A data fusion task has recently been posed in the context of the IEEE Visualization 2014 contest. The works by Günther et al. [279] and Elshehaly et al. [280] presented solutions that fill spatio-temporal gaps between multiple satellite observations and trajectory model output. Notably, Elshehaly et al. [280] proposed a GPU-accelerated workflow incorporating expert knowledge in an interactive process to fill gaps in the data and to provide a coherent view of the atmospheric processes. Fig. 17 shows a result of Kuhn et al. [278], who approached the contest dataset with topological methods, extracting structures in the data that allow for clustering and comparison. For example, the temporal evolution of extremal structures is detected via segmentation and displayed in a space-time graph; Fig. 17 shows the temporal evolution of detected volcano eruption events. Related to data fusion is *seamless prediction* (cf. Sect. 2.2). Visualization of such multi-scale data (cf. [269, Ch. 28]) has been addressed in for atmospheric data by Shen et al. [249] and Treinish [281]. For instance, Treinish [281] discussed flow visualization and stream line seeding for multi-resolution

(a) (b)

Fig. 18. Alternatives to spaghetti plots recently suggested in the literature. (a) Whitaker et al. [289] proposed a generalization of box plots (cf. Fig. 10) to contour lines. (Reprinted from [289], © 2013 IEEE. Used with permission.) (b) Ferstl et al. [293] clustered an ensemble of lines and produced “variability plots”, depicting for each cluster a lobe that represents the variability of the cluster’s lines around a medium line. (Reprinted from [293], © 2016 The Author(s). © 2016 The Eurographics Association and John Wiley & Sons Ltd. Used with permission.)

of further studies (also with respect to communication). For instance, Cox et al. [295] proposed an alternative display to the official National Hurricane Center error cones. Based on the current ensemble prediction and historical tracks, they produce synthetic hurricane tracks that dynamically appear and fade out. A user study confirmed that users were better at estimating the hurricane strike probability at a given location. The method was further developed by Liu et al. [296], who used the storm tracks generated to estimate a time-dependent likelihood field for hurricane risk, allowing the user to view a time animation of a risk ellipse encoding different risk values. In a subsequent study, the authors approached the issue of larger risk ellipses being misinterpreted as larger size or strength of the hurricane [297], evaluating display alternatives based on subsampling hurricane positions. Ruginski et al. [298] further evaluated display alternatives including the method by Cox et al. [295] with a non-expert user study.

Further studies investigated methods aimed at IVA of ensemble prediction data. Potter et al. [299] investigated the usage of multiple linked 2D views, concluding that the combination of standard statistical displays (spaghetti plots, maps of mean and standard deviation) with user interaction facilitates clearer presentation and simpler exploration of the data. Similarly, Sanyal et al. [291] highlighted the positive effect of interactivity and linked views on the user. Recently, Quinan and Meyer [300] proposed *WeaVER*, an interactive tool to support meteorological analysis of ensemble data. *WeaVER* supports standard location-based techniques as well as interactive spaghetti plots, allowing the user to highlight selected contour lines in order to decrease visual saliency of other members’ contours. Quinan and Meyer [300] also employed the contour boxplot technique [289], obtaining positive feedback about the technique from collaborating meteorologists. An approach using interactive brushing and linking to analyze ensembles of scalar fields was presented by Demir et al. [301]. By providing a combination of diagram techniques in a “multi-chart”, they enable the user to interactively explore visual summaries of ensemble properties at different regions and at different solutions. Demir et al. [301] provided examples from the analysis of an ECMWF forecast. A similar approach was presented by Höllt et al. [302], who used linked views to facilitate

the interactive exploration of height field ensembles from ocean forecasts. Recently, Wang, Biswas et al. [303], [304] proposed methods to investigate ensembles generated by varying spatial resolution and convective parametrization parameters in the WRF model. Wang et al. introduced a *Nested Parallel Coordinates Plot* to investigate parameter correlations, Biswas et al. approached the sensitivity and accuracy of simulated precipitation to input parameters influencing the parametrization and to model resolution. They combined abstract views displaying statistical quantities from, e.g., multi-dimensional scaling and clustering techniques with map views, and described a number of meteorological findings made with the technique by a collaborating atmospheric scientist. Kumpf et al. [305] presented an interactive approach to cluster ECMWF ENS forecasts, focusing on visualization of the robustness of the clustering result with respect to slight changes in the used data region. Specific to forecasting during atmospheric field campaigns, Rautenhaus et al. [214] proposed an interactive method to predict and visualize in 3D an occurrence probability for Warm Conveyor Belt features, using Lagrangian particle trajectories for feature detection and transparent isosurfaces for probability visualization. The method is integrated into Met.3D (cf. Sect. 5.2), thereby achieving interactive combination with further ensemble display methods. Recently, Demir et al. [306] approached the challenge of rendering an ensemble of 3D isosurfaces by displaying a mean isosurface surrounded by a spaghetti plot of silhouettes of the individual members’ surfaces.

With respect to 1D series of scalar data, Potter et al. [307] discussed variations of box plots that, compared to the classic version (cf. Fig. 10), convey additional information on the depicted probability distribution. They proposed enhanced plots depicting joint summaries of the distributions of two parameters, showing joint data series of ensemble predictions of temperature and humidity. Lampe and Hauser [308] used a generalization of kernel density estimates to create smooth depictions of probability information along time series (applying their technique to temperature time series). With respect to comparing *entire ensembles* to each other, Köthür et al. [309] proposed a correlation-based approach to visually compare time series of multiple ensembles of paleoclimate data.

In addition to the (mostly 2D) spaghetti plot alternatives discussed above, further work has investigated the depiction of uncertain 2D and 3D isocontours from both parametric and nonparametric uncertainty models (also cf. references listed in [310]). Here, examples with relation to meteorology include the drawing of uncertainty bands, fuzzy and random 2D contours [284], [311] and the usage of kernel density estimates [310]. Pfaffelmoser and Westermann [312] investigated how visual ambiguities in spaghetti plots can be prevented. In 3D, normals on 3D isosurfaces have been used as “3D error bars” [313], [314], and probabilistic rendering approaches have been investigated to depict the positional uncertainty of 3D isosurfaces [313], [315], [316]. Pfaffelmoser et al. [317] have proposed a glyph-based approach to depict the uncertainty of gradients in 2D scalar fields, revealing regions in which isocontours of an ensemble temperature forecast are stably oriented.

Methods to investigate the topological structure of un-

certain forecasts were recently proposed by Mihai and Westermann [318] and Liebmann and Scheuermann [319] and applied to temperature field ensembles from ECMWF forecasts. For instance, Mihai and Westermann [318] analyzed the stability of critical points, proposing summary maps that show how stable critical points are with respect to location and type. The modality of forecast distributions was subject of an article by Bensema et al. [320], who classified simulated temperature fields of a 50-member ensemble climate simulation according to its modality, in particular highlighting the stability of bimodal regions.

With respect to vector field ensembles, glyphs have been used to display, e.g., uncertainty in wind fields [321]. Jarema et al. [322] performed a local clustering of wind directions of ECMWF wind fields. They displayed the results using glyphs per grid point (similar to the wind roses in Fig. 10 but indicating the modality of the local distribution). The depiction of uncertain trajectory data has been investigated by Boller et al. [323]. Considering uncertainty stemming from the numerical advection scheme used to compute trajectories, they map uncertainty to line thickness. Further approaches to visualizing ensemble trajectories to reveal differences in the ensemble's flow fields were presented by Guo et al. [324] and Ferstl et al. [292]. For instance, Guo et al. [324] used a Lagrangian metric to specify the distance between path lines computed from the ensemble members' wind fields, an improvement of which was recently described by Liu et al. [325], who used longest common subsequences to measure path lines distance. Results are visualized, e.g., via 3D volume rendering. Guo et al. [257] also investigated uncertain FTLE and LCS methods to analyze transport behavior in time-varying uncertain forecasts.

5.8 Interactive visual analysis

Meteorological analysis almost always builds on the combination of multiple views on a dataset. IVA techniques [326], [327] add the ability to interactively emphasize data subsets in multiple-view displays. ParaView, as shown in Fig. 12, provides support for some IVA techniques that can readily be applied by meteorological researchers. Also, visualization experts at institutions including DKRZ have applied the SimVis framework [326] to climate research [328]. Nevertheless, IVA techniques are largely unknown to atmospheric researchers. Tominski et al. [329] conducted a survey with 76 participants to evaluate the application of IVA methods in the climate sciences. They found that state-of-the-art techniques are rarely applied.

A number of studies, however, have demonstrated the potential of applying IVA techniques to atmospheric data. In the context of the IEEE Visualization 2004 contest, Doleisch et al. [331] applied interactive brushing and linking and focus+context techniques in SimVis to the exploration of the Hurricane Isabel dataset. They showed how brushing in attribute space (i.e., the simulated parameters at the grid points) can highlight relevant features in a linked volume rendering (e.g., brushing of pressure and wind speed highlights the hurricane's eye), thereby facilitating interactive exploration of features. Fig. 19 shows an example of similar techniques used by Kehrler, Ladstädter et al. [330], [332], who used SimVis with ECMWF reanalysis and ECHAM datasets.

(a) (b) (c)

Fig. 19. Example of IVA techniques applied to atmospheric data. The geopotential height field trend of the ECMWF ERA-40 reanalysis dataset is analyzed. The turquoise rectangle in (a) brushes outliers in the time-series view (selected outliers are shown in red). Linked views immediately show where the brushed outliers are located in the (b) pressure and (c) latitude dimensions. (Reprinted from [330], © 2010 American Meteorological Society. Used with permission.)

Without employing prior knowledge of the data, the interactive visual exploration techniques in the tool were used to generate hypotheses about possible indicator parameters and regions for climate change. Similarly, Jin and Guo [333] coupled a map view with parallel coordinates and a self-organizing map to facilitate an interactive exploration of climate change patterns. Qu et al. [334] applied IVA techniques to air pollution observations from the city of Hong Kong, discussing the effectiveness of polar plots, parallel coordinates, and a graph-like display for the analysis. Diehl et al. [335] presented a web-based system using linked views designed to provide forecast visualization for meteorologists in Argentina, proposing a "minimap timeline" that uses small depictions of the plotted meteorological maps. Kerren et al. [336] proposed an interactive viewer for long climate time series. The work by Jänicke et al. [337], [338] focused on applying IVA techniques to analyze temporal variability in climate simulations. By reducing the high-dimensional attribute vectors consisting of the simulated parameters to 2D [337], they facilitated brushing and linking able to identify and visualize different seasonal patterns of precipitation changes in a climate change simulation. Also, they showed how wavelet analysis can be applied to multivariate climate simulations, facilitating a visual analysis of changes in variability due to global warming [338].

These studies are closely related to statistical data analysis methods well established in meteorology [37]. A number of visualization studies have considered how information visualization techniques can be used in the statistical analysis process, and how interactivity and graphical display can be improved. For example, Steed et al. [339], [340] approached the issue that atmospheric workflows often involve simultaneous statistical and graphical analysis and integrated an interactive parallel coordinates visualization with statistical computations. A case study of the technique's application to an analysis of North Atlantic hurricane trends showed a significant speedup of the analysis process [339]. Radial depiction of information (for a general overview see [341]) was adapted by Li et al. [342], who investigated the challenge of analyzing spatially distributed time series of atmospheric surface observations to discover climate change patterns. Further studies have considered correlation analysis [343], the application of diffusion maps to create temporally and spatially compressed depictions of NWP output [344], the adaptation of boxplots to sequences

of 2D maps and images to analyze time series of maps of climate simulation output [345], and the usage of self-organizing maps to visualize patterns in multivariate atmospheric data [333], [346]. For example, Lundblad et al. [346] proposed a technique based on self-organizing maps to reduce dimensionality of the multivariate forecast data in order to analyze clusters, and described meteorological information systems using IVA methods to provide specific forecasting techniques for ship and road traffic in Sweden [346], [347], [348]. The application of visual data mining techniques in climate sciences has also been extensively discussed by Nocke et al. [147], [349], [350]. For instance, Nocke et al. [349] discussed visualization of clusters computed in the analysis of climate simulations by means of visual analysis methods. Recently, Nocke et al. [13] provided a review of how visual analytics techniques can be applied to the study of climate networks. As is the case for the above discussed visualization topics, further studies for interactive visual statistical analysis have considered the common meteorological datasets. For example, Staib et al. [351] demonstrated an enhancement of scatterplots by multi-dimensional focal blur using Hurricane Isabel.

Recently, big-data issues of IVA techniques have been discussed. Wong et al. [352] described the application of several interactive visual analytics techniques to large-scale climate simulation output, discussing computational aspects as well as user feedback. Notably, they touch upon major challenges to facilitate visual analytics of large-scale datasets [353]. In this respect, Steed et al. [354] have approached the issue of where the data to be analyzed is physically stored and presented a web-based visual analytics framework for climate model data to minimize movements of the large data volumes. As described in Sects. 5.6 and 5.7, IVA techniques have also increasingly been applied for comparative and ensemble visualization. In this respect, Dasgupta et al. [355] have recently discussed lessons learned from a study in which IVA methods for comparative visualization have been developed (cf. [271], [272], discussed in Sect. 5.6). They argued that IVA techniques can play a key role in bridging the gap between relatively short simulation run-times and long data analysis times.

5.9 Efficient rendering

The specific grid and data topologies encountered in meteorology (cf. Sect. 2.2) pose computational challenges for rendering (see [21] for a discussion). Therefore, many existing visualization tools require data resampling to a regular grid structure (cf. Sect. 4.3). A number of studies approached the challenge of rendering nonuniform data from atmospheric models and observations. Djurcilov and Pang [356] discussed various approaches to deal with incomplete data from point measurements or sparse measurement structures, including point rendering, scattered data interpolation, and point cloud triangulation. Gerstner et al. [357] and Moreno et al. [358] discussed the generation of a multiresolution representation and the gridding of scattered observational data, respectively, and demonstrated combined volume and terrain rendering to put the observations in spatial context. Riley et al. [21] pointed out that resampling introduces grid artifacts and can increase the

required memory. They presented a GPU volume-rendering algorithm operating on the structured non-uniform grids output by the WRF model, using approximate texture-mappings. Riley et al. applied their renderer to simulations of a tornado outbreak and of Hurricane Isabel, and showed the utility of rendering 3D Doppler radar data. Also using texture-mapping, Met.3D [22] (cf. Sect. 5.2) implements visualization algorithms that can handle the vertical ECMWF hybrid sigma-pressure coordinate (cf. Fig. 2). Xie et al. [359], [360] described how the geodesic grids of modern weather and climate models can be efficiently volume-rendered by single GPUs as well as by GPU clusters. Křištof et al. [361] presented a volume rendering approach using an adaptive octree representation for operational 3D Doppler radar data. They tackled the challenge of temporal misalignment via linear interpolation in time, and used GPU raycasting to achieve interactive rendering.

5.10 Scalability and reproducibility

Continuous data growth in weather forecasting and atmospheric research (e.g., [30], [362], [363]) poses significant challenges to data processing and visualization (cf. Sect. 4.3). The computational power of computers has grown much faster than storage capacity and disk speed [363]. As a consequence, datasets increasingly need to be analyzed directly on the supercomputers and also, increasingly smaller parts of model results can be stored in a timely manner. Approaches to this challenge include remote and parallelized visualization, compression, and in-situ visualization (i.e., a part of the visualization pipeline is run within the model code; e.g., the extraction of isosurface geometry). At DKRZ, e.g., remote visualization servers integrated into the supercomputer enable users to interactively explore large data without the need to transfer data. Similarly, ECMWF follows web-based approaches (cf. Sect. 4.3).

Vapor's wavelet-based approach to data compression was described in Sect. 4.4; scientists working with general-purpose tools including Python and ParaView have access to big-data-analysis libraries developed in the corresponding communities. An example is ParaView *Catalyst*, a library for in-situ data processing and visualization for which Ayachit et al. [364] have recently demonstrated use in atmospheric modeling to significantly reduce visualization data output. In-situ capabilities have also been integrated in some numerical models; e.g., Olbrich et al. [365], [366], [367] demonstrated the in-situ extraction of isosurfaces and other 3D geometry from an LES model and facilitated interactive 3D remote visualization via streaming. Client/server-based rendering for parallel visualization is available in only few tools. ParaView, as well, can be run in client/server mode, allowing visualization of data on multiple compute nodes simultaneously. A further option for parallel rendering is the recent volume visualization technology *Index* by Nvidia [368]. It allows the use of multiple GPU nodes to visualize large time-dependent irregular volumetric datasets at interactive rates; *Index* is available as a ParaView plugin.

The *Ultrascale Visualization Climate Data Analysis Tools* (UV-CDAT) target both big-data and reproducibility issues; they have been developed as a “*workflow-based, provenance-enabled system that integrates climate data*

analysis libraries and visualization tools” [369], [370]. The approach is to couple a collection of existing domain specific and general purpose tools including Python, the *Climate Data Analysis Tools* (CDAT) [371], ParaView, and the visualization workflow and provenance system *VisTrails* [372] in a unified environment. By integrating this variety of components, users can select their favorite tools and develop workflows for reproducible visualizations.

6 SUMMARY AND DISCUSSION

Our survey has highlighted how weather and climate data are visualized in operational forecasting and meteorological research environments to suit the meteorological users’ needs, and has provided an overview of recent visualization research related to meteorology.

We briefly summarize key aspects we have identified: Heterogeneous and often large data encountered in meteorology make visualization an essential tool for the analysis of observations and numerical simulations. Current observation and simulation systems capture atmospheric processes at various spatiotemporal scales; datasets are increasingly stored on grid structures that are challenging for efficient visualization. In recent years, consideration of uncertainty has received increased attention in the meteorological community; in particular ensemble techniques gain increasing importance in predicting future weather and climate. Visualization in meteorology is dominated by 2D depictions, most of which are static. Interactive and 3D methods have received interest since the early days of computer graphics, however, challenges including perceptual issues and user acceptance have in the past delayed the use of meaningful 3D depiction. In operational forecasting, visualization tasks are largely pre-defined, allowing the design of specialized but efficient visualization techniques and systems. Here, traditional 2D meteorological maps and diagrams are the most common visualization types. In recent years, feature-based, as well as ensemble visualization methods have received increased attention. Visualization in meteorological research is more diverse and requires more flexibility. Although most research is based on scriptable data analysis and 2D plotting software, interactive and 3D visualization is increasingly encountered. Visualization research targeting meteorological challenges has covered a wide range of topics from the visualization domain, including the fields of display design, 3D visualization, flow dynamics, comparative visualization, data fusion, ensemble visualization, interactive visual analysis, efficiency, scalability, and reproducibility.

In the following, we discuss what we view to be the most important demands arising in the meteorology community that entail further visualization research in the coming years. Although overlapping in many areas, visualization demands will continue to be different in forecasting and research. In forecasting, seamless prediction systems [29] and ensemble methods can be expected to be key topics in the next decade (cf. Sect. 2). This has recently been emphasized by Bauer et al.’s [30] survey on the state of weather prediction, and is listed as a key priority in ECMWF’s current 10-year strategy [373]. Forecasting will be extended to cover smaller and larger spatiotemporal scales

than today [30]; we expect the increasing model output complexity and increasing data volumes to give rise to further automated data mining and analysis methods including, e.g., feature-based methods. Visualization techniques need to enable forecasters to effectively analyze the output of such systems. In meteorological research, visualization demands will remain to be manifold. Scientific meteorological challenges will continue to include the development and evaluation of numerical models, the analysis of observations and numerical simulations, and the analysis of uncertainties (cf. Sect. 2); technological challenges including the handling of large data volumes and the heterogeneity of data sources and modalities can be expected to even increase in the future [30], [362], [363].

We expect that visualization research will contribute much to the advancement of data analysis in meteorology in coming years. To do so, however, different types of challenges need to be approached. New methods need to be *developed* or *adapted* from other application domains, and, equally or possibly even more important, the *benefit* of using them in meteorological practice needs to be demonstrated.

Demonstration of benefit. The need for visualization research to clearly evaluate and demonstrate the benefits, strengths and limitations of any new method (cf. Johannson et al. [374]) is an important consideration. For example, a number of visual abstractions have been proposed to improve 2D spaghetti plots (cf. Sect. 5.7). Contour boxplots and variability plots, for example, show the variability range of an ensemble of lines at a glance; however, they hide small-scale detail that might be relevant to the user. For which tasks are they meteorologically meaningful? The problem becomes even more complex in 3D. As another example, a major objective of meteorological visualization is to support the generation of a mental model of the current atmospheric situation by the user (cf. Sect. 2). In this respect, further method evaluations and perceptual research will be required to determine how well proposed methods support this goal. For instance, designing an interactive visualization sketchpad as suggested, e.g., by Trafton and Hoffman [11], could improve the generation of a mental model and help in communicating this model to colleagues. Method evaluations can be user studies, and in our opinion also take the form of case studies demonstrating a method’s value by applying it to an actual meteorological research question. Both user and case studies will often encompass enough material to be studies on their own, and we would like to see more visualization researchers working together with meteorologists to incorporate new visualization methods into the meteorologists’ workflow and reporting on the added value. Such studies would increase the exchange between the meteorological and visualization communities, raise awareness and show users how novel visualization developments can have value for their work.

Availability and training. To increase impact, new techniques also need to be more easily available to meteorologists for evaluation with their own data. Most visualization tools used in meteorology are open-source (cf. Sect. 4.3). Thus, when developing a new visualization technique, the benefit of making it available to users may be worth the overhead of implementing into an existing tool. Also, more training needs to be provided to change the ways meteorol-

ogists explore their data. Here, we agree with Szoke et al. [212] that increased teaching of advanced visualization concepts in meteorological university courses will be helpful.

Interactive visual analysis and further not-yet-common techniques. With respect to development and adaptation of methods, we believe there is potential in bringing more interactive and further not-yet-common visualization techniques into meteorology. In particular in the areas of IVA, flow visualization, and 3D rendering, many techniques have been proposed in visualization research that have not yet been applied to meteorological data. For example, flow visualization techniques (cf. [239], [240]) including integral line rendering, LCS, and feature-based methods may be beneficial. Similarly, the use of IVA techniques (e.g., brushing and linking) and techniques from information visualization should be further investigated. In this respect, Dasgupta et al. [355], too, recently argued for an increased use of interactive, iterative, human-in-the-loop analysis techniques in climate research. There is, however, still much skepticism of domain experts with respect to interactive and automated analysis techniques (e.g., [9], [355]; cf. Sect. 4.3); skepticism that we can confirm from our experience with forecasters and atmospheric researchers. However, we can also confirm Nocke’s [9] observation that in particular young atmospheric researchers are increasingly used to interactive usage of software. We hence expect interactive visual analysis tools to become of increased importance. An in our opinion important aspect for the success of interactive techniques will be transparency of the data flow, and further effort should be invested into the design of methods for data provenance and reproducible visualization – here, reproducibility still is a clear advantage of script-based systems (cf. Sect. 4.3).

Seamless visualization and data fusion. A key to effective analysis of future meteorological datasets will be visualization techniques and systems that are able to depict data at multiple temporal and spatial resolutions (e.g., from seamless prediction), and able to fuse data from heterogeneous sources (cf. the datasets from the IEEE SciVis contests 2014 [375] and 2017 [376]). Challenges include dealing with model grids of differing resolutions, and also to dealing with data of entirely different topology (as typical, e.g., for the analysis of field campaign data). Visualizations need to make resolution and data topology transparent; such *seamless visualization* will enable forecasters and atmospheric researchers to analyze data at different scales to obtain a holistic picture of a weather situation.

Uncertainty and ensemble visualization. Visualization of uncertainty, in particular from ensemble forecasts, remains a particular challenge. Due to a lack of analytic and visualization methods, uncertainty is yet to be fully exploited; new types of visualization can have large potential value. Open issues range from the further improvement of established techniques (e.g., spaghetti plots and clustering) to questions including how to visualize ensemble variability and similarity for specific atmospheric features. For example, clustering ensemble members in a physically meaningful way is an extremely hard problem; clustering results depend on many details of the chosen method. How can such method uncertainty be visualized? With respect to features, questions include [214]: Do features develop

similarly to each other in different members but shifted in space and time? Can feature variability be visually depicted in a single image? Another challenge is to compare *entire ensembles*. A forecaster can be interested in how forecast scenarios differ in subsequent ensemble prediction runs; a researcher may be interested in the difference in ensemble properties with respect to changing a model parameterization or assimilating additional observation data.

3D visualization. An example of the demonstration of benefit is the use of interactive 3D visualization. Several studies have discussed benefits (cf. Sect. 5.2), including the argumentation that 3D depictions are much closer to conceptual models used by meteorologists (e.g., [201]), thereby reducing the time in which simulation data can be explored (e.g., [214]), and minimizing the risk of missing critical features (e.g., [212]). Obviously, potential benefit depends on the actual analysis task and data to be visualized. In operational forecasting, the horizontal movement of weather features can be well depicted on a 2D map (cf. Sect. 4). Nevertheless, 3D visualization could be beneficial to capture fully the spatial structure of small and large-scale features including convective cells, fronts and the tropopause. This could be particularly important for forecasting with a specific focus, such as planning a research flight. However, integration of 3D visualization into forecasting means a change to long established working practices. Software that combines the power of interactive 3D displays with traditional 2D maps (e.g., Met.3D [22]) might be able to ease the transition; first tests at ECMWF have shown that there is interest for analysts in viewing 2D maps in their 3D context.

We see many further open issues for 3D visualization, in particular with respect to the design of *meaningful* visualizations and their implementation as interactive graphics algorithms. For example, there are often large difference between horizontal and vertical scales, and this poses difficulties for meaningful 3D depictions. Which horizontal projections should be used with which vertical scaling? Distances perceived in the visualization may not physically make sense and may not be representative of reality. Also, an important aspect is to achieve good spatial perception in the 3D view. It must be obvious where the features displayed are located in space. In some cases (e.g., for visualizing a front), a meaningful depiction of the atmosphere could resemble the look of a “miniature plastic model” sitting on the scientist’s desk. In other cases (e.g., for visualization of clouds), a photo-realistic look resembling a picture taken from an airplane may be appropriate. Such visualizations touch upon issues in real-time rendering with global illumination; representative scenarios have just recently been provided by the IEEE SciVis contest 2017 [376]. Also, the benefit of using the third visualization dimension for a non-spatial coordinate (e.g., time or ensemble member) could be further investigated.

Technological challenges: big data and data modalities. Two technical factors will increasingly become challenging for visualization (in particular with respect to achieving interactivity): data sizes and the structure of the data (e.g., model grids). The continuously growing amount of data output by numerical models and observation systems already requires specific strategies at institutions including DKRZ and ECMWF (cf. Sect. 5.10); the increasing gap

between data production and storage [362], [363] has implications for visual data analysis as well. It will be challenging to make interactive visualization techniques and systems scale with growing data volumes; of importance can be compression and in-situ visualization approaches (cf. Sect. 5.10). It is of interest, e.g., to further investigate the application of wavelet compression to meteorological data (cf. Sect. 4.4). With respect to in-situ visualization, the trade-off between specifying “interesting” parts of a simulation before run-time and storing as much information as possible is challenging. Approaches that automate visualization output based on further in-situ analyses could be beneficial.

With respect to grid topologies, new model generations using irregular grids with local mesh refinements (cf. Sect. 2) bring technical challenges in particular for real-time and 3D rendering. For scientists, it is often important to inspect data on the original model grid (cf. Sect. 4.3); interpolation to regular grids to simplify visualization algorithms and increase performance may often not be acceptable.

7 CONCLUSION

We aimed at providing a comprehensive overview of visualization for data analysis in weather forecasting and meteorological research, from the origins of computer-based methods in the 1960s (Sect. 3) to today. Visualization research (Sect. 5) has approached many relevant topics in meteorological visualization to improve upon the current state of the art in the application domain (Sect. 4). Nevertheless, our discussion (Sect. 6) revealed many open challenges that we expect to motivate future visualization research with potentially large impact on meteorological practice; topics include, e.g., demonstration of benefit, interactive visual analysis, seamless visualization, uncertainty, 3D rendering and big data. Cooperation and exchange between visualization researchers and meteorologists will in this respect be fruitful for both communities; we expect exciting progress in meteorological visualization in coming years.

ACKNOWLEDGMENTS

This work was partly supported by the European Union under the ERC Advanced Grant 291372-SaferVis and the ERC Proof-of-Concept Grant “Vis4Weather”, and by the Transregional Collaborative Research Center SFB/TRR 165 “Waves to Weather” funded by the German Research Foundation (DFG). The fifth and sixth authors acknowledge the support of National Science Foundation (NSF) grant IIS-1212806.

REFERENCES

- [1] C. D. Ahrens, *Meteorology Today*, 9th ed. Brooks Cole, Jul. 2008.
- [2] M. E. McIntyre, “Numerical weather prediction: A vision of the future,” *Weather*, vol. 43, no. 8, pp. 294–298, 1988.
- [3] P. M. Inness and S. Dorling, *Operational Weather Forecasting*. Wiley-Blackwell, 2013.
- [4] T. V. Papathomas, J. A. Schiavone, and B. Julesz, “Applications of computer graphics to the visualization of meteorological data,” *SIGGRAPH Comput. Graph.*, vol. 22, no. 4, pp. 327–334, 1988.
- [5] J. A. Schiavone and T. V. Papathomas, “Visualizing meteorological data,” *Bull. Amer. Meteor. Soc.*, vol. 71, no. 7, pp. 1012–1020, 1990.
- [6] M. Böttinger, V. Gülzow, and J. Biercamp, “Visualisierung als Werkzeug zur Analyse von Klimasimulationsdaten,” in *Umwelt-informatik '98: Vernetzte Strukturen in Informatik, Umwelt und Wirtschaft*, H. D. Haasis and K. C. Ranze, Eds., 1998.
- [7] D. Middleton, T. Scheitlin, and B. Wilhelmson, “Visualization in weather and climate research,” in *The Visualization Handbook*, C. D. Hansen and C. Johnson, Eds. Academic Press, 2005, ch. 44, pp. 845–871.
- [8] T. Nocke, T. Sterzel, M. Böttinger, and M. Wrobel, “Visualization of climate and climate change data: An overview,” in *Digital Earth Summit on Geoinformatics 2008: Tools for Global Change Research (ISDE'08)*, Ehlers, Ed. Heidelberg: Wichmann, 2008, pp. 226–232.
- [9] T. Nocke, “Images for data analysis: The role of visualization in climate research processes,” in *Image Politics of Climate Change*, B. Schneider and T. Nocke, Eds. Bielefeld: transcript Verlag, 2014.
- [10] M. Monmonier, *Air Apparent: How Meteorologists Learned to Map, Predict, and Dramatize Weather*. University of Chicago Press, Chicago, 1999.
- [11] J. G. Trafton and R. R. Hoffman, “computer-aided visualization in meteorology,” in *Expertise Out of Context: Proc. of the Sixth Int'l Conf. on Naturalistic Decision Making*, R. R. Hoffman, Ed. Lawrence Erlbaum Associates, Mahwah, NJ, 2007, pp. 337–357.
- [12] E. M. Stephens, T. L. Edwards, and D. Demeritt, “Communicating probabilistic information from climate model ensembles—lessons from numerical weather prediction,” *WIREs Clim Change*, vol. 3, no. 5, pp. 409–426, Sep. 2012.
- [13] T. Nocke, S. Buschmann, J. F. Donges, N. Marwan, H. J. Schulz, and C. Tominski, “Review: visual analytics of climate networks,” *Nonlinear Processes in Geophysics*, vol. 22, no. 5, pp. 545–570, 2015.
- [14] B. Schneider, “Climate model simulation visualization from a visual studies perspective,” *WIREs Clim Change*, vol. 3, no. 2, pp. 185–193, Mar. 2012.
- [15] Intergovernmental Panel on Climate Change, Ed., *Climate Change 2013 - The Physical Science Basis*. Cambridge University Press, 2014.
- [16] H. J. Koppert, F. Schröder, E. Hergenröther, M. Lux, and A. Trembilski, “3D visualisation in daily operation at the DWD,” in *Proc. of the 6th ECMWF Workshop on Meteorological Operational Systems, 17-21 Nov. 1997, Reading, England*, 1998, pp. 119–142.
- [17] World Meteorological Organization. Manual on the global data-processing and forecasting system. <https://www.wmo.int/pages/prog/www/DPFS/Manual/GDPFS-Manual.html>. Accessed 23 Nov. 2017.
- [18] M. Rautenhaus, “Interactive 3D visualization of ensemble weather forecasts,” Ph.D. dissertation, Technische Universität München, 2015.
- [19] R. R. Hoffman, J. G. Trafton, P. J. Roebber, H. M. Mogil, and D. S. LaDue, *Minding the Weather: How Expert Forecasters Think* (MIT Press). The MIT Press, Jul. 2017.
- [20] M. Z. Jacobson, *Fundamentals of Atmospheric Modeling*, 2nd ed. Cambridge University Press, Jun. 2005.
- [21] K. Riley, Y. Song, M. Kraus, D. S. Ebert, and J. J. Levitt, “Visualization of structured nonuniform grids,” *IEEE Comput. Graphics Appl.*, vol. 26, no. 1, pp. 46–55, Jan. 2006.
- [22] M. Rautenhaus, M. Kern, A. Schäfler, and R. Westermann, “Three-dimensional visualization of ensemble weather forecasts – Part 1: The visualization tool Met3D (version 1.0),” *Geosci. Model Dev.*, vol. 8, no. 7, pp. 2329–2353, 2015.
- [23] W. C. Skamarock, J. B. Klemp, J. Dudhia, D. O. Gill, D. M. Barker, M. G. Duda, X.-Y. Huang, W. Wang, and J. G. Powers, “A description of the advanced research WRF version 3,” National Center for Atmospheric Research, Boulder, Colorado, USA, Tech. Rep., 2008.
- [24] M. Baldauf, A. Seifert, J. Förstner, D. Majewski, M. Raschendorfer, and T. Reinhardt, “Operational convective-scale numerical weather prediction with the COSMO model: Description and sensitivities,” *Mon. Wea. Rev.*, vol. 139, no. 12, pp. 3887–3905, 2011.
- [25] J. M. Prusa, P. K. Smolarkiewicz, and A. A. Wyszogrodzki, “EU-LAG, a computational model for multiscale flows,” *Computers & Fluids*, vol. 37, no. 9, pp. 1193–1207, Oct. 2008.
- [26] ECMWF, “IFS documentation – Cy40r1, Part III: Dynamics and numerical procedures,” European Centre for Medium-Range Weather Forecasting, Reading, UK, Tech. Rep., 2013.
- [27] W. C. Skamarock, J. B. Klemp, M. G. Duda, L. D. Fowler, S.-H. Park, and T. D. Ringler, “A multiscale nonhydrostatic atmo-

- spheric model using centroidal Voronoi tessellations and C-grid staggering," *Mon. Wea. Rev.*, vol. 140, no. 9, pp. 3090–3105, 2012.
- [28] M. Hortal and A. J. Simmons, "Use of reduced Gaussian grids in spectral models," *Mon. Wea. Rev.*, vol. 119, no. 4, pp. 1057–1074, Apr. 1991.
- [29] B. Hoskins, "The potential for skill across the range of the seamless weather-climate prediction problem: a stimulus for our science," *Q.J.R. Meteorol. Soc.*, vol. 139, no. 672, pp. 573–584, 2013.
- [30] P. Bauer, A. Thorpe, and G. Brunet, "The quiet revolution of numerical weather prediction," *Nature*, vol. 525, no. 7567, pp. 47–55, Sep. 2015.
- [31] G. Zängl, D. Reinert, P. Ripodas, and M. Baldauf, "The ICON (icosahedral non-hydrostatic) modelling framework of DWD and MPI-M: Description of the non-hydrostatic dynamical core," *Q.J.R. Meteorol. Soc.*, May 2014.
- [32] B. Stevens, M. Giorgetta, M. Esch, T. Mauritsen, T. Crueger, S. Rast, M. Salzmann, H. Schmidt, J. Bader, K. Block, R. Brokopf, I. Fast, S. Kinne, L. Kornbluh, U. Lohmann, R. Pincus, T. Reichler, and E. Roeckner, "Atmospheric component of the MPI-M earth system model: ECHAM6," *J. of Advances in Modeling Earth Systems*, vol. 5, no. 2, pp. 146–172, Jun. 2013.
- [33] F. Branski, "Pioneering the collection and exchange of meteorological data," *World Meteorological Organization (WMO) Bulletin*, vol. 59, no. 1, p. 12, 2010.
- [34] G. Visconti, P. Di Carlo, W. H. Brune, M. Schoeberl, and A. Wahner, Eds., *Observing Systems for Atmospheric Composition: Satellite, Aircraft, Sensor Web and Ground-Based Observational Methods and Strategies*. New York: Springer, Oct. 2007.
- [35] C. R. Johnson and A. R. Sanderson, "A next step: Visualizing errors and uncertainty," *IEEE Comput. Graphics Appl.*, vol. 23, no. 5, pp. 6–10, Sep. 2003.
- [36] G.-P. Bonneau, H.-C. Hege, C. Johnson, M. Oliveira, K. Potter, P. Rheingans, and T. Schultz, "Overview and state-of-the-art of uncertainty visualization," in *Scientific Visualization*, ser. Mathematics and Visualization, C. D. Hansen, M. Chen, C. R. Johnson, A. E. Kaufman, and H. Hagen, Eds. Springer London, 2014, pp. 3–27.
- [37] D. S. Wilks, *Statistical Methods in the Atmospheric Sciences*, 3rd ed. Academic Press, Jun. 2011.
- [38] T. Gneiting and A. E. Raftery, "Weather forecasting with ensemble methods," *Science*, vol. 310, no. 5746, pp. 248–249, 2005.
- [39] M. Leutbecher and T. Palmer, "Ensemble forecasting," *J. Comput. Phys.*, vol. 227, no. 7, pp. 3515–3539, Mar. 2008.
- [40] T. Palmer and R. Hagedorn, Eds., *Predictability of Weather and Climate*. Cambridge University Press, Aug. 2006.
- [41] E. N. Lorenz, "Atmospheric predictability experiments with a large numerical model," *Tellus*, vol. 34, no. 6, pp. 505–513, 1982.
- [42] L. S. R. Froude, L. Bengtsson, and K. I. Hodges, "Atmospheric predictability revisited," *Tellus A*, vol. 65, no. 19022, Jun. 2013.
- [43] Global Climate & Weather Modeling Branch. (2016) Ensemble publication and documentation page. <http://www.emc.ncep.noaa.gov/GEFS/doc.php>. Accessed 23 Nov. 2017.
- [44] M. A. Giorgetta, J. Jungclaus, C. H. Reick, S. Legutke, J. Bader, M. Böttinger, V. Brovkin, T. Crueger, M. Esch, K. Fieg, K. Glushak, V. Gayler, H. Haak, H.-D. Hollweg, T. Ilyina, S. Kinne, L. Kornbluh, D. Matei, T. Mauritsen, U. Mikolajewicz, W. Mueller, D. Notz, F. Pithan, T. Raddatz, S. Rast, R. Redler, E. Roeckner, H. Schmidt, R. Schnur, J. Segschneider, K. D. Six, M. Stockhause, C. Timmreck, J. Wegner, H. Widmann, K.-H. Wieners, M. Claussen, J. Marotzke, and B. Stevens, "Climate and carbon cycle changes from 1850 to 2100 in MPI-ESM simulations for the coupled model intercomparison project phase 5," *J. Adv. Model. Earth Syst.*, vol. 5, no. 3, pp. 572–597, Jul. 2013.
- [45] V. Eyring, M. Righi, M. Evaldsson, A. Lauer, S. Wenzel, C. Jones, A. Anav, O. Andrews, I. Cionni, E. L. Davin, C. Deser, C. Ehbrecht, P. Friedlingstein, P. Gleckler, K. D. Gottschaldt, S. Hagemann, M. Juckes, S. Kindermann, J. Krasting, D. Kunert, R. Levine, A. Loew, J. Mäkelä, G. Martin, E. Mason, A. Phillips, S. Read, C. Rio, R. Roehrig, D. Senftleben, A. Sterl, L. H. van Ulft, J. Walton, S. Wang, and K. D. Williams, "ESMValTool (v1.0) – a community diagnostic and performance metrics tool for routine evaluation of earth system models in CMIP," *Geosci. Model Dev.*, vol. 9, no. 5, pp. 1747–1802, 2016.
- [46] J. Marotzke, W. A. Müller, F. S. E. Vamborg, P. Becker, U. Cubasch, H. Feldmann, F. Kaspar, C. Kottmeier, C. Marini, I. Polkova, K. Prömmel, H. W. Rust, D. Stammer, U. Ulbrich, C. Kadow, A. Köhl, J. Kröger, T. Kruschke, J. G. Pinto, H. Pohlmann, M. Rey-ers, M. Schröder, F. Sienz, C. Timmreck, and M. Ziese, "MiKlip - a national research project on decadal climate prediction," *Bull. Amer. Meteor. Soc.*, Jun. 2016.
- [47] M. Collins, B. Booth, G. Harris, J. Murphy, D. Sexton, and M. Webb, "Towards quantifying uncertainty in transient climate change," *Climate Dynamics*, vol. 27, no. 2-3, pp. 127–147, 2006.
- [48] C. Tebaldi and R. Knutti, "The use of the multi-model ensemble in probabilistic climate projections," *Phil. Trans. of the Royal Society of London A: Mathematical, Physical and Engineering Sciences*, vol. 365, no. 1857, pp. 2053–2075, Aug. 2007.
- [49] W. J. Saucier, *Principles of Meteorological Analysis*. Dover Publications, 1955.
- [50] W. M. Washington, B. T. Olear, J. Takamine, and D. Robertson, "The application of CRT contour analysis to general circulation experiments," *Bull. Amer. Meteor. Soc.*, vol. 49, pp. 882–888, 1968.
- [51] A. Kasahara and W. M. Washington, "NCAR global general circulation model of the atmosphere," *Mon. Wea. Rev.*, vol. 95, no. 7, pp. 389–402, Jul. 1967.
- [52] R. Grotjahn and R. M. Chervin, "Animated graphics in meteorological research and presentations," *Bull. Amer. Meteor. Soc.*, vol. 65, no. 11, pp. 1201–1208, Nov. 1984.
- [53] A. F. Hasler, "Stereographic observations from geosynchronous satellites: An important new tool for the atmospheric sciences," *Bull. Amer. Meteor. Soc.*, vol. 62, no. 2, pp. 194–212, Feb. 1981.
- [54] A. F. Hasler, M. des Jardins, and A. J. Negri, "Artificial stereo presentation of meteorological data fields," *Bull. Amer. Meteor. Soc.*, vol. 62, no. 7, pp. 970–973, Jul. 1981.
- [55] A. F. Hasler, H. Pierce, K. R. Morris, and J. Dodge, "Meteorological data fields "in perspective,"" *Bull. Amer. Meteor. Soc.*, vol. 66, no. 7, pp. 795–801, Jul. 1985.
- [56] W. L. Hibbard, "Computer-generated imagery for 4-D meteorological data," *Bull. Amer. Meteor. Soc.*, vol. 67, no. 11, pp. 1362–1369, Nov. 1986.
- [57] T. V. Papathomas, J. Schiavone, and B. Julesz, "Stereo animation for very large data bases: Case study- meteorology," *IEEE Comput. Graphics Appl.*, vol. 7, no. 9, pp. 18–27, 1987.
- [58] E. Smith, "The McIDAS system," *IEEE Trans. on Geoscience Electronics*, vol. 13, no. 3, pp. 123–136, Jul. 1975.
- [59] V. E. Suomi, R. Fox, S. S. Limaye, and W. L. Smith, "McIDAS III: A modern interactive data access and analysis system," *J. Climate Appl. Meteor.*, vol. 22, no. 5, pp. 766–778, May 1983.
- [60] M. A. Lazzara, J. M. Benson, R. J. Fox, D. J. Laitsch, J. P. Rueden, D. A. Santek, D. M. Wade, T. M. Whittaker, and J. T. Young, "The man computer interactive data access system: 25 years of interactive processing," *Bull. Amer. Meteor. Soc.*, vol. 80, no. 2, pp. 271–284, Feb. 1999.
- [61] W. L. Hibbard, "4-D display of meteorological data," in *Proc. of the 1986 Workshop on Interactive 3D Graphics*, ser. I3D '86. New York, NY, USA: ACM, 1987, pp. 23–36.
- [62] T. H. Von der Haar, A. C. Meade, R. J. Craig, and D. L. Reinke, "Four-dimensional imaging for meteorological applications," *J. Atmos. Oceanic Technol.*, vol. 5, no. 1, pp. 136–143, Feb. 1988.
- [63] W. L. Hibbard, D. Santek, L. Uccellini, and K. Brill, "Application of the 4-D McIDAS to a model diagnostic study of the presidents' day cyclone," *Bull. Amer. Meteor. Soc.*, vol. 70, no. 11, pp. 1394–1403, Nov. 1989.
- [64] W. Hibbard and D. Santek, "Visualizing large data sets in the earth sciences," *Computer*, vol. 22, no. 8, pp. 53–57, Aug. 1989.
- [65] —, "Interactivity is the key," in *Proc. of the 1989 Chapel Hill Workshop on Volume Visualization*, ser. VVS '89. New York, NY, USA: ACM, 1989, pp. 39–43.
- [66] R. B. Wilhelmson, B. F. Jewett, C. Shaw, L. J. Wicker, M. Arrott, C. B. Bushell, M. Bajuk, J. Thingvold, and J. B. Yost, "A study of the evolution of a numerically modeled severe storm," *Int. J. High Perform. C.*, vol. 4, no. 2, pp. 20–36, Jun. 1990.
- [67] W. L. Hibbard, "Vis5D, Cave5D, and VisAD," in *The Visualization Handbook*, C. D. Hansen and C. Johnson, Eds. Academic Press, 2005, ch. 34, pp. 673–688.
- [68] B. Hibbard and D. Santek, "The VIS-5D system for easy interactive visualization," in *Proc. of the 1st Conf. on Visualization '90*, ser. VIS '90. Los Alamitos, CA, USA: IEEE Computer Society Press, 1990, pp. 28–35.
- [69] W. L. Hibbard, B. E. Paul, D. A. Santek, C. R. Dyer, A. L. Battaiola, and M. F. V. Martinez, "Interactive visualization of earth and space science computations," *Computer*, vol. 27, no. 7, pp. 65–72, Jul. 1994.

- [70] W. L. Hibbard, J. Anderson, I. Foster, B. E. Paul, R. Jacob, C. Schafer, and M. K. Tyree, "Exploring coupled atmosphere-ocean models using Vis5D," *Int. J. High Perform. C.*, vol. 10, no. 2-3, pp. 211–222, Jun. 1996.
- [71] J. Daabeck and B. Hibbard, "Large operational user of visualization," *SIGGRAPH Comput. Graph.*, vol. 37, no. 3, pp. 5–9, 2003.
- [72] F. Schröder, *Visualisierung meteorologischer Daten*. Berlin, Heidelberg: Springer, 1997.
- [73] C. Upson, T. Faulhaber, D. Kamins, D. Laidlaw, D. Schlegel, J. Vroom, R. Gurwitz, and A. Van Dam, "The application visualization system: a computational environment for scientific visualization," *IEEE Comput. Graphics Appl.*, vol. 9, no. 4, pp. 30–42, Jul. 1989.
- [74] J. M. Favre and M. Valle, "AVS and AVS/Express," in *The Visualization Handbook*, C. D. Hansen and C. Johnson, Eds. Academic Press, 2005, ch. 33, pp. 655–672.
- [75] J. Walton, "NAG's IRIS Explorer," in *The Visualization Handbook*, C. D. Hansen and C. Johnson, Eds. Academic Press, 2005, ch. 32, pp. 633–654.
- [76] G. Abram and L. Treinish, "An extended data-flow architecture for data analysis and visualization," in *Proc. of the 6th Conf. on Visualization '95*, ser. VIS '95. Washington, DC, USA: IEEE Computer Society, 1995.
- [77] D. Watson, "Meteorological data visualisation using IBM visualisation data explorer," in *Proc. of the 5th ECMWF Workshop on Meteorological Operational Systems*, 13-17 Nov. 1995, Reading, England, 1995, pp. 238–251.
- [78] D. Stalling, M. Westerhoff, and H.-C. Hege, "amira: A highly interactive system for visual data analysis," in *The Visualization Handbook*, C. D. Hansen and C. Johnson, Eds. Academic Press, 2005, ch. 38, pp. 749–767.
- [79] W. R. Gregg and I. R. Tannehill, "International standard projections for meteorological charts," *Mon. Wea. Rev.*, vol. 65, no. 12, pp. 411–415, Dec. 1937.
- [80] D. Heizenreder and S. Haucke, "Das meteorologische Visualisierungs- und Produktionssystem NinJo," *promet*, vol. 35, pp. 57–69, 2009.
- [81] D. M. Schultz, S. Anderson, J. G. Fairman, D. Lowe, G. McFiggans, E. Lee, and R. Seo-Zindy, "ManUniCast: a real-time weather and air-quality forecasting portal and app for teaching," *Weather*, vol. 70, no. 6, pp. 180–186, Jun. 2015.
- [82] M. Sprenger and H. Wernli, "The LAGRANTO Lagrangian analysis tool – version 2.0," *Geosci. Model Dev.*, vol. 8, no. 8, pp. 2569–2586, 2015.
- [83] I. Glatt, A. Dörnbrack, S. Jones, J. Keller, O. Martius, A. Müller, D. H. W. Peters, and V. Wirth, "Utility of Hovmöller diagrams to diagnose rossby wave trains," *Tellus A*, vol. 63, no. 5, pp. 991–1006, Oct. 2011.
- [84] K. E. Taylor, "Summarizing multiple aspects of model performance in a single diagram," *J. Geophys. Res.*, vol. 106, no. D7, pp. 7183–7192, Apr. 2001.
- [85] V. Lakshmanan, R. Rabin, J. Otkin, J. S. Kain, and S. Dembek, "Visualizing model data using a fast approximation of a radiative transfer model," *J. Atmos. Oceanic Technol.*, vol. 29, no. 5, pp. 745–754, Mar. 2012.
- [86] S. Dance, E. Ebert, and D. Scurrah, "Thunderstorm strike probability nowcasting," *J. Atmos. Oceanic Technol.*, vol. 27, no. 1, pp. 79–93, 2010.
- [87] V. K. Meyer, H. Höller, and H. D. Betz, "Automated thunderstorm tracking: utilization of three-dimensional lightning and radar data," *Atmos. Chem. Phys.*, vol. 13, no. 10, pp. 5137–5150, 2013.
- [88] T. D. Hewson and H. A. Titley, "Objective identification, typing and tracking of the complete life-cycles of cyclonic features at high spatial resolution," *Met. Apps*, vol. 17, no. 3, pp. 355–381, 2010.
- [89] C. Roy and R. Kovordányi, "Tropical cyclone track forecasting techniques – a review," *Atmospheric Research*, vol. 104–105, pp. 40–69, Feb. 2012.
- [90] P. Joe, S. Dance, V. Lakshmanan, D. Heizenreder, P. James, P. Lang, T. Hengstebeck, Y. Feng, P. W. Li, H.-Y. Yeung, O. Suzuki, K. Doi, and J. Dai, "Automated processing of doppler radar data for severe weather warnings," in *Doppler Radar Observations - Weather Radar, Wind Profiler, Ionospheric Radar, and Other Advanced Applications*, J. Bech and J. L. Chau, Eds. Rijeka, Croatia: InTech, 2012, pp. 33–74.
- [91] J. T. Dawe and P. H. Austin, "Statistical analysis of an LES shallow cumulus cloud ensemble using a cloud tracking algorithm," *Atmos. Chem. Phys.*, vol. 12, no. 2, pp. 1101–1119, 2012.
- [92] S. Limbach, E. Schömer, and H. Wernli, "Detection, tracking and event localization of jet stream features in 4-d atmospheric data," *Geosci. Model Dev.*, vol. 5, no. 2, pp. 457–470, Apr. 2012.
- [93] C. Keil, A. Tafferner, and T. Reinhardt, "Synthetic satellite imagery in the Lokal-Modell," *Atmospheric Research*, vol. 82, no. 1-2, pp. 19–25, Nov. 2006.
- [94] T. A. Gleeson, "Probability predictions of geostrophic winds," *J. Appl. Meteor.*, vol. 6, no. 2, pp. 355–359, Apr. 1967.
- [95] E. S. Epstein and R. J. Fleming, "Depicting stochastic dynamic forecasts," *J. Atmos. Sci.*, vol. 28, no. 4, pp. 500–511, May 1971.
- [96] T. P. Legg, K. R. Mylne, and C. Woolcock, "Use of medium-range ensembles at the Met Office I: PREVIN - a system for the production of probabilistic forecast information from the ECMWF EPS," *Met. Apps*, vol. 9, no. 3, pp. 255–271, Sep. 2002.
- [97] K. Mylne, "Predictability from a forecast provider's perspective," in *Predictability of Weather and Climate*, T. Palmer and R. Hagedorn, Eds. Cambridge: Cambridge University Press, Aug. 2006, ch. 23, pp. 596–613.
- [98] W. J. Tennant, Z. Toth, and K. J. Rae, "Application of the NCEP ensemble prediction system to medium-range forecasting in South Africa: New products, benefits, and challenges," *Wea. Forecasting*, vol. 22, no. 1, pp. 18–35, Feb. 2007.
- [99] D. R. Novak, D. R. Bright, and M. J. Brennan, "Operational forecaster uncertainty needs and future roles," *Wea. Forecasting*, vol. 23, no. 6, pp. 1069–1084, Dec. 2008.
- [100] T. Schumann, "Nutzung von Ensemble-Prognosen im Vorhersagedienst," *promet*, vol. 35, pp. 23–29, 2009.
- [101] M. Denhard, "Herausforderungen in der Interpretation und Kommunikation von probabilistischen Vorhersagen," *promet*, vol. 37, pp. 72–78, 2011.
- [102] A. Persson and E. Andersson, *User guide to ECMWF forecast products, version 1.1*, European Centre for Medium-Range Weather Forecasts (ECMWF), Reading, UK, 2013.
- [103] J. Gill, J. Rubiera, C. Martin, I. Cacic, K. Mylne, C. Dehui, G. Jiafeng, T. Xu, M. Yamaguchi, A. K. Foamouhoue, E. Poolman, and J. Guiney, *Guidelines on communicating forecast uncertainty*, World Meteorological Organization WMO/TD No. 1422, 2008.
- [104] I. Ihász and D. Tajti, "Use of ECMWF's ensemble vertical profiles at the Hungarian meteorological service," *ECMWF Newsletter*, vol. 129, pp. 25–29, 2011.
- [105] S. Theis and C. Gebhardt, "Grundlagen der Ensembletechnik und Wahrscheinlichkeitsaussagen," *promet*, vol. 35, pp. 104–110, 2009.
- [106] F. Lalaurette, "Early detection of abnormal weather conditions using a probabilistic extreme forecast index," *Q.J.R. Meteorol. Soc.*, vol. 129, no. 594, pp. 3037–3057, Oct. 2003.
- [107] T. I. Petroliaigis and P. Pinson, "Early warnings of extreme winds using the ECMWF extreme forecast index," *Met. Apps*, vol. 21, no. 2, pp. 171–185, Apr. 2014.
- [108] L. Ferranti and S. Corti, "New clustering products," *ECMWF Newsletter*, vol. 127, pp. 6–11, 2011.
- [109] F. Atger, "Tubing: An alternative to clustering for the classification of ensemble forecasts," *Wea. Forecasting*, vol. 14, no. 5, pp. 741–757, Oct. 1999.
- [110] L. Ferranti, S. Corti, and M. Janousek, "Flow-dependent verification of the ECMWF ensemble over the Euro-Atlantic sector," *Q.J.R. Meteorol. Soc.*, Aug. 2014.
- [111] C. E. P. Brooks, C. S. Durst, and N. Carruthers, "Upper winds over the world: Part I. the frequency distribution of winds at a point in the free air," *Q.J.R. Meteorol. Soc.*, vol. 72, no. 311, pp. 55–73, Jan. 1946.
- [112] H. L. Crutcher, "On the standard vector-deviation wind rose," *J. Meteor.*, vol. 14, no. 1, pp. 28–33, Feb. 1957.
- [113] T. D. Hewson, "Objective identification of frontal wave cyclones," *Met. Apps*, vol. 4, no. 4, pp. 311–315, Dec. 1997.
- [114] —, "Objective fronts," *Met. Apps*, vol. 5, no. 1, pp. 37–65, 1998.
- [115] —, "Tracking fronts and extra-tropical cyclones," *ECMWF Newsletter*, vol. 121, pp. 9–19, 2009.
- [116] P. G. Gill and P. Buchanan, "An ensemble based turbulence forecasting system," *Met. Apps*, vol. 21, no. 1, pp. 12–19, Jan. 2014.
- [117] L. S. R. Froude, L. Bengtsson, and K. I. Hodges, "The prediction of extratropical storm tracks by the ECMWF and NCEP ensemble prediction systems," *Mon. Wea. Rev.*, vol. 135, no. 7, pp. 2545–2567, Jul. 2007.

- [118] T. M. Hamill, M. J. Brennan, B. Brown, M. DeMaria, E. N. Rappaport, and Z. Toth, "NOAA's future ensemble-based hurricane forecast products," *Bull. Amer. Meteor. Soc.*, vol. 93, no. 2, pp. 209–220, 2012.
- [119] D. B. Stephenson and F. J. Doblas-Reyes, "Statistical methods for interpreting monte carlo ensemble forecasts," *Tellus A*, vol. 52, no. 3, pp. 300–322, May 2000.
- [120] Z. Toth, E. Kalnay, S. M. Tracton, R. Wobus, and J. Irwin, "A synoptic evaluation of the NCEP ensemble," *Wea. Forecasting*, vol. 12, no. 1, pp. 140–153, Mar. 1997.
- [121] R. S. Schumacher and C. A. Davis, "Ensemble-based forecast uncertainty analysis of diverse heavy rainfall events," *Wea. Forecasting*, vol. 25, no. 4, pp. 1103–1122, Mar. 2010.
- [122] M. Böttinger, H. Pohlmann, N. Röber, K. Meier-Fleischer, and D. Spickermann, "Visualization of 2D uncertainty in decadal climate predictions," in *Proc. Workshop on Visualization in Environmental Sciences (EnvirVis 2015)*, 2015.
- [123] K. Potter, A. Wilson, P.-T. Bremer, D. Williams, C. Doutriaux, V. Pascucci, and C. Johhson, "Visualization of uncertainty and ensemble data: Exploration of climate modeling and weather forecast data with integrated VisUS-CDAT systems," *J. of Physics: Conf. Series*, vol. 180, no. 1, pp. 012 089+, Jul. 2009.
- [124] Unidata. AWIPS II. <http://www.unidata.ucar.edu/software/awips2>. Accessed 23 Nov. 2017.
- [125] Norwegian Meteorological Institute. Diana. <https://diana.wiki.met.no>. Accessed 23 Nov. 2017.
- [126] L. Bergholt, "Diana - an opensource production and visualisation package," in *Proc. of the 11th ECMWF Workshop on Meteorological Operational Systems*, 12–16 Nov. 2007, Reading, England, 2008, pp. 150–152.
- [127] Meteo France Int'l. SYNERGIE web. <http://www.mfi.fr/en/page/meteorological-information-systems/synergie-web-forecasting.php>. Accessed 23 Nov. 2017.
- [128] ibl software engineering. Visual weather. <http://www.iblsoft.com/products/visualweather>. Accessed 23 Nov. 2017.
- [129] J. Daabeck, "Overview of meteorological workstation development in Europe," in *21st Int'l Conf. on Interactive Information Processing Systems (IIPS) for Meteorology, Oceanography, and Hydrology*, 9 – 13 Jan. 2005, 2005.
- [130] EGOWS. European working group on operational [meteorological] workstations. <https://en.wikipedia.org/wiki/EGOWS>. Accessed 23 Nov. 2017.
- [131] S. Limbach, M. Sprenger, E. Schömer, and H. Wernli, "IWAL - an interactive weather analysis laboratory," *Bull. Amer. Meteor. Soc.*, vol. 96, no. 6, pp. 903–909, 2014.
- [132] R. Blakeslee, J. Hall, M. Goodman, P. Parker, L. Freudinger, and M. He, "The real time mission monitor- a situational awareness tool for managing experiment assets," in *NASA Science and Technology Conf. 2007*, 19–21 Jun. 2007, College Park, MD, 2007.
- [133] M. Rautenhaus, G. Bauer, and A. Dörnbrack, "A web service based tool to plan atmospheric research flights," *Geosci. Model Dev.*, vol. 5, no. 1, pp. 55–71, Jan. 2012.
- [134] Meteorology and Oceanography Domain Working Group. MetOceanDWG web. http://external.opengeospatial.org/twiki_public/MetOceanDWG/WebHome. Accessed 23 Nov. 2017.
- [135] S. Lamy-Thépaut, C. Sahin, and B. Raoult, "ecCharts service," *ECMWF Newsletter*, vol. 134, pp. 7–9, 2013.
- [136] ADAGUC Consortium. Atmospheric data access for the geospatial user community. <http://adaguc.knmi.nl>. Accessed 23 Nov. 2017.
- [137] University Corporation for Atmospheric Research. NCAR Command Language. <http://www.ncl.ucar.edu>. Accessed 23 Nov. 2017.
- [138] Center for Ocean-Land-Atmosphere Studies. Grid Analysis and Display System (GrADS). <http://cola.gmu.edu/grads/>. Accessed 23 Nov. 2017.
- [139] NOAA Pacific Marine Environmental Laboratory. Ferret. <http://www.ferret.noaa.gov/>. Accessed 23 Nov. 2017.
- [140] School of Ocean and Earth Science and Technology, University of Hawaii at Manoa. The Generic Mapping Tools. <https://www.soest.hawaii.edu/gmt/>. Accessed 23 Nov. 2017.
- [141] F. Pérez, B. E. Granger, and J. D. Hunter, "Python: An ecosystem for scientific computing," *Comput. Sci. Eng.*, vol. 13, no. 2, pp. 13–21, Mar. 2011.
- [142] Harris Geospatial Solutions. Interactive Data Language (IDL). <http://www.harrisgeospatial.com/ProductsandSolutions/GeospatialProducts/IDL.aspx>. Accessed 23 Nov. 2017.
- [143] MathWorks, Inc. Matlab. <http://www.mathworks.com/products/matlab>. Accessed 23 Nov. 2017.
- [144] European Centre for Medium-Range Weather Forecasts. Metview. <http://software.ecmwf.int/metview>. Accessed 23 Nov. 2017.
- [145] I. Russell, S. Siemen, F. Ii, S. Kertész, S. Lamy-Thépaut, and V. Karhila, "Metview 4 – ECMWF's latest generation meteorological workstation," *ECMWF Newsletter*, vol. 126, pp. 23–27, 2010.
- [146] H.-J. Schulz, T. Nocke, M. Heitzler, and H. Schumann, "A design space of visualization tasks," *IEEE Trans. Visual. Comput. Graphics*, vol. 19, no. 12, pp. 2366–2375, 2013.
- [147] T. Nocke, M. Flechsig, and U. Böhm, "Visual exploration and evaluation of climate-related simulation data," in *Simulation Conf., 2007 Winter*. IEEE, Dec. 2007, pp. 703–711.
- [148] Koninklijk Nederlands Meteorologisch Instituut. Weather3DExplorer. <http://projects.knmi.nl/w3dx>. Accessed 23 Nov. 2017.
- [149] W. Schroeder, K. Martin, and B. Lorensen, *Visualization Toolkit: An object-oriented Approach to 3D Graphics*, 4th ed. Kitware, 2006.
- [150] M. Koutek, S. de Haan, F. Debie, S. Tjemkes, I. van der Neut, and P. de Valk, "3D exploration of weather data in combination with IASI l2 products for better understanding of potential applications," in *EUMETSAT Conf., 22–26 Sep. 2014, Geneva, Switzerland*, 2014.
- [151] M. Koutek, I. van der Neut, K. Lemcke, F. Debie, H. T. Pelkewijk, and R. van Westrhenen, "Exploration of severe weather events in virtual reality environments: Lessons learned from interactive 3D visualization of meteorological models," in *11th EMS Annual Meeting and 10th European Conf. on Applications of Meteorology*, 12–15 Sep. 2011, Berlin, Germany, 2011.
- [152] W. Hibbard, C. R. Dyer, and B. Paul, "Display of scientific data structures for algorithm visualization," in *Proc. of the 3rd conference on Visualization '92*. IEEE Computer Society Press Los Alamitos, CA, USA, Oct. 1992, pp. 139–146.
- [153] W. L. Hibbard, "Future directions in 3-D meteorological display," in *Proc. of the 6th ECMWF Workshop on Meteorological Operational Systems*, 17–21 Nov. 1997, Reading, England, 1997, pp. 186–190.
- [154] B. Hibbard, "VisAD: Connecting people to computations and people to people," *SIGGRAPH Comput. Graph.*, vol. 32, no. 3, pp. 10–12, Aug. 1998.
- [155] D. Murray, B. Hibbard, T. Whittaker, and J. Kelly, "Using VisAD to build tools for visualizing and analyzing remotely sensed data," in *IEEE 2001 Int'l Geoscience and Remote Sensing Symp., IGARSS '01*, vol. 1. IEEE, 2001, pp. 204–206.
- [156] D. Murray and J. McWhirter, "Evolving IDV – creating better tools for the community," in *23th Conf. on Int'l Interactive Information and Processing Systems (IIPS) for Meteorology, Oceanography, and Hydrology*. American Meteorological Society, 2007.
- [157] D. Murray, J. McWhirter, Y. Ho, and T. M. Whittaker, "IDV at 5: New features and future," in *25th Conf. on Int'l Interactive Information and Processing Systems (IIPS) for Meteorology, Oceanography, and Hydrology*. American Meteorological Society, 2009.
- [158] T. Achtor, T. Rink, T. Whittaker, D. Parker, and D. Santek, "McIDAS-V: a powerful data analysis and visualization tool for multi and hyperspectral environmental satellite data," *Proc. SPIE*, vol. 7085, 2008.
- [159] S. Yalda, G. Zoppetti, R. Clark, and K. Mackin, "Interactive immersion learning: Flying through weather data onboard the GEOpod," *Bull. Amer. Meteor. Soc.*, vol. 93, no. 12, pp. 1811–1813, Dec. 2012.
- [160] L. Orf, R. Wilhelmson, and L. Wicker, "Visualization of a simulated long-track EF5 tornado embedded within a supercell thunderstorm," *Parallel Computing*, vol. 55, pp. 28–34, Jul. 2016.
- [161] A. Norton and J. Clyne, "The VAPOR visualization application," in *High Performance Visualization*, E. W. Bethel, H. Childs, and C. Hansen, Eds. CRC Press, 2012, ch. 20, pp. 415–428.
- [162] J. Clyne, P. Mininni, A. Norton, and M. Rast, "Interactive desktop analysis of high resolution simulations: application to turbulent plume dynamics and current sheet formation," *New J. Phys.*, vol. 9, no. 8, pp. 301+, Aug. 2007.
- [163] L. Orf, R. Wilhelmson, B. Lee, C. Finley, and A. Houston, "Evolution of a long-track violent tornado within a simulated supercell," *Bull. Amer. Meteor. Soc.*, May 2016.
- [164] J. Clyne, "Progressive data access for regular grids," in *High Performance Visualization*, E. W. Bethel, H. Childs, and C. Hansen, Eds. CRC Press, 2012, ch. 8, pp. 145–169.

- [165] M. I. Jubair, U. Alim, N. Röber, J. Clyne, A. Mahdavi-Amiri, and F. Samavati, "Multiresolution visualization of digital earth data via hexagonal box-spline wavelets," in *Poster at IEEE Visualization 2015*, 2015.
- [166] A. Henderson, J. Ahrens, and C. Law, *The ParaView Guide*. Kitware Clifton Park, NY, 2004.
- [167] U. Ayachit, B. Geveci, K. Moreland, J. Patchett, and J. Ahrens, "The ParaView visualization application," in *High Performance Visualization*, E. W. Bethel, H. Childs, and C. Hansen, Eds. CRC Press, 2012, ch. 18, pp. 383–400.
- [168] J. Dyer and P. Amburn, "Desktop visualization of meteorological data using ParaView," *Kitware Source*, vol. 14, pp. 7–10, Jul. 2010.
- [169] N. Röber, P. Adamidis, and J. Behrens, "Visualization and analysis of climate simulation performance data," in *EGU General Assembly Conf. Abstracts*, ser. EGU General Assembly Conf. Abstracts, vol. 17, Apr. 2015, pp. 15318+.
- [170] N. Röber, *Paraview Tutorial – For the visualization of Earth- and Climate Science Data*, Deutsches Klimarechenzentrum, Bundesstrasse 45a, 20146 Hamburg, Germany, 2014.
- [171] Fei. Avizo. <http://www.fei.com/software/avizo3d/>. Accessed 23 Nov. 2017.
- [172] M. Böttinger, C. Ulmen, and K. Meier-Fleischer. (2014) Avizo climatology profile tutorial by DKRZ. http://www.dkrz.de/pdfs/docs/Getting_started_with_Avizo_Green_8.1.pdf. Accessed 23 Nov. 2017.
- [173] N. Röber, M. Salim, A. Gierisch, M. Böttinger, and H. Schlünzen, "Visualization of Urban Micro-Climate Simulations," in *Workshop on Visualisation in Environmental Sciences (EnvirVis)*, O. Kolditz, K. Rink, and G. Scheuermann, Eds. The Eurographics Association, 2013.
- [174] T. Theubl, H. P. Dasari, I. Hoteit, and M. Srinivasan, "Simulation and visualization of the cyclonic storm chapala over the Arabian sea: a case study," in *2016 4th Saudi Int'l Conf. on Information Technology (Big Data Analysis) (KACSTIT)*. IEEE, Nov. 2016, pp. 1–6.
- [175] T. M. Smith and V. Lakshmanan, "Real-time, rapidly updating severe weather products for virtual globes," *Computers & Geosciences*, vol. 37, no. 1, pp. 3–12, Jan. 2011.
- [176] A. Chen, G. Leptoukh, S. Kempler, C. Lynnes, A. Savtchenko, D. Nadeau, and J. Farley, "Visualization of A-train vertical profiles using Google Earth," *Computers & Geosciences*, vol. 35, no. 2, pp. 419–427, Feb. 2009.
- [177] F. Joseph Turk, J. Hawkins, K. Richardson, and M. Surratt, "A tropical cyclone application for virtual globes," *Computers & Geosciences*, vol. 37, no. 1, pp. 13–24, Jan. 2011.
- [178] P. Liu, J. Gong, and M. Yu, "Graphics processing unit-based dynamic volume rendering for typhoons on a virtual globe," *Int'l J. of Digital Earth*, vol. 8, no. 6, pp. 431–450, Jun. 2015.
- [179] P. W. Webley, "Virtual globe visualization of ash-aviation encounters, with the special case of the 1989 Redoubt-KLM incident," *Computers & Geosciences*, vol. 37, no. 1, pp. 25–37, Jan. 2011.
- [180] X. Sun, S. Shen, G. G. Leptoukh, P. Wang, L. Di, and M. Lu, "Development of a web-based visualization platform for climate research using Google earth," *Computers & Geosciences*, vol. 47, pp. 160–168, Oct. 2012.
- [181] Y. Wang, G. Huynh, and C. Williamson, "Integration of Google Maps/Earth with microscale meteorology models and data visualization," *Computers & Geosciences*, vol. 61, pp. 23–31, Dec. 2013.
- [182] IEEE Visualization 2004. (2004) IEEE Visualization 2004 Contest. <http://vis.computer.org/vis2004contest/data.html>. Accessed 23 Nov. 2017.
- [183] R. R. Hoffman, M. Detweiler, J. A. Conway, and K. Lipton, "Some considerations in using color in meteorological displays," *Wea. Forecasting*, vol. 8, no. 4, pp. 505–518, Dec. 1993.
- [184] A. J. Teuling, R. Stöckli, and S. I. Seneviratne, "Bivariate colour maps for visualizing climate data," *Int. J. Climatol.*, vol. 31, no. 9, pp. 1408–1412, Jul. 2011.
- [185] R. Stauffer, G. J. Mayr, M. Dabernig, and A. Zeileis, "Somewhere over the rainbow: How to make effective use of colors in meteorological visualizations," *Bull. Amer. Meteor. Soc.*, vol. 96, no. 2, pp. 203–216, Feb. 2015.
- [186] N. R. Kaye, A. Hartley, and D. Hemming, "Mapping the climate: guidance on appropriate techniques to map climate variables and their uncertainty," *Geosci. Model Dev.*, vol. 5, no. 1, pp. 245–256, Feb. 2012.
- [187] D. P. Retchless and C. A. Brewer, "Guidance for representing uncertainty on global temperature change maps," *Int. J. Climatol.*, vol. 36, no. 3, pp. 1143–1159, Mar. 2016.
- [188] A. Dasgupta, J. Poco, Y. Wei, R. Cook, E. Bertini, and C. T. Silva, "Bridging theory with practice: An exploratory study of visualization use and design for climate model comparison," *IEEE Trans. Visual. Comput. Graphics*, vol. 21, no. 9, pp. 996–1014, 2015.
- [189] M. Hegarty, "The cognitive science of visual-spatial displays: Implications for design," *Topics in Cognitive Science*, vol. 3, no. 3, pp. 446–474, Jul. 2011.
- [190] M. Hegarty, M. S. Canham, and S. I. Fabrikant, "Thinking about the weather: How display salience and knowledge affect performance in a graphic inference task," *J. Exp. Psychol. Learn.*, vol. 36, no. 1, pp. 37–53, 2010.
- [191] K. A. Bowden, P. L. Heinselman, and Z. Kang, "Exploring applications of eye-tracking in operational meteorology research," *Bull. Amer. Meteor. Soc.*, 2016.
- [192] B. Jobard and W. Lefer, "Creating evenly-spaced streamlines of arbitrary density," in *Visualization in Scientific Computing '97*, ser. Eurographics, W. Lefer and M. Grave, Eds. Springer Vienna, 1997, pp. 43–55.
- [193] B. Jobard, J. M. Favre, A. Mangli, M. Ballabio, M. Consoli, C. Ponti, D. Maric, G. de Morsier, P. Kaufmann, M. Arpagaus, J. M. Bettems, E. Zala, and J. Quiby, "Advanced flow representations applied to wind visualization," in *Proc. of the 8th ECMWF Workshop on Meteorological Operational Systems*, 12–16 Nov. 2001, Reading, England, 2001, pp. 172–178.
- [194] J. P. Martin, J. E. Swan, R. J. Moorhead, Z. Liu, and S. Cai, "Results of a user study on 2D hurricane visualization," *Comput. Graphics Forum*, vol. 27, no. 3, pp. 991–998, May 2008.
- [195] M. P. Paterson and S. F. Benjamin, "Better than a wind rose," *Atmos. Env.*, vol. 9, no. 5, pp. 537–542, 1975.
- [196] T. E. Graedel, "The wind boxplot: An improved wind rose," *J. Appl. Meteor.*, vol. 16, no. 4, pp. 448–450, Apr. 1977.
- [197] C. Ware and M. D. Plumlee, "Designing a better weather display," *Information Visualization*, vol. 12, no. 3–4, pp. 221–239, 2013.
- [198] C. Beccario. (2017) Earth: a global map of wind, weather, and ocean conditions. <https://earth.nullschool.net>. Accessed 23 Nov. 2017.
- [199] D. H. F. Pilar and C. Ware, "Representing flow patterns by using streamlines with glyphs," *IEEE Trans. Visual. Comput. Graphics*, vol. 19, no. 8, pp. 1331–1341, 2013.
- [200] L. A. Treinish, "Weather forecasting for the 1996 olympics," *IEEE Comput. Graphics Appl.*, vol. 16, no. 4, pp. 10–13, Jul. 1996.
- [201] L. A. Treinish and L. P. Rothfus, "Three-dimensional visualization for support of operational forecasting at the 1996 centennial olympic games," in *Proc. of the 13th IIPS Conf.*, 2–7 Feb. 1997, Long Beach, CA, 1997, pp. 2–8.
- [202] L. A. Treinish, "Task-specific visualization design: a case study in operational weather forecasting," in *Proc. Visualization '98, Research Triangle Park, North Carolina*, 1998, pp. 405–409.
- [203] P. T. McCaslin, P. A. McDonald, and E. J. Szoke, "3D visualization development at NOAA forecast systems laboratory," *ACM SIGGRAPH Comput. Graph.*, vol. 34, pp. 41–44, 2000.
- [204] M. Lux and T. Frühauf, "A visualization system for operational meteorological use," in *Proc. of the Sixth Int'l Conf. in Central Europe on Computer Graphics and Visualization (WSCG'98)*, 9–13 Feb. 1998, Plzen, Czech Republic, 1998, pp. 525–534.
- [205] F. Schröder, "Animation meteorologischer Daten für Massenmedien," in *Dynamische Visualisierung*, G. Buziek, D. Dransch, and W.-D. Rase, Eds. Springer Berlin Heidelberg, 2000, pp. 159–174.
- [206] H. Haase, M. Bock, E. Hergenröther, C. Knöpfle, H. J. Koppert, F. Schröder, A. Trembilski, and J. Weidenhausen, "Where weather meets the eye – a case study on a wide range of meteorological visualisations for diverse audiences," in *Data Visualization '99*, ser. Eurographics, E. Gröller, H. Löffelmann, and W. Ribarsky, Eds. Springer Vienna, 1999, pp. 261–266.
- [207] H. Haase, M. Bock, E. Hergenröther, C. Knöpfle, H. J. Koppert, F. Schröder, A. Trembilski, and J. Weidenhausen, "Meteorology meets computer graphics - a look at a wide range of weather visualisations for diverse audiences," *Computers & Graphics*, vol. 24, no. 3, pp. 391–397, Jun. 2000.
- [208] E. J. Szoke, U. H. Grote, P. T. McCaslin, and P. A. McDonald, "D3D: Overview, update, and future plans," in *Proc. of the 18th IIPS Conf.*, 13–18 Jan. 2002, Orlando, Florida, 2002.

- [209] A. I. Watson, J. D. Fournier, T. P. Lericos, and E. J. Szoke, "The use of D3D when examining tropical cyclones," in *Proc. of the 18th IIPS Conf.*, 13-18 Jan. 2002, Orlando, Florida, 2002.
- [210] D. B. Barjenbruch, E. Thaler, and E. J. Szoke, "Operational applications of three dimensional air parcel trajectories using AWIPS D3D," in *Proc. of the 18th IIPS Conf.*, 13-18 Jan. 2002, Orlando, Florida, 2002.
- [211] D. D. Niefeld, "The synoptic environment of the 11 April 2001 central plains tornado outbreak viewed in three dimensions," in *Proc. of the 19th IIPS Conf.*, 9-13 Feb. 2003, Long Beach, California, 2003.
- [212] E. J. Szoke, U. H. Grote, P. T. McCaslin, and P. A. McDonald, "D3D update: Is it being used?" in *Proc. of the 19th IIPS Conf.*, 9-13 Feb. 2003, Long Beach, California, 2003.
- [213] M. Rautenhaus, C. M. Grams, A. Schäfer, and R. Westermann, "GPU based interactive 3D visualization of ECMWF ensemble forecasts," *ECMWF Newsletter*, vol. 138, pp. 34–38, 2014.
- [214] —, "Three-dimensional visualization of ensemble weather forecasts – Part 2: Forecasting warm conveyor belt situations for aircraft-based field campaigns," *Geosci. Model Dev.*, vol. 8, no. 7, pp. 2355–2377, 2015.
- [215] Met.3D contributors. (2017) Met.3D. <http://met3d.wavestowweather.de>. Accessed 23 Nov. 2017.
- [216] J. Kniss, C. Hansen, M. Grenier, and T. Robinson, "Volume rendering multivariate data to visualize meteorological simulations: a case study," in *Proc. of the Symp. on Data Visualisation 2002*, ser. VISSYM '02. Aire-la-Ville, Switzerland, Switzerland: Eurographics Association, 2002, pp. 189–ff.
- [217] Y. Song, J. Ye, N. Svakhine, S. Lasher-Trapp, M. Baldwin, and D. S. Ebert, "An atmospheric visual analysis and exploration system," *IEEE Trans. Visual. Comput. Graphics*, vol. 12, no. 5, pp. 1157–1164, 2006.
- [218] D. K. Arthur, S. Lasher-Trapp, A. Abdel-Haleem, N. Klosterman, and D. S. Ebert, "A new three-dimensional visualization system for combining aircraft and radar data and its application to RICO observations," *J. Atmos. Oceanic Technol.*, vol. 27, no. 5, pp. 811–828, May 2010.
- [219] M. Berberich, P. Amburn, R. Moorhead, J. Dyer, and M. Brill, "Geospatial visualization using hardware accelerated real-time volume rendering," in *OCEANS 2009, MTS/IEEE Biloxi - Marine Technology for Our Future: Global and Local Challenges*. IEEE, Oct. 2009, pp. 1–5.
- [220] S. Ziegler, R. J. Moorhead, P. J. Croft, and D. Lu, "The MetVR case study: meteorological visualization in an immersive virtual environment," in *Proc. of the 2001 IEEE Visualization Conf.*, 2001, pp. 489–596.
- [221] M. Koutek, "Scientific visualization in virtual reality: Interaction techniques and application development," Ph.D. dissertation, Delft University of Technology, 2003.
- [222] W. A. Gallus, D. N. Yarger, C. Cruz-Neira, and R. Heer, "An example of a virtual reality learning environment," *Bull. Amer. Meteor. Soc.*, vol. 84, no. 1, pp. 18–20, Jan. 2003.
- [223] W. A. Gallus, C. Cervato, C. Cruz-Neira, G. Faidley, and R. Heer, "Learning storm dynamics with a virtual thunderstorm," *Bull. Amer. Meteor. Soc.*, vol. 86, no. 2, pp. 162–163, Feb. 2005.
- [224] C. Helbig, H.-S. Bauer, K. Rink, V. Wulfmeyer, M. Frank, and O. Kolditz, "Concept and workflow for 3D visualization of atmospheric data in a virtual reality environment for analytical approaches," *Environ. Earth Sci.*, vol. 72, no. 10, pp. 3767–3780, 2014.
- [225] C. Helbig, L. Bilke, H.-S. Bauer, M. Böttinger, and O. Kolditz, "MEVA - an interactive visualization application for validation of multifaceted meteorological data with multiple 3D devices," *PLoS ONE*, vol. 10, no. 4, pp. e0123811+, Apr. 2015.
- [226] G. Y. Gardner, "Visual simulation of clouds," *SIGGRAPH Comput. Graph.*, vol. 19, no. 3, pp. 297–304, Jul. 1985.
- [227] N. Max, R. Crawfis, and D. Williams, "Visualizing wind velocities by advecting cloud textures," in *Proc. IEEE Conf. on Visualization*, 1992. IEEE, 1992, pp. 179–184.
- [228] —, "Visualization for climate modeling," *IEEE Comput. Graphics Appl.*, vol. 13, no. 4, pp. 34–40, Jul. 1993.
- [229] K. Riley, D. Ebert, C. Hansen, and J. Levit, "Visually accurate multi-field weather visualization," in *Visualization 2003, VIS 2003*, IEEE, 2003, pp. 279–286.
- [230] K. Riley, D. S. Ebert, M. Kraus, J. Tessoroff, and C. Hansen, "Efficient rendering of atmospheric phenomena," in *Proc. of the Fifteenth Eurographics Conf. on Rendering Techniques*, ser. EGSR'04. Aire-la-Ville, Switzerland, Switzerland: Eurographics Association, 2004, pp. 375–386.
- [231] S.-K. Ueng and S.-C. Wang, "Interpolation and visualization for advected scalar fields," in *Visualization, 2005. VIS 05. IEEE*. IEEE, Oct. 2005, pp. 615–622.
- [232] A. Trembilski, "Two methods for cloud visualisation from weather simulation data," *The Visual Computer*, vol. 17, no. 3, pp. 179–184, 2001.
- [233] E. Hergenrother, A. Bleile, D. Middleton, and A. Trembilski, "The abalone interpolation: a visual interpolation procedure for the calculation of cloud movement," in *15th Brazilian Symp. on Computer Graphics and Image Processing*. IEEE Comput. Soc, 2002, pp. 381–387.
- [234] Y. Dobashi, K. Kaneda, H. Yamashita, T. Okita, and T. Nishita, "A simple, efficient method for realistic animation of clouds," in *Proc. of the 27th Annual Conf. on Computer Graphics and Interactive Techniques*, ser. SIGGRAPH '00. New York, NY, USA: ACM Press/Addison-Wesley Publishing Co., 2000, pp. 19–28.
- [235] Y. Dobashi, T. Yamamoto, and T. Nishita, "Interactive and realistic visualization system for earth-scale clouds," *Proc. of the Pacific Graphics, Switzerland: Eurographics Association Press*, 2009.
- [236] M. J. Harris and A. Lastra, "Real-time cloud rendering," *Comput. Graphics Forum*, vol. 20, no. 3, pp. 76–85, Sep. 2001.
- [237] M. J. Harris, W. V. Baxter, T. Scheuermann, and A. Lastra, "Simulation of cloud dynamics on graphics hardware," in *Proc. of the ACM SIGGRAPH/EUROGRAPHICS Conf. on Graphics Hardware*, ser. HWWS '03. Aire-la-Ville, Switzerland: Eurographics Association, 2003, pp. 92–101.
- [238] R. Hufnagel and M. Held, "A survey of cloud lighting and rendering techniques," in *Proc. 20th Internat. Conf. Comput. Graphics, Visualizat., Comput. Vision (WSCG'12)*, 2012, pp. 53–63.
- [239] T. McLoughlin, R. S. Laramée, R. Peikert, F. H. Post, and M. Chen, "Over two decades of integration-based, geometric flow visualization," *Comput. Graphics Forum*, vol. 29, no. 6, pp. 1807–1829, 2010.
- [240] M. Edmunds, R. S. Laramée, G. Chen, N. Max, E. Zhang, and C. Ware, "Surface-based flow visualization," *Computers & Graphics*, vol. 36, no. 8, pp. 974–990, Dec. 2012.
- [241] N. Cuntz, M. Leidl, A. Kolb, C. Rezk-Salama, and M. Böttinger, "GPU-based dynamic flow visualization for climate research applications," in *Proc. Simulation and Visualization*, 2007.
- [242] H. Doraiswamy, V. Natarajan, and R. S. Nanjundiah, "An exploration framework to identify and track movement of cloud systems," *IEEE Trans. Visual. Comput. Graphics*, vol. 19, no. 12, pp. 2896–2905, 2013.
- [243] T.-Y. Lee, P. C. Wong, S. Hagos, X. Tong, H.-W. Shen, and L. R. Leung, "Feature tracking and visualization of the Madden-Julian oscillation in climate simulation," *IEEE Comput. Graphics Appl.*, vol. 33, no. 4, pp. 29–37, Jul. 2013.
- [244] M. Maskey and T. S. Newman, "Directional texture for visualization - new technique and application study," in *19th Int'l Conf. on Information Visualisation (IV)*, 2015. IEEE, 2015, pp. 1–8.
- [245] W. Kendall, J. Huang, and T. Peterka, "Geometric quantification of features in large flow fields," *IEEE Comput. Graphics Appl.*, vol. 32, no. 4, pp. 46–54, Jul. 2012.
- [246] M. Edmunds, R. S. Laramée, R. Malki, I. Masters, T. N. Croft, G. Chen, and E. Zhang, "Automatic stream surface seeding: A feature centered approach," *Comput. Graphics Forum*, vol. 31, no. 3pt2, pp. 1095–1104, Jun. 2012.
- [247] H. Guo, F. Hong, Q. Shu, J. Zhang, J. Huang, and X. Yuan, "Scalable lagrangian-based attribute space projection for multivariate unsteady flow data," in *Visualization Symp. (PacificVis)*, 2014 IEEE Pacific. IEEE, Mar. 2014, pp. 33–40.
- [248] B. W. Shen, W. K. Tao, and B. Green, "Coupling advanced modeling and visualization to improve high-impact tropical weather prediction," *Comput. Sci. Eng.*, vol. 13, no. 5, pp. 56–67, 2011.
- [249] B.-W. Shen, B. Nelson, W.-K. Tao, and Y.-L. Lin, "Advanced visualizations of scale interactions of tropical cyclone formation and tropical waves," *Comput. Sci. Eng.*, vol. 15, no. 2, pp. 47–59, Mar. 2013.
- [250] B. Jobard and W. Lefer, "Unsteady flow visualization by animating evenly-spaced streamlines," *Comput. Graphics Forum*, vol. 19, no. 3, pp. 31–39, Sep. 2000.
- [251] W. Lefer, B. Jobard, and C. Leduc, "High-quality animation of 2D steady vector fields," *IEEE Trans. Visual. Comput. Graphics*, vol. 10, no. 1, pp. 2–14, 2004.

- [252] B. Jobard, N. Ray, and D. Sokolov, "Visualizing 2D flows with animated arrow plots," May 2012.
- [253] L. Yu, A. Lu, W. Ribarsky, and W. Chen, "Automatic animation for time-varying data visualization," *Comput. Graphics Forum*, vol. 29, no. 7, pp. 2271–2280, Sep. 2010.
- [254] W. Tang, P. W. Chan, and G. Haller, "Lagrangian coherent structure analysis of terminal winds detected by Lidar. part I: Turbulence structures," *J. Appl. Meteor. Climatol.*, vol. 50, no. 2, pp. 325–338, Oct. 2010.
- [255] F. J. Beron-Vera, M. J. Olascoaga, M. G. Brown, and H. Koçak, "Zonal jets as meridional transport barriers in the subtropical and polar lower stratosphere," *J. Atmos. Sci.*, vol. 69, no. 2, pp. 753–767, Sep. 2011.
- [256] T. Sapsis and G. Haller, "Inertial particle dynamics in a hurricane," *J. Atmos. Sci.*, vol. 66, no. 8, pp. 2481–2492, Aug. 2009.
- [257] H. Guo, W. He, T. Peterka, H.-W. Shen, S. M. Collis, and J. J. Helmus, "Finite-time Lyapunov exponents and Lagrangian coherent structures in uncertain unsteady flows," *IEEE Trans. Visual. Comput. Graphics*, vol. 22, no. 6, pp. 1672–1682, 2016.
- [258] H. Jänicke, M. Böttinger, X. Tricoche, and G. Scheuermann, "Automatic detection and visualization of distinctive structures in 3D unsteady multi-fields," *Comput. Graphics Forum*, vol. 27, no. 3, pp. 767–774, May 2008.
- [259] F. H. Post, B. Vrolijk, H. Hauser, R. S. Laramée, and H. Doleisch, "The state of the art in flow visualisation: Feature extraction and tracking," *Comput. Graphics Forum*, vol. 22, no. 4, pp. 775–792, 2003.
- [260] E. J. Griffith, F. H. Post, M. Koutek, T. Heus, and H. J. J. Jonker, "Feature tracking in VR for cumulus cloud life-cycle studies," in *Proc. of the 11th Eurographics Conf. on Virtual Environments*, ser. EGVE'05. Aire-la-Ville, Switzerland: Eurographics Association, 2005, pp. 121–128.
- [261] T. Heus, H. J. J. Jonker, H. E. A. Van den Akker, E. J. Griffith, M. Koutek, and F. H. Post, "A statistical approach to the life cycle analysis of cumulus clouds selected in a virtual reality environment," *J. Geophys. Res.*, vol. 114, no. D6, pp. D06208+, 2009.
- [262] L. G. Orf, B. D. Semeraro, and R. B. Wilhelmson, "Vortex detection in a simulated supercell thunderstorm," *Atmosph. Sci. Lett.*, vol. 8, no. 1, pp. 29–35, Jan. 2007.
- [263] C. Peng, S. Sahani, and J. Rushing, "A GPU-accelerated approach for feature tracking in time-varying imagery datasets," *IEEE Trans. Visual. Comput. Graphics*, vol. 23, no. 10, pp. 2262–2274, 2017.
- [264] J. J. Caban, A. Joshi, and P. Rheingans, "Texture-based feature tracking for effective time-varying data visualization," *IEEE Trans. Visual. Comput. Graphics*, vol. 13, no. 6, pp. 1472–1479, Nov. 2007.
- [265] P. C. Wong, H. Foote, R. Leung, E. Jurrus, D. Adams, and J. Thomas, "Vector fields simplification—a case study of visualizing climate modeling and simulation data sets," in *Proc. Visualization 2000*. IEEE, Oct. 2000, pp. 485–488.
- [266] M. Kern, T. Hewson, F. Sadlo, R. Westermann, and M. Rautenhaus, "Robust detection and visualization of jet-stream core lines in atmospheric flow," *IEEE Trans. Visual. Comput. Graphics*, vol. preprint, 2017.
- [267] A. Tafferner, C. Forster, M. Hagen, C. Keil, T. Zinner, and H. Volkert, "Development and propagation of severe thunderstorms in the upper Danube catchment area: Towards an integrated now-casting and forecasting system using real-time data and high-resolution simulations," *Meteorology and Atmospheric Physics*, vol. 101, no. 3–4, pp. 211–227, Oct. 2008.
- [268] M. Gleicher, D. Albers, R. Walker, I. Jusufi, C. D. Hansen, and J. C. Roberts, "Visual comparison for information visualization," *Information Visualization*, vol. 10, no. 4, pp. 289–309, Oct. 2011.
- [269] C. D. Hansen, M. Chen, C. R. Johnson, A. E. Kaufman, and H. Hagen, *Scientific Visualization: Uncertainty, Multifield, Biomedical, and Scalable Visualization*. Springer Publishing Company, Incorporated, 2014.
- [270] Q. Shen, A. Pang, and S. Uselton, "Data level comparison of wind tunnel and computational fluid dynamics data," in *Proc. Visualization 1998*. IEEE, 1998, pp. 415–418.
- [271] J. Poco, A. Dasgupta, Y. Wei, W. Hargrove, C. R. Schwalm, D. N. Huntzinger, R. Cook, E. Bertini, and C. T. Silva, "Visual reconciliation of alternative similarity spaces in climate modeling," *IEEE Trans. Visual. Comput. Graphics*, vol. 20, no. 12, pp. 1923–1932, 2014.
- [272] J. Poco, A. Dasgupta, Y. Wei, W. Hargrove, C. Schwalm, R. Cook, E. Bertini, and C. Silva, "SimilarityExplorer: A visual inter-comparison tool for multifaceted climate data," *Comput. Graphics Forum*, vol. 33, no. 3, pp. 341–350, Jun. 2014.
- [273] Y. H. Wang, C. R. Fan, J. Zhang, T. Niu, S. Zhang, and J. R. Jiang, "Forecast verification and visualization based on Gaussian mixture model co-estimation," *Comput. Graphics Forum*, vol. 34, no. 6, pp. 99–110, Sep. 2015.
- [274] Y. Tang, H. Qu, Y. Wu, and H. Zhou, "Natural textures for weather data visualization," in *Tenth Int'l Conf. on Information Visualization (IV)*, 2006. IEEE, 2006, pp. 741–750.
- [275] N. Sauber, H. Theisel, and H. P. Seidel, "Multifield-graphs: An approach to visualizing correlations in multifield scalar data," *IEEE Trans. Visual. Comput. Graphics*, vol. 12, no. 5, pp. 917–924, 2006.
- [276] H. Jänicke, A. Wiebel, G. Scheuermann, and W. Kollmann, "Multifield visualization using local statistical complexity," *IEEE Trans. Visual. Comput. Graphics*, vol. 13, no. 6, pp. 1384–1391, Nov. 2007.
- [277] S. Nagaraj, V. Natarajan, and R. S. Nanjundiah, "A gradient-based comparison measure for visual analysis of multifield data," *Comput. Graphics Forum*, vol. 30, no. 3, pp. 1101–1110, Jun. 2011.
- [278] A. Kuhn, W. Engelke, M. Flatken, H.-C. Hege, and I. Hotz, "topology-based analysis for multimodal atmospheric data of volcano eruptions," in *Topological Methods in Data Analysis and Visualization IV*, ser. Mathematics and Visualization, H. Carr, C. Garth, and T. Weinkauff, Eds. Springer Int'l Publishing, 2017, pp. 35–50.
- [279] T. Günther, M. Schulze, A. Friederici, and H. Theisel, "Visualizing volcanic clouds in the atmosphere and their impact on air traffic," *IEEE Comput. Graphics Appl.*, vol. 36, no. 3, pp. 36–47, May 2016.
- [280] M. Elshehaly, D. Gračanin, M. Gad, H. G. Elmongui, and K. Matković, "Interactive fusion and tracking for multi-modal spatial data visualization," *Comput. Graphics Forum*, vol. 34, no. 3, pp. 251–260, Jun. 2015.
- [281] L. A. Treinish, "Multi-resolution visualization techniques for nested weather models," in *Proc. Visualization 2000*. IEEE, Oct. 2000, pp. 513–516.
- [282] A. T. Pang, C. M. Wittenbrink, and S. K. Lodha, "Approaches to uncertainty visualization," *The Visual Computer*, vol. 13, no. 8, pp. 370–390, Nov. 1997.
- [283] A. M. MacEachren, A. Robinson, S. Hopper, S. Gardner, R. Murray, M. Gahegan, and E. Hetzler, "Visualizing geospatial information uncertainty: What we know and what we need to know," *Cartography and Geographic Information Science*, vol. 32, no. 3, pp. 139–160, Jan. 2005.
- [284] K. Brodlić, R. Allendes Osorio, and A. Lopes, "A review of uncertainty in data visualization," in *Expanding the Frontiers of Visual Analytics and Visualization*, J. Dill, R. Earnshaw, D. Kasik, J. Vince, and P. C. Wong, Eds. Springer London, 2012, pp. 81–109.
- [285] K. Potter, P. Rosen, and C. Johnson, "From quantification to visualization: A taxonomy of uncertainty visualization approaches," in *Uncertainty Quantification in Scientific Computing*, ser. IFIP Advances in Information and Communication Technology, A. Dienstfrey and R. Boisvert, Eds. Springer Berlin Heidelberg, 2012, vol. 377, pp. 226–249.
- [286] H. Obermaier and K. I. Joy, "Future challenges for ensemble visualization," *IEEE Comput. Graphics Appl.*, vol. 34, no. 3, pp. 8–11, May 2014.
- [287] L. Nadav-Greenberg, S. L. Joslyn, and M. U. Taing, "The effect of uncertainty visualizations on decision making in weather forecasting," *J. of Cognitive Engineering and Decision Making*, pp. 24–47, 2008.
- [288] S. Savelli and S. Joslyn, "The advantages of predictive interval forecasts for non-expert users and the impact of visualizations," *Appl. Cognit. Psychol.*, vol. 27, no. 4, pp. 527–541, Jul. 2013.
- [289] R. T. Whitaker, M. Mirzargar, and R. M. Kirby, "Contour boxplots: A method for characterizing uncertainty in feature sets from simulation ensembles," *IEEE Trans. Visual. Comput. Graphics*, vol. 19, no. 12, pp. 2713–2722, 2013.
- [290] M. Mirzargar, R. T. Whitaker, and R. M. Kirby, "Curve boxplot: Generalization of boxplot for ensembles of curves," *IEEE Trans. Visual. Comput. Graphics*, vol. 20, no. 12, pp. 2654–2663, 2014.
- [291] J. Sanyal, S. Zhang, J. Dyer, A. Mercer, P. Amburn, and R. Moorhead, "Noodles: A tool for visualization of numerical weather model ensemble uncertainty," *IEEE Trans. Visual. Comput. Graphics*, vol. 16, no. 6, pp. 1421–1430, 2010.

- [292] F. Ferstl, K. Bürger, and R. Westermann, "Streamline variability plots for characterizing the uncertainty in vector field ensembles," *IEEE Trans. Visual. Comput. Graphics*, vol. 22, no. 1, pp. 767–776, 2016.
- [293] F. Ferstl, M. Kanzler, M. Rautenhaus, and R. Westermann, "Visual analysis of spatial variability and global correlations in ensembles of iso-contours," *Comput. Graphics Forum*, vol. 35, no. 3, 2016.
- [294] —, "Time-hierarchical clustering and visualization of weather forecast ensembles," *IEEE Trans. Visual. Comput. Graphics*, vol. 23, no. 1, pp. 831–840, 2017.
- [295] J. Cox, D. House, and M. Lindell, "Visualizing uncertainty in predicted hurricane tracks," *Int. J. Uncertainty Quant.*, vol. 3, no. 2, pp. 143–156, 2013.
- [296] L. Liu, M. Mirzargar, R. M. Kirby, R. Whitaker, and D. H. House, "Visualizing time-specific hurricane predictions, with uncertainty, from storm path ensembles," *Comput. Graphics Forum*, vol. 34, no. 3, pp. 371–380, 2015.
- [297] L. Liu, A. Boone, I. Ruginski, L. Padilla, M. Hegarty, S. H. Creem-Regehr, W. B. Thompson, C. Yuksel, and D. H. House, "Uncertainty visualization by representative sampling from prediction ensembles," *IEEE Trans. Visual. Comput. Graphics*, vol. 23, no. 9, Sep. 2017.
- [298] I. T. Ruginski, A. P. Boone, L. M. Padilla, L. Liu, N. Heydari, H. S. Kramer, M. Hegarty, W. B. Thompson, D. H. House, and S. H. Creem-Regehr, "Non-expert interpretations of hurricane forecast uncertainty visualizations," *Spatial Cognition & Computation*, vol. 16, no. 2, pp. 154–172, Apr. 2016.
- [299] K. Potter, A. Wilson, P. T. Bremer, D. Williams, C. Doutriaux, V. Pascucci, and C. R. Johnson, "Ensemble-Vis: A framework for the statistical visualization of ensemble data," in *Int'l Conf. on Data Mining Workshops, Miami, Florida*. Los Alamitos, CA, USA: IEEE Computer Society, 2009, pp. 233–240.
- [300] P. S. Quinan and M. Meyer, "Visually comparing weather features in forecasts," *IEEE Trans. Visual. Comput. Graphics*, vol. 22, no. 1, pp. 389–398, 2016.
- [301] I. Demir, C. Dick, and R. Westermann, "Multi-charts for comparative 3D ensemble visualization," *IEEE Trans. Visual. Comput. Graphics*, vol. 20, no. 12, pp. 2694–2703, Dec. 2014.
- [302] T. Höllt, A. Magdy, P. Zhan, G. Chen, G. Gopalakrishnan, I. Hoteit, C. D. Hansen, and M. Hadwiger, "Ovis: A framework for visual analysis of ocean forecast ensembles," *IEEE Trans. Visual. Comput. Graphics*, vol. 20, no. 8, pp. 1114–1126, 2014.
- [303] J. Wang, X. Liu, H.-W. Shen, and G. Lin, "Multi-resolution climate ensemble parameter analysis with nested parallel coordinates plots," *IEEE Trans. Visual. Comput. Graphics*, vol. 23, no. 1, pp. 81–90, 2017.
- [304] A. Biswas, G. Lin, X. Liu, and H.-W. Shen, "Visualization of time-varying weather ensembles across multiple resolutions," *IEEE Trans. Visual. Comput. Graphics*, vol. 23, no. 1, pp. 841–850, 2017.
- [305] A. Kumpf, B. Tost, M. Baumgart, M. Riemer, R. Westermann, and M. Rautenhaus, "Visualizing confidence in cluster-based ensemble weather forecast analyses," *IEEE Trans. Visual. Comput. Graphics*, vol. preprint, 2017.
- [306] I. Demir, J. Kehrner, and R. Westermann, "Screen-space silhouettes for visualizing ensembles of 3D isosurfaces," in *2016 IEEE Pacific Visualization Symp. (PacificVis)*. IEEE, 2016, pp. 204–208.
- [307] K. Potter, J. Kniss, R. Riesenfeld, and C. R. Johnson, "Visualizing summary statistics and uncertainty," *Comput. Graphics Forum*, vol. 29, no. 3, pp. 823–832, 2010.
- [308] O. D. Lampe and H. Hauser, "Curve density estimates," *Comput. Graphics Forum*, vol. 30, no. 3, pp. 633–642, Jun. 2011.
- [309] P. Köthur, C. Witt, M. Sips, N. Marwan, S. Schinkel, and D. Dransch, "Visual analytics for correlation-based comparison of time series ensembles," *Comput. Graphics Forum*, vol. 34, no. 3, pp. 411–420, Jun. 2015.
- [310] K. Pöthkow and H.-C. Hege, "Nonparametric models for uncertainty visualization," *Comput. Graphics Forum*, vol. 32, no. 3, pp. 131–140, 2013.
- [311] R. S. Allendes Osorio and K. W. Brodlić, "Contouring with uncertainty," in *Proc. 6th Theory & Practice of Computer Graphics Conf.*, I. S. Lim and W. Tang, Eds. UK Chapter of the Eurographics Association, 2008, pp. 59–66.
- [312] T. Pfaffelmoser and R. Westermann, "Visualizing contour distributions in 2D ensemble data," in *EuroVis-Short Papers*. The Eurographics Association, 2013, pp. 55–59.
- [313] K. Pöthkow and H. C. Hege, "Positional uncertainty of iso-contours: Condition analysis and probabilistic measures," *IEEE Trans. Visual. Comput. Graphics*, vol. 17, no. 10, pp. 1393–1406, 2011.
- [314] B. Zehner, N. Watanabe, and O. Kolditz, "Visualization of gridded scalar data with uncertainty in geosciences," *Comput. Geosci.*, vol. 36, no. 10, pp. 1268–1275, Oct. 2010.
- [315] K. Pöthkow, B. Weber, and H.-C. Hege, "Probabilistic mapping cubes," *Comput. Graphics Forum*, vol. 30, no. 3, pp. 931–940, 2011.
- [316] T. Pfaffelmoser, M. Reitingner, and R. Westermann, "Visualizing the positional and geometrical variability of isosurfaces in uncertain scalar fields," *Comput. Graphics Forum*, vol. 30, no. 3, pp. 951–960, Jun. 2011.
- [317] T. Pfaffelmoser, M. Mihai, and R. Westermann, "Visualizing the variability of gradients in uncertain 2D scalar fields," *IEEE Trans. Visual. Comput. Graphics*, vol. 19, no. 11, pp. 1948–1961, Nov. 2013.
- [318] M. Mihai and R. Westermann, "Visualizing the stability of critical points in uncertain scalar fields," *Computers & Graphics*, vol. 41, pp. 13–25, Jun. 2014.
- [319] T. Liebmann and G. Scheuermann, "Critical points of Gaussian-distributed scalar fields on simplicial grids," *Comput. Graphics Forum*, vol. 35, no. 3, pp. 361–370, Jun. 2016.
- [320] K. Benesma, L. Gosink, H. Obermaier, and K. Joy, "Modality-driven classification and visualization of ensemble variance," *IEEE Trans. Visual. Comput. Graphics*, vol. 22, no. 10, pp. 2289–2299, 2016.
- [321] C. M. Wittenbrink, A. T. Pang, and S. K. Lodha, "Glyphs for visualizing uncertainty in vector fields," *IEEE Trans. Visual. Comput. Graphics*, vol. 2, no. 3, pp. 266–279, Sep. 1996.
- [322] M. Jarema, I. Demir, J. Kehrner, and R. Westermann, "Comparative visual analysis of vector field ensembles," in *IEEE Conf. on Visual Analytics Science and Technology (VAST)*, 2015. IEEE, 2015, pp. 81–88.
- [323] R. A. Boller, S. A. Braun, J. Miles, and D. Laidlaw, "Application of uncertainty visualization methods to meteorological trajectories," *Earth Science Informatics*, vol. 3, no. 1-2, pp. 119–126, May 2010.
- [324] H. Guo, X. Yuan, J. Huang, and X. Zhu, "Coupled ensemble flow line advection and analysis," *IEEE Trans. Visual. Comput. Graphics*, vol. 19, no. 12, pp. 2733–2742, 2013.
- [325] R. Liu, H. Guo, J. Zhang, and X. Yuan, "Comparative visualization of vector field ensembles based on longest common subsequence," in *2016 IEEE Pacific Visualization Symp. (PacificVis)*. IEEE, Apr. 2016, pp. 96–103.
- [326] H. Doleisch and H. Hauser, "Interactive visual exploration and analysis of multivariate simulation data," *Comput. Sci. Eng.*, vol. 14, no. 2, pp. 70–77, Mar. 2012.
- [327] J. Kehrner and H. Hauser, "Visualization and visual analysis of multifaceted scientific data: A survey," *IEEE Trans. Visual. Comput. Graphics*, vol. 19, no. 3, pp. 495–513, Mar. 2013.
- [328] N. Röber, *Visualization of Data using SimVis in the Context of Earth System and Climate Research*, Deutsches Klimarechenzentrum, Bundesstrasse 45a, 20146 Hamburg, Germany, 2011.
- [329] C. Tominski, J. F. Donges, and T. Nocke, "Information visualization in climate research," in *15th Int'l Conf. on Information Visualisation (IV)*. IEEE, Jul. 2011, pp. 298–305.
- [330] F. Ladstädter, A. K. Steiner, B. C. Lackner, B. Pirscher, G. Kirchengast, J. Kehrner, H. Hauser, P. Muigg, and H. Doleisch, "Exploration of climate data using interactive visualization," *J. Atmos. Oceanic Technol.*, vol. 27, no. 4, pp. 667–679, 2010.
- [331] H. Doleisch, P. Muigg, and H. Hauser, "Interactive visual analysis of Hurricane Isabel with SimVis," in *IEEE Visualization 2004 Contest, Austin, Texas*, 2004.
- [332] J. Kehrner, F. Ladstädter, P. Muigg, H. Doleisch, A. Steiner, and H. Hauser, "Hypothesis generation in climate research with interactive visual data exploration," *IEEE Trans. Visual. Comput. Graphics*, vol. 14, no. 6, pp. 1579–1586, 2008.
- [333] H. Jin and D. Guo, "Understanding climate change patterns with multivariate geovisualization," in *IEEE Int'l Conf. on Data Mining Workshops, 2009. ICDMW'09*. IEEE, 2009, pp. 217–222.
- [334] H. Qu, W.-Y. Chan, A. Xu, K.-L. Chung, K.-H. Lau, and P. Guo, "Visual analysis of the air pollution problem in hong kong," *IEEE Trans. Visual. Comput. Graphics*, vol. 13, no. 6, pp. 1408–1415, Nov. 2007.
- [335] A. Diehl, L. Pelorosso, C. Delrieux, C. Saulo, J. Ruiz, M. E. Gröller, and S. Bruckner, "Visual analysis of spatio-temporal data: Applications in weather forecasting," *Comput. Graphics Forum*, vol. 34, no. 3, pp. 381–390, Jun. 2015.
- [336] A. Kerren, I. Jusufi, and J. Liu, "Multi-scale trend visualization of long-term temperature data sets," in *Proc. of SIGRAD 2014, Visual*

- Computing*, Jun. 12-13, 2014, Göteborg, Sweden, no. 106. Linköping University Electronic Press, 2014, pp. 91–94.
- [337] H. Jänicke, M. Böttinger, and G. Scheuermann, “Brushing of attribute clouds for the visualization of multivariate data,” *IEEE Trans. Visual. Comput. Graphics*, vol. 14, no. 6, pp. 1459–1466, 2008.
- [338] H. Jänicke, M. Böttinger, U. Mikolajewicz, and G. Scheuermann, “Visual exploration of climate variability changes using wavelet analysis,” *IEEE Trans. Visual. Comput. Graphics*, vol. 15, no. 6, pp. 1375–1382, 2009.
- [339] C. A. Steed, J. E. Swan, T. J. Jankun-Kelly, and P. J. Fitzpatrick, “Guided analysis of hurricane trends using statistical processes integrated with interactive parallel coordinates,” in *IEEE Symp. on Visual Analytics Science and Technology, 2009. VAST 2009*. IEEE, 2009, pp. 19–26.
- [340] C. A. Steed, G. Shipman, P. Thornton, D. Ricciuto, D. Erickson, and M. Branstetter, “Practical application of parallel coordinates for climate model analysis,” *Procedia Computer Science*, vol. 9, pp. 877–886, 2012.
- [341] G. M. Draper, Y. Livnat, and R. F. Riesenfeld, “A survey of radial methods for information visualization,” *IEEE Trans. Visual. Comput. Graphics*, vol. 15, no. 5, pp. 759–776, 2009.
- [342] J. Li, K. Zhang, and Z.-P. Meng, “Vismate: Interactive visual analysis of station-based observation data on climate changes,” in *IEEE Conf. on Visual Analytics Science and Technology (VAST), 2014*. IEEE, 2014, pp. 133–142.
- [343] J. Sukharev, C. Wang, K.-L. Ma, and A. T. Wittenberg, “Correlation study of time-varying multivariate climate data sets,” in *IEEE Pacific Visualization Symp., 2009.*, vol. 0. Los Alamitos, CA, USA: IEEE, Apr. 2009, pp. 161–168.
- [344] A. Fernández, A. M. González, J. Díaz, and J. R. Dorronsoro, “Diffusion maps for dimensionality reduction and visualization of meteorological data,” *Neurocomputing*, vol. 163, pp. 25–37, 2015.
- [345] M. G. Genton, C. Johnson, K. Potter, G. Stenchikov, and Y. Sun, “Surface boxplots,” *STAT*, vol. 3, no. 1, pp. 1–11, Mar. 2014.
- [346] P. Lundblad, H. Löfving, A. Elovsson, and J. Johansson, “Exploratory visualization for weather data verification,” in *15th Int’l Conf. on Information Visualisation (IV)*. IEEE, Jul. 2011, pp. 306–313.
- [347] P. Lundblad, O. Eurenus, and T. Heldring, “Interactive visualization of weather and ship data,” in *13th Int’l Conf. on Information Visualisation (IV)*. IEEE, Jul. 2009, pp. 379–386.
- [348] P. Lundblad, J. Thoursie, and M. Jern, “Swedish road weather visualization,” in *14th Int’l Conf. on Information Visualisation (IV)*. IEEE, Jul. 2010, pp. 313–321.
- [349] T. Nocke, H. Schumann, and U. Böhm, “Methods for the visualization of clustered climate data,” *Computational Statistics*, vol. 19, no. 1, pp. 75–94, Feb. 2004.
- [350] T. Nocke, “Visuelles Data Mining und Visualisierungsdesign für die Klimaforschung,” Ph.D. dissertation, Universität Rostock, 2007.
- [351] J. Staib, S. Grottel, and S. Gumhold, “Enhancing scatterplots with multi-dimensional focal blur,” *Comput. Graphics Forum*, vol. 35, no. 3, pp. 11–20, Jun. 2016.
- [352] P. C. Wong, H.-W. Shen, R. Leung, S. Hagos, T.-Y. Lee, X. Tong, and K. Lu, “Visual analytics of large-scale climate model data,” in *IEEE 4th Symp. on Large Data Analysis and Visualization (LDAV)*. IEEE, Nov. 2014, pp. 85–92.
- [353] P. C. Wong, H.-W. Shen, C. R. Johnson, C. Chen, and R. B. Ross, “The top 10 challenges in extreme-scale visual analytics,” *IEEE Comput. Graphics Appl.*, vol. 32, no. 4, pp. 63–67, Jul. 2012.
- [354] C. A. Steed, K. J. Evans, J. F. Harney, B. C. Jewell, G. Shipman, B. E. Smith, P. E. Thornton, and D. N. Williams, “Web-based visual analytics for extreme scale climate science,” in *IEEE Int’l Conf. on Big Data, 2014*. IEEE, 2014, pp. 383–392.
- [355] A. Dasgupta, J. Poco, E. Bertini, and C. T. Silva, “Reducing the analytical bottleneck for domain scientists: Lessons from a climate data visualization case study,” *Comput. Sci. Eng.*, vol. 18, no. 1, pp. 92–100, Jan. 2016.
- [356] S. Djurcilov and A. Pang, “Visualizing sparse gridded data sets,” *IEEE Comput. Graphics Appl.*, vol. 20, no. 5, pp. 52–57, Sep. 2000.
- [357] T. Gerstner, D. Meetschen, S. Crewel, M. Griebel, and C. Simmer, “A case study on multiresolution visualization of local rainfall from weather radar measurements,” in *Proc. Visualization 2002*. IEEE, Nov. 2002, pp. 533–536.
- [358] A. Moreno, A. G. Mujika, and A. Segura, “Visual analytics of multi-sensor weather information georeferenciation of doppler weather radar and weather stations,” in *2014 Int’l Conf. on Information Visualization Theory and Applications (IVAPP)*. IEEE, Jan. 2014, pp. 329–336.
- [359] J. Xie, H. Yu, and K.-L. Ma, “Interactive ray casting of geodesic grids,” *Comput. Graphics Forum*, vol. 32, no. 3pt4, pp. 481–490, 2013.
- [360] —, “Visualizing large 3D geodesic grid data with massively distributed GPUs,” in *IEEE 4th Symp. on Large Data Analysis and Visualization (LDAV), 2014*. IEEE, 2014, pp. 3–10.
- [361] P. Kristof, B. Benes, C. X. Song, and L. Zhao, “A system for large-scale visualization of streaming doppler data,” in *IEEE Int’l Conf. on Big Data 2013*. IEEE, Oct. 2013, pp. 33–40.
- [362] J. M. Kunkel, M. Kuhn, and T. Ludwig, “Exascale storage systems – an analytical study of expenses,” *Supercomputing Frontiers and Innovations*, vol. 1, no. 1, Sep. 2014.
- [363] M. Kuhn, J. Kunkel, and T. Ludwig, “Data compression for climate data,” *Supercomputing Frontiers and Innovations*, vol. 3, no. 1, Jun. 2016.
- [364] U. Ayachit, A. Bauer, B. Geveci, P. O’Leary, K. Moreland, N. Fabian, and J. Mauldin, “ParaView catalyst: Enabling in situ data analysis and visualization,” in *Proc. of the First Workshop on In Situ Infrastructures for Enabling Extreme-Scale Analysis and Visualization*, ser. ISAV2015. New York, NY, USA: ACM, 2015, pp. 25–29.
- [365] S. Olbrich, H. Pralle, and S. Raasch, “Using streaming and parallelization techniques for 3D visualization in a high performance computing and networking environment,” in *High-Performance Computing and Networking*, ser. Lecture Notes in Computer Science, B. Hertzberger, A. Hoekstra, and R. Williams, Eds. Springer Berlin Heidelberg, 2001, vol. 2110, pp. 231–240.
- [366] N. Jensen, S. Olbrich, H. Pralle, and S. Raasch, “An efficient system for collaboration in tele-immersive environments,” in *Proc. of the Fourth Eurographics Workshop on Parallel Graphics and Visualization*, ser. EGPGV ’02. Aire-la-Ville, Switzerland, Switzerland: Eurographics Association, 2002, pp. 123–131.
- [367] S. Manten, M. Vetter, and S. Olbrich, “Evaluation of a scalable in-situ visualization system approach in a parallelized computational fluid dynamics application,” in *Virtual Realities*, G. Brunnett, S. Coquillart, and G. Welch, Eds. Springer Vienna, 2011, pp. 225–238.
- [368] NVIDIA Corporation. (2017) NVIDIA IndeX. <https://developer.nvidia.com/index>. Accessed 23 Nov. 2017.
- [369] E. Santos, J. Poco, Y. Wei, S. Liu, B. Cook, D. N. Williams, and C. T. Silva, “UV-CDAT: Analyzing climate datasets from a user’s perspective,” *Comput. Sci. Eng.*, vol. 15, no. 1, pp. 94–103, 2013.
- [370] D. N. Williams, T. Bremer, C. Doutriaux, J. Patchett, S. Williams, G. Shipman, R. Miller, D. R. Pugmire, B. Smith, C. Steed, E. W. Bethel, H. Childs, H. Krishnan, P. Prabhat, M. Wehner, C. T. Silva, E. Santos, D. Koop, T. Ellqvist, J. Poco, B. Geveci, A. Chaudhary, A. Bauer, A. Pletzer, D. Kindig, G. L. Potter, and T. P. Maxwell, “Ultrascale visualization of climate data,” *Computer*, vol. 46, no. 9, pp. 68–76, Sep. 2013.
- [371] D. N. Williams, C. M. Doutriaux, R. S. Drach, and R. B. McCoy, “The flexible climate data analysis tools (CDAT) for multi-model climate simulation data,” in *Proc. Int’l Conf. on Data Mining Workshops*. Los Alamitos, CA, USA: IEEE Computer Society, 2009, pp. 254–261.
- [372] S. P. Callahan, J. Freire, E. Santos, C. E. Scheidegger, C. T. Silva, and H. T. Vo, “VisTrails: Visualization meets data management,” in *Proc. of the 2006 ACM SIGMOD Int’l Conf. on Management of Data*, ser. SIGMOD ’06. New York, NY, USA: ACM, 2006, pp. 745–747.
- [373] European Centre for Medium-Range Weather Forecasts, *ECMWF Strategy 2016-2025*, European Centre for Medium-Range Weather Forecasts, Shinfield Road, Reading RG2 9AX, UK, 2016.
- [374] J. Johansson, T.-S. S. Neset, and B.-O. Linnér, “Evaluating climate visualization: An information visualization approach,” in *14th Int’l Conf. on Information Visualisation (IV), 2010*. IEEE, 2010, pp. 156–161.
- [375] IEEE SciVis Contest 2014 Team. (2013) 2014 IEEE Scientific Visualization Contest. <http://www.viscontest.rwth-aachen.de>. Accessed 23 Nov. 2017.
- [376] IEEE SciVis Contest 2017 Team. (2016) SciVis contest 2017: Visualization of clouds and atmospheric processes. <https://www.dkrz.de/SciVis>. Accessed 23 Nov. 2017.